HIGHWAY RESEARCH RECORD

Number 243

Soil Properties From In Situ Measurements

A Symposium

7 Reports

Subject Area

61 Exploration-Classification (Soils)
63 Mechanics (Earth Mass)

HIGHWAY RESEARCH BOARD
DIVISION OF ENGINEERING NATIONAL RESEARCH COUNCIL
NATIONAL ACADEMY OF SCIENCES—NATIONAL ACADEMY OF ENGINEERING

Washington, D.C., 1968

Publication 1631

Department of Soils, Geology and Foundations

Eldon J. Yoder, Chairman
Purdue University, Lafayette, Indiana

Chester McDowell, Vice Chairman
Texas Highway Department, Austin

HIGHWAY RESEARCH BOARD STAFF

J. W. Guinnee

DIVISION C

O. L. Lund, Chairman
Nebraska Department of Roads, Lincoln

L. F. Erickson, Vice Chairman
Idaho Department of Highways, Boise

COMMITTEE ON SOIL AND ROCK PROPERTIES
(As of December 31, 1967)

G. A. Leonards, Chairman
Purdue University, Lafayette, Indiana

George B. Clark
Robert W. Cunny
E. D'Appolonia
Robert C. Deen
Victor Dolmage
Wilbur I. Duvall
Austin H. Emery
Charles L. Emery
Emmericus C. W. A. Geuze
Bernard B. Gordon
James P. Gould
Stanley J. Johnson
Ernest Jonas
Robert L. Kondner
Charles C. Ladd
Thurmul F. McMahon
Victor Milligan
Roy E. Olson
William H. Perloff
Shailer S. Philbrick
Gregory P. Tschebotarioff
William G. Weber, Jr.
T. H. Wu

Foreword

Quantitative measurements of soil properties (or parameters) are needed in calculations of stability and settlement of structures founded on, or constructed with, soil. Such measurements are usually made by testing small samples in the laboratory. The papers comprising this RECORD represent a first attempt to examine the validity of these measurements in the light of computed values obtained from field observations.

Two papers, by Soderman, Milligan, and Kim, and by Hanna and Adams, compare values of the modulus of elasticity of clay till deposits obtained from a variety of laboratory and plate loading tests, and the latter paper includes modular values inferred from in-place ground movements. The papers give good indication of the effects of various test procedures on the modulus of elasticity of dense clayey tills.

The paper by Bromwell and Lambe compares laboratory values of the coefficient of consolidation during unloading (excavation) with those inferred from in situ measurements of pore pressure dissipation rates. The field values are found to be much larger than those obtained from laboratory tests but factors other than sampling and testing, such as the assumptions made in the interpretation of the pore pressure measurements, obscure the errors that might be attributed to the laboratory technique. On the other hand, Schmidt and Gould found that laboratory values of the coefficient of consolidation, when used with simple consolidation theory, predicted the rate of settlement of embankments whose foundations were stabilized by sand drains with acceptable precision for design purposes. It is not known to what extent compensating errors contributed to the good result obtained in this case.

Weber computed values of the coefficient of consolidation using compressibilities determined from oedometer tests and permeabilities computed from field measurements (drawdown rates in boreholes). For a number of embankments in California Weber showed that better predictions of settlement rates were obtained compared with computations using the coefficient of consolidation interpreted solely from oedometer tests.

Butt, Demirel, and Handy report the results of preliminary investigations involving the use of a spherical penetration device for the purpose of estimating the bearing capacity of footings. The device may prove to be a helpful indicator of stress-strain relations in clays and might be developed as a useful supplement to plate bearing tests.

Finally, an excellent summary and evaluation of the six papers is presented by Geuze.

—G. A. Leonards

Contents

Field and Laboratory Studies of Modulus of Elasticity of a Clay Till

L. G. SODERMAN and Y. D. KIM, University of Western Ontario, and
V. MILLIGAN, H. Q. Golder and Associates Ltd., Cooksville, Ontario

As part of a settlement study of structures founded on clay till in southern Ontario, factors influencing the modulus of elasticity of the till have been investigated. In situ plate tests and laboratory tests on tube and block samples were carried out under repetitive loading cycles, during which pore pressures were measured. Remolded samples were also tested and the results are compared with the field and undisturbed laboratory tests.

The results of the study indicate that the modulus of elasticity is extremely sensitive to sample disturbance; that the modulus of elasticity should be defined for the specific level of stress considered; and that definite relationships seem to exist between the undrained shear strength, consolidation pressure, and modulus of elasticity for this specific clay till. Pore pressure behavior during undrained repetitive loading in the laboratory and in the field was similar.

•IN the prediction of both immediate and time-dependent deformations resulting from the application of loads to a soil mass, general use is made of the theory of elasticity, incorporating soil properties that must, in most cases, be arrived at from laboratory tests made on the "best samples" that can be obtained from the particular soil deposit. In addition to the inherent problem of sample disturbance, the inelastic and nonlinear load-deformation characterisitc of soils necessitates an arbitrary definition of modulus of elasticity that must be used in the classical elastic theory solutions for stresses and deformations.

The results reported in this paper relate specifically to the practical determination of a modulus of elasticity to be used in predicting the immediate settlement of a highway embankment underlain by a deep deposit of near-normally consolidated clay till. A very common and characteristic feature of this clay till deposit is a relatively stiff desiccated surface crust having a thickness of about 20 ft; below this depth, the deposit is considered to be normally consolidated. The significance of the relative stiffness of the surface layer in evaluating the stress distribution throughout the deposit led to a detailed study of elastic modulus determination for this layer. The results obtained are reported in terms of total stresses only, since these data are sufficient to emphasize the sensitivity of the modulus of elasticity as determined in the laboratory to such factors as (a) sample type and size, (b) test type and procedure, (c) stress ratio, (d) rate of strain, and (e) number of cycles of repetitive load applied. The structure has been instrumented to monitor settlements; consequently, the field average value of the modulus will be forthcoming.

The stress-strain modulus used most commonly in nondynamic soil engineering problems dealing with saturated clay is that obtained from an undrained compression test either unconfined or confined in a triaxial test cell. Practical justification for the undrained tests in problems having to do with deformation immediately following a load application is found in the fact that the permeability of the clay soil is such that significant drainage is precluded during the relatively short time interval involved during

Paper sponsored by Committee on Soil and Rock Properties and presented at the 47th Annual Meeting.

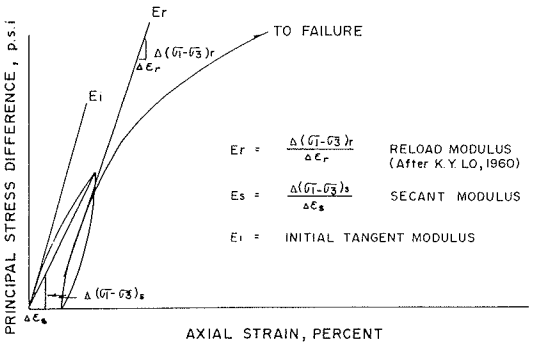

Figure 1. Definitions of moduli [$\Delta \epsilon_s$, $\Delta \epsilon_r$ = axial strain increment; $\Delta (\sigma_1 - \sigma_3)s$, $\Delta (\sigma_1 - \sigma_3)r$ = principal stress difference increment].

loading. The most frequently defined moduli from such undrained compression tests (Fig. 1) and (a) initial tangent modulus E_i, taken as the slope of the virgin stress-strain curve, and (b) the secant modulus, E_S, taken as the ratio of stress to strain at a particular stress value on the virgin loading curve. It has been previously suggested (7) that the modulus defined by the virgin loading curve is a quantity that involves both pseudoplastic and elastic effects and is not a true elastic modulus. Cyclic or repetitive loading results in a more linear compression curve and the true modulus of elasticity may be calculated from this curve. This modulus is shown in Figure 1 and is termed "reload modulus" denoted by Er. A number of investigators have compared moduli determined from first loading and reloading stress-strain curves on laboratory samples (2, 10), showing that the ratio of reloading modulus to initial loading modulus from laboratory compression tests varied from about 3 to 10. A notable exception to this is reported by Klohn (5), who states that the initial tangent modulus from unconfined compression tests and the reloading modulus from triaxial compression are sensibly the same for a dense glacial till. Moduli of elasticity determined from in situ plate loading tests were found to be "of the same general order of magnitude as those obtained from field observations," whereas laboratory compression test values varied from about one-half to one-tenth of those found from plate loading tests (5). The best agreement between plate test values and values obtained from structure performance was obtained by "using the average slope of the hysteresis loop that develops when the plate is subjected to cyclic loading." Simons (8), reporting on settlements of two structures in Norway, found that E values from Q tests gave values lower than those measured from actual settlement, while E values from R tests were too high. (Q test is an unconsolidated undrained triaxial test; R test is a consolidated undrained triaxial test.)

SITE LOCATION AND SOIL CONDITIONS

The site investigated is located in southwestern Ontario about 35 miles east of Detroit at the point where the MacDonald-Cartier Freeway crosses Tilbury Creek. The general geotechnical properties of the clay till deposit have been summarized by Soderman et al (9), and the gelogical origin of the till has been discussed by Dreimanis (3), who suggested that the till sheet was deposited during the Wisconsin Ice Age. The soil profile is shown in Figure 2. In general, the soil is of remarkably uniform composition and, with the exception of the desiccated upper crust, the deposit appears to be near-normally consolidated. The index properties and mineralogical composition, provided by R. M. Quigley, are given in Table 1. Occasional shale fragments of about ½-inch size were found throughout the entire deposit. The water table was found to be at a depth of 3½ ft and this coincided with the water level in Tilbury Creek. No artesian conditions were found either in the bedrock or overburden.

SAMPLING AND TESTING

The postconstruction investigation was carried out in two stages. The initial stage consisted of deep borings from which thin-walled Shelby tube (area ratio < 10 percent) samples were removed in diameters of 2 and 3 in. The boreholes were positioned on a 10-ft grid and undisturbed samples were taken so that the different diameter samples were from the same depth in adjacent boreholes. All samples were carefully wax-sealed immediately upon removal and stored in a humidity cabinet until tested.

TABLE 1

TILBURY CLAY TILL PROPERTIES

Property	Value
Natural moisture content, W	22 percent
Liquid limit, W_L	30 percent
Plastic limit, W_P	18 percent
Clay fraction (<0.002)	42 percent
Activity	0.30
S_u (in desiccated crust depth 0-20 ft)	1.5-3.0 kips/sq ft
S_u (below desiccated crust)	0.7-1.2 kips/sq ft
Sensitivity	2-3
ϕ' = Angle of shearing resistance in terms of effective stress	26 deg
c' = Apparent cohesion in terms of effective stress	100-200 psf
pH—pore fluid	8.5
Salinity—pore fluid (equivalent NaCl)	2.7 gm/liter
Clay minerals—illite, chlorite	
Nonclay minerals—quartz, feldspar, calcite, dolomite	
Ratio—calcite to dolomite	1.3

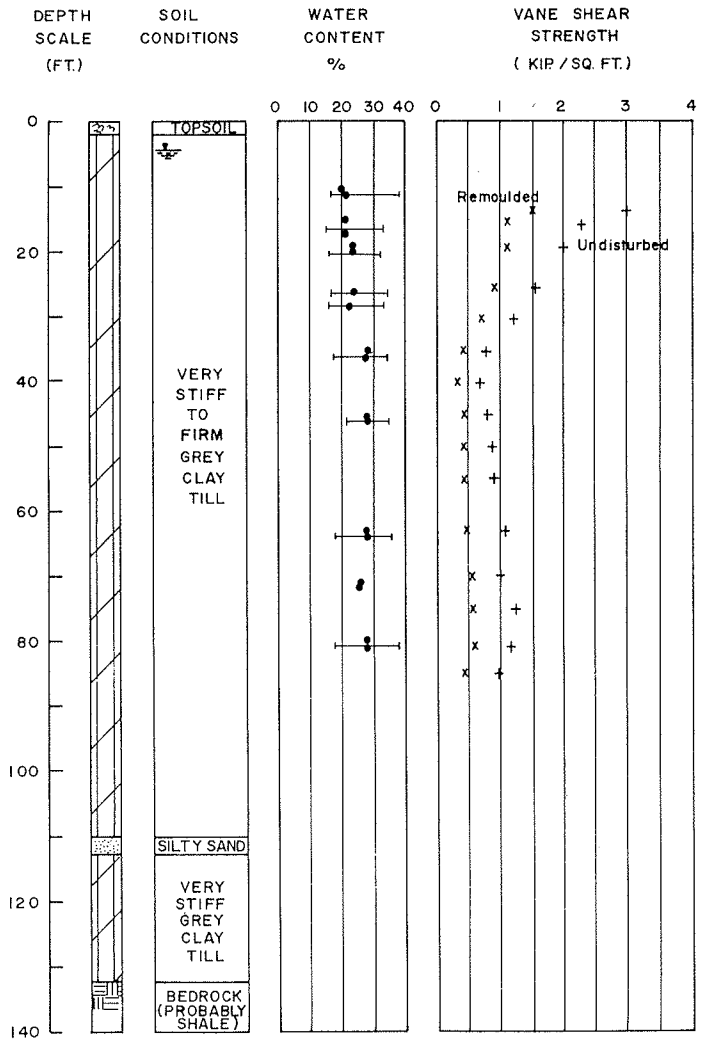

Figure 2. Generalized soil conditions, Tilbury test site.

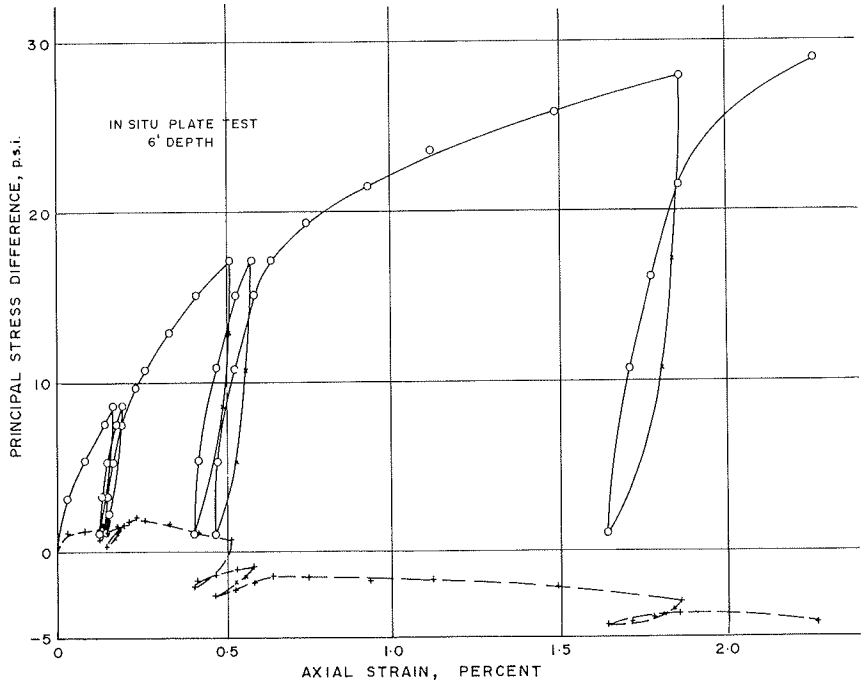

Figure 3. Stress-strain-pore water pressure relationship, 6-in. diameter plate test.

The second stage of the investigation was limited to the upper crust material and consisted of a test trench excavation so that horizontal benches at depths of 6, 10, and 14 ft resulted. Samples were taken at each bench elevation using thin-walled Shelby tubes about 18 in. long with diameters varying from 2 to 4 in. These sampling tubes were driven or pushed into the undisturbed soil to a depth of 15 in. and then dug out, rather than being rotated and pulled out. The inside clearance was zero percent for the tubes used (10), allowing no expansion of sample in the tubes. Both horizontal and vertical tube samples were taken. Plate loading tests using a cyclic loading procedure (Fig. 3) were carried out at each bench elevation both in a horizontal and vertical direction. The plate tests were limited to a single plate having a diameter of 6 in. The

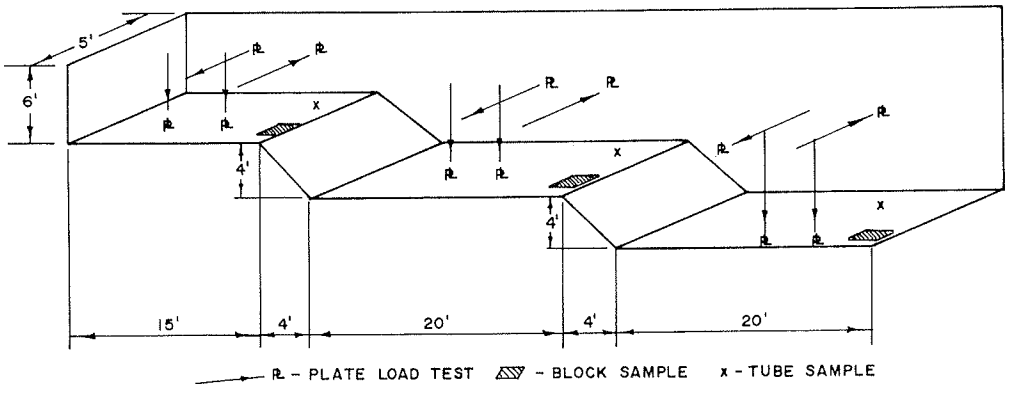

Figure 4. Schematic diagram of location samples in test pit.

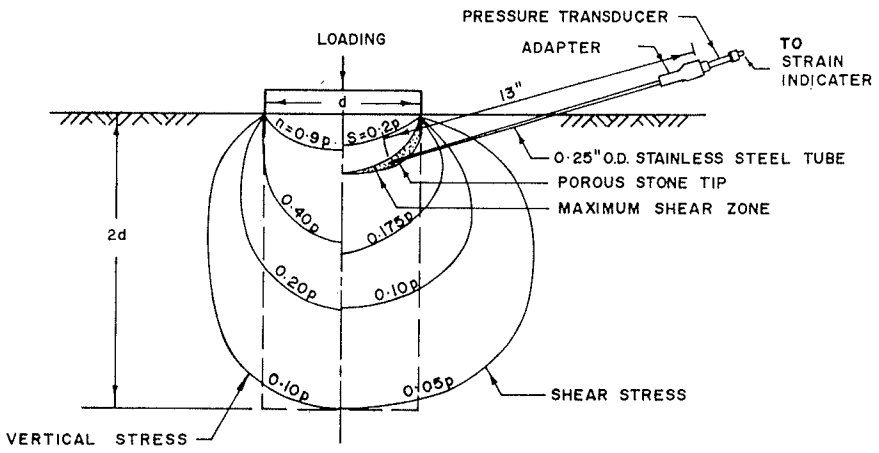

Figure 5. Distribution of stresses under a circular footing (after Jurgenson, 1934).

test trench details are shown in Figure 4. A transducerized porous-tipped needle was inserted into the theoretical maximum shear zone below the loading plate (Fig. 5) and pore water pressures were continuously recorded during the cyclic plate load tests (Fig. 3). All tube samples were wax-sealed immediately upon recovery and stored with the borehole samples until laboratory tested. In addition to the tube sampling and plate testing in the trench, block samples approximately 12 by 12 by 8 in. were carefully taken at each bench elevation. These were sealed with alternate layers of wax and cheesecloth immediately upon recovery.

Triaxial Testing

In addition to routine index tests performed on all samples recovered, a special cyclic triaxial testing program consisting of both unconsolidated undrained and consolidated undrained tests ($\overline{Q}$ and $\overline{R}$ tests) with pore water pressures measured at the base of the sample using pressure transducers was carried out. Back pressures varying from 40 to 70 psi were used for all tests. The cyclic loading procedure consisted of loading the undisturbed specimens to $\frac{1}{3}$ the maximum expected principal stress difference and unloading to zero load. This was repeated three times, the next reloading cycle was taken to a principal stress difference of about 50 percent of the estimated maximum and two unload-reload cycles were carried out. This repetitive procedure was also carried out at about 75 percent of estimated failure stress and at failure stress.

Strain Rate

All compression tests were carried out as strain-controlled tests, and the rate of strain used varied from about 2.5 percent to 4.5 percent per hour. Ladd (6) points out that as much as a threefold variation in modulus has been reported when strain rates vary from 0.12 percent per hour to 60 percent per hour. A series of tests carried out on undrained consolidated specimens using remolded and undisturbed material (Fig. 6) showed

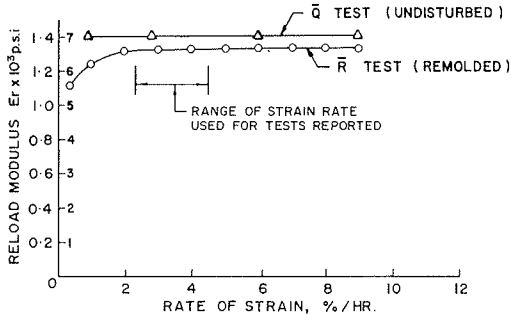

Figure 6. Variation in reload modulus with rate of strain.

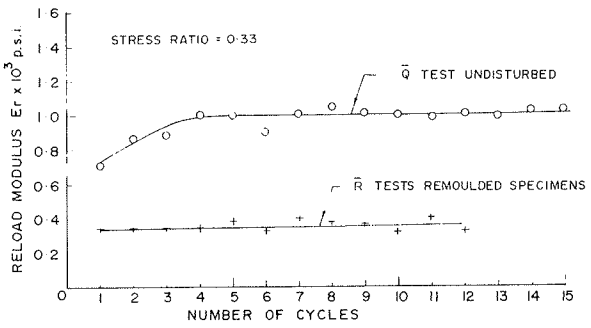

Figure 7. Variation in reload modulus with number of cycles.

that the value of reload modulus (E_r) was sensibly constant when the strain rate varied from about 0.5 percent per hour to 13 percent per hour. A similar insignificant sensitivity to strain rate was reported for the Sunnybrook till, Toronto (2).

Number of Load Cycles

Use of the recompression curves in the stress-strain diagram to define the modulus of elasticity has been discussed by a number of investigators (2, 6, 7, 10, 11). In addition to eliminating initial seating errors in the test setup, the use of the recompression curve has the advantage of causing fissures and partings in undisturbed samples of overconsolidated clays to close, thereby minimizing deformation that is not true strain (10). In order to determine the influence of a number of cycles on reload modulus, a series of $\bar{Q}$ and $\bar{R}$ tests was carried out on both undisturbed and remolded specimens with cycles varying from 1 to 15. The data obtained are shown in Figure 7. Three cycles were used for most of the laboratory and all of the plate load tests reported. Crawford and Burn (2) found that about 20 cycles were required to result in constant value of E_r, whereas Lo (7) found that recompression curves were parallel for all cycles up to two-thirds of the peak stress in each cycle.

Percentage Unloading

Wilson and Dietrich (11) have defined a static modulus of elasticity (E_{static}) obtained from repetitive load tests during which small on-off load increments were used. This procedure eliminates creep effects but has the disadvantage that a stiffening effect results when successively smaller off-on loads are used. This effect is demonstrated in Figure 8, which shows that the reload modulus obtained from a 25 percent unloading is about twice the value obtained from 100 percent unloading. Undoubtedly the modulus defined by Wilson and Dietrich is the modulus that should be used in some practical problems, but it does not apply directly to the problem of immediate deformation under a highway embankment loading.

Modulus From Plate Load Tests

The three most commonly used moduli for applied static loadings are shown in Figure 1. The reload modulus determined after two to three cycles of repetitive loadings at a specific stress ratio is the one chosen for this comparative study to demonstrate the influence of sample disturbance on the modulus value. The use of in situ plate load tests to evaluate the modulus of elasticity has been discussed by Burmister (1) and the method suggested in his discussion has been adopted. The Bousinesq equation for a rigid circular bearing plate with a uniformly distributed contact pressure has been used. This equation is as follows:

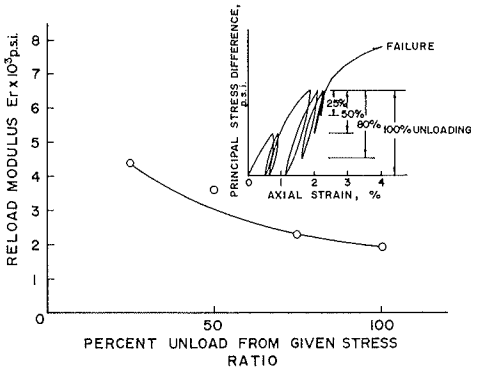

Figure 8. Variation in reload modulus with percent unload.

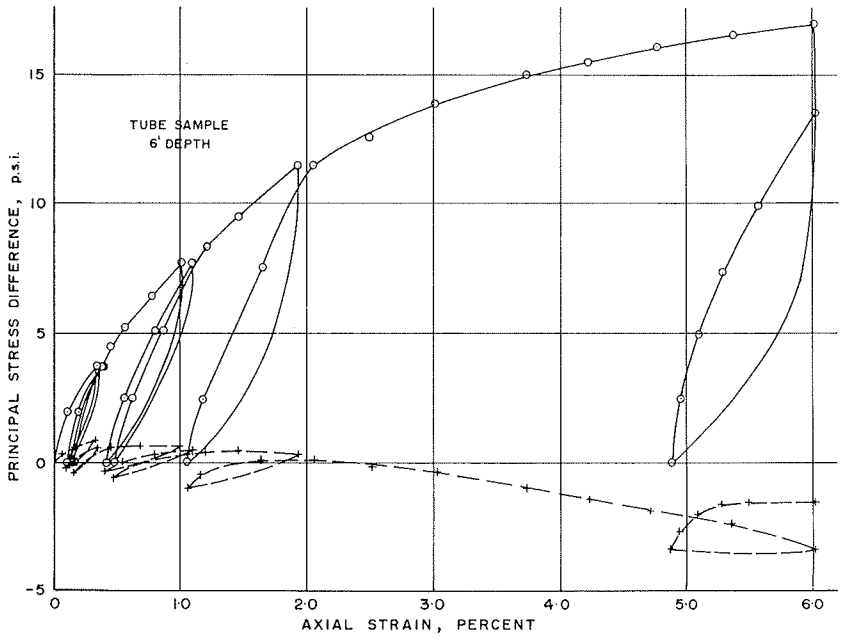

Figure 9. Stress-strain-pore water pressure relationship $\overline{Q}$ test.

$$\Delta = \frac{\pi}{2} \frac{(1 - \mu^2)}{E} pr$$

where $\mu = 0.5$, p = contact pressure, r = plate radius, Δ = deflection, and E = modulus of elasticity.

In order to develop a stress-strain curve as shown in Figure 3, the depth of soil below the loading plate assumed to be deformed by the surface plate load has been taken as two plate diameters (Fig. 5). The principal stress difference is determined from the elastic equation using the surface contact pressure and a restraint factor as discussed by Burmister (1).

The small diameter plate has been used because (a) the small plate minimized equipment weight; (b) the variation in modulus with depth in the crust will have less influence for small plates than larger plates; and (c) the length of laboratory samples tested varied from 4 to 8 in., which is reasonably close to the depth of soil influenced by 6-in. diameter plate. Pore water pressures were measured at a point in the zone of estimated maximum shear stress below the loaded plate using a porous insert and a pressure transducer. The stress-strain-pore water pressure curves from a cyclic triaxial laboratory test on an undisturbed specimen and an in situ cyclic plate load test are compared in Figures 3 and 9. The pattern of pore water pressure behavior is remarkably similar in both tests.

RESULTS

The results obtained from the first stage of the investigation using undisturbed borehole samples are shown in Figure 10. This figure shows that

1. The reload modulus E_r was found to be about 50 percent greater than the secant modulus for stress ratios varying from 0.2 to 0.7 (Fig. 10).
2. The reload modulus as determined from 3-in. diameter samples was consistently greater than values determined from 2-in. diameter samples. At low stress ratios the modulus for 2-in. undisturbed samples was only about 20 percent larger than that found

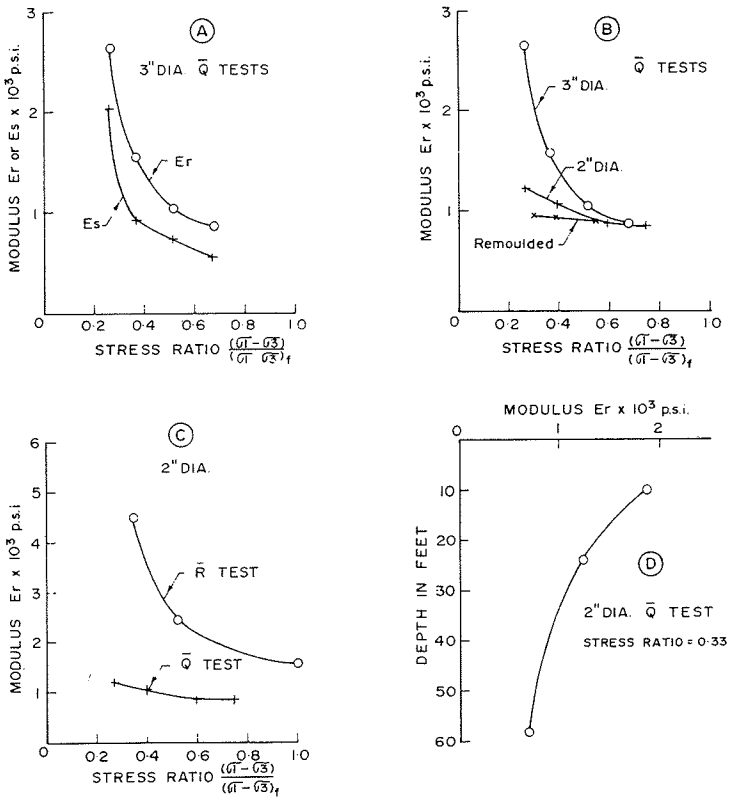

Figure 10. Influence of sample size and test type on moduli shown using borehole samples [$(\sigma_1 - \sigma_3)$ = applied principal stress difference; $(\sigma_1 - \sigma_3)$ f = principal stress difference at failure].

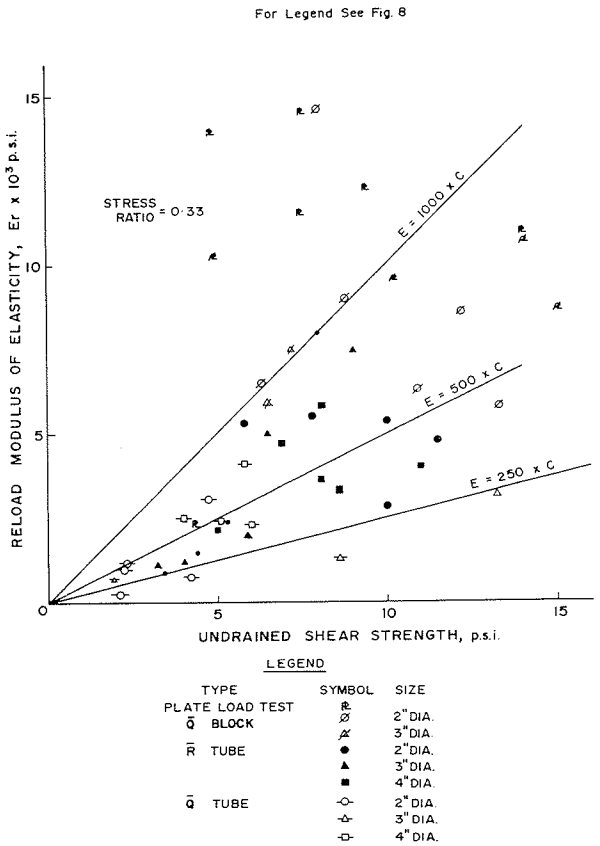

Figure 11. Strength vs modulus relationship.

from tests on remolded specimens; at high stress levels all results were similar (Fig. 7).

3. For the same size undisturbed samples the reload modulus as determined from consolidated undrained tests (R tests) varied from 2 to 4 times the value obtained from Q tests (Fig. 8).

4. The reload modulus was found to decrease markedly with depth through the crust zone and in a manner similar to the decrease in strength with depth. This is presumably related to desiccation (Fig. 6).

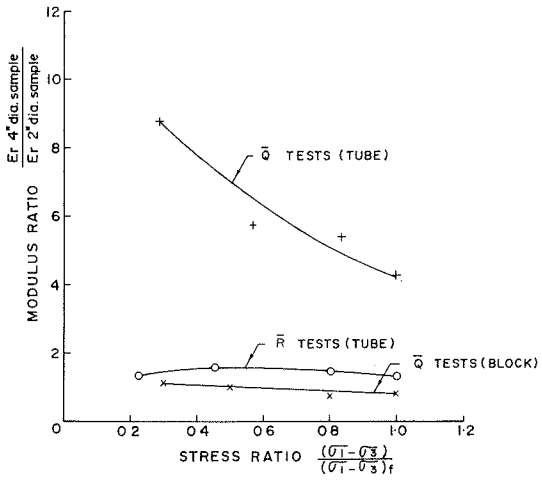

Figure 12. Influence of sample diameter and test type on reload modulus.

An attempt was made to determine the E_r/S_u ratio but no order was found in the data at hand (Fig. 11). These points are not new and similar patterns have been reported by others (4, 6).

The results of the second stage of the investigation are shown in Figures 12 and 13, which indicate that the influence of sample disturbance vs stress ratio for any one test type is shown by the ratio of reload modulus for 4-in. and 2-in. samples:

5. For $\bar{Q}$ tests on tube samples this modular ratio, $\frac{Er\text{-}4}{Er\text{-}2}$, varies by 100 percent for the stress ratio range of 0.25 to 1.0.

6. For $\bar{R}$ tests, which are recommended by Ladd (6), on tube samples the modular ratio varies from 1.5 to 2.0 for a stress ratio range of 0.25 to 1.0.

7. For $\bar{Q}$ tests on specimens cut from block samples the modular ratio was only slightly above 1 for a stress ratio range of 0.25 to 1.0.

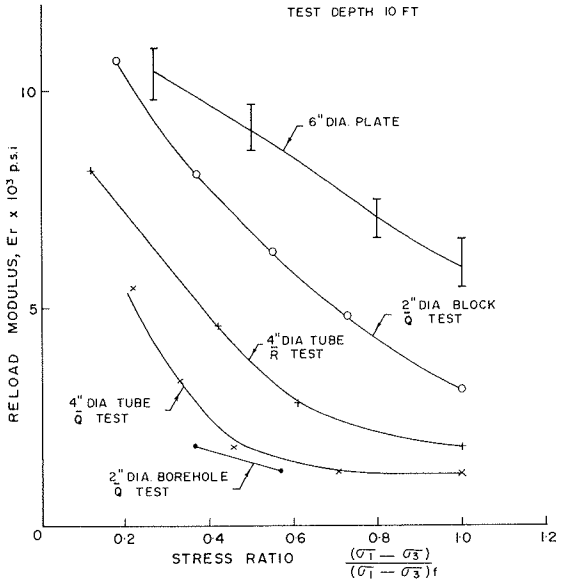

Figure 13. Reload modulus vs stress ratio for sample size and test type shown.

The significant findings of the complete study have been summarized in Figure 13. It was found that

8. All types of samples, regardless of test type, show a decrease in modulus with increase in stress ratio. This decrease is about 50 percent for all tests when the stress ratio varies from about 20 to 100 percent.

9. The largest value of reload modulus was obtained from in situ plate bearing tests for all stress ratios.

10. The plate loading tests gave values of reload modulus generally twice the value obtained from $\bar{R}$ tests on 4-in. diameter tube samples.

11. The $\bar{Q}$ tests on specimens trimmed from block samples gave reload modulus values nearest those obtained from plate loading tests.

The variation in modulus vs depth for the crust zone is shown in

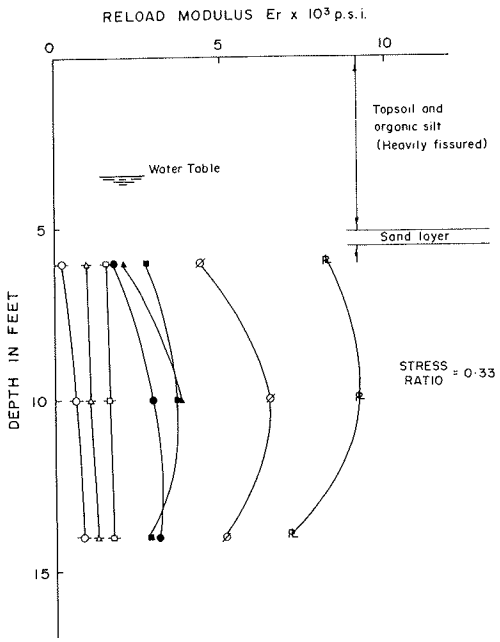

Figure 14. Reload modulus vs depth (see Fig. 11 for legend).

Figure 14. This shows clearly the wide discrepancy between moduli determined from laboratory tests on undisturbed samples and moduli determined from in situ plate bearing tests.

CONCLUSIONS

1. A decrease in the value of reloading modulus (E_r) with increase in stress ratio occurs regardless of test type and sample type. For Tilbury clay till this decrease was found to be about 50 percent when stress ratio was increased from 20 percent to 100 percent. This decrease in modulus is believed to be due to a breakdown of the soil structure as the specimen develops large strains near the failure stress ratio of unity.

2. The comparative tests on samples subjected to various degrees of sampling disturbance show clearly that carefully trimmed specimens from block samples subjected to unconsolidated undrained triaxial tests ($\overline{Q}$ tests) gave values of E_r nearest to values obtained from in situ cyclic plate load tests. The E_r values from consolidated undrained tests ($\overline{R}$ tests) on tube samples were about 50 percent of the values found from cyclic plate loading tests.

3. The presentation of data obtained in terms of undrained shear strength vs reload modulus or any other modulus of elasticity commonly used did not show an acceptable correlation between modulus and strength. In general the value of E_r/S_u was markedly higher for plate test data than for laboratory test data.

4. The pore water pressure developed in the zone of maximum shear stress below the bearing plate during the in situ cyclic loading exhibited a behavior pattern similar to the water pressures measured during cyclic triaxial tests on tube samples in the laboratory.

ACKNOWLEDGMENTS

The studies reported in this paper were supported by a grant from the National Research Council of Canada to the senior author. The test data form part of Y. D. Kim's doctoral thesis at the University of Western Ontario. Assistance was given by D. L. Townsend, Queen's University, in helpful discussion and review of the manuscript.

REFERENCES

1. Burmister, D. M. General Discussion at Symposium on Load Tests of Bearing Capacity of Soils. ASTM STP 79, p. 139-148, 1947.
2. Crawford, C. B., and Burn, K. N. Settlement Studies on Mt. Sinai Hospital, Toronto. Eng. Jour. (Canada), p. 31-37, Dec. 1962.
3. Dreimanis, A. Tills of Southern Ontario. In Soils in Canada (rev. ed.), R. F. Legett, ed., Univ. of Toronto Press, 1965.
4. Hanna, T. H. Engineering Properties of Glacial-Lake Clays Near Sarnia, Ontario. Ontario Hydro's Res. Quart., Vol. 18, No. 2, 1966.
5. Klohn, E. J. The Elastic Properties of a Dense Glacial Till Deposit. Canad. Geotech. Jour., Vol. 2, No. 2, p. 116-128, 1965.
6. Ladd, C. C. Stress-Strain Modulus of Clay in Undrained Shear. Jour. Soil Mech. and Found. Div., p. 103-132, Sept. 1964.

7. Lo, K. Y. Stress-Strain Relationship and Pore Water Pressure Characteristics of a Normally-Consolidated Clay. Norweg. Geotech. Publ., No. 45, Oslo, 1961.
8. Simons, N. Settlement Studies on Two Structures in Norway. Proc. Fourth Internat. Conf. on Soil and Found. Eng., Vol. 1, 431 pp.
9. Soderman, L. G., Kenney, T. C., and Loh, A. K. Geotechnical Properties of Glacial Clays in Lake St. Clair Region of Ontario. Proc. 14th Canad. Soil Mech. Conf., 1961.
10. Ward, W. H., Samuels, S. E., and Butler, M. E. Further Studies of the Properties of London Clay. Geotechnique, Vol. 9, p. 33-58, 1959.
11. Wilson, S. D., and Dietrich, R. J. Effect of Consolidation Pressure on Elastic and Strength Properties of Clay. ASCE Res. Conf. on Shear Strength of Cohesive Soils, Boulder, Colo., p. 419-435, 1960.
12. Jurgenson, L. Application of Theories of Elasticity and Plasticity to Foundation Problems. Jour. Boston Soc. Civil Eng., July, 1934.

Comparison of Field and Laboratory Measurements of Modulus of Deformation of a Clay

THOMAS H. HANNA, Sheffield University, England, and
JOHN I. ADAMS, The Hydro Electric Power Commission of Ontario, Canada

The results are presented of a field and laboratory study of the deformability of a natural clay from a site in southwestern Ontario tested under undrained loading conditions. It was found that the laboratory-determined modulus of deformation is very sensitive to the test load system used and the stress level applied as well as the magnitude of the undrained shear strength. Moduli of deformation determined in-place by plate loading tests and inferred from in-place ground movements resulting from construction work generally were different from and in most cases greater than the laboratory-determined values.

•WHEN a soil mass is loaded it will deform and work will be done. The work done may be conveniently divided into an irrecoverable component (plastic) associated with particle slippage and a recoverable component (elastic) associated with pressure changes. In routine testing the sum of the components is measured. Perfectly elastic materials have a linear stress-strain behavior. Ductile materials, however, can tolerate strain beyond the limit of elasticity following elastic-plastic behavior, and their deformation may be studied by "perfect" theories of plasticity. Soils are at the soft end of the range of engineering materials and have stress-strain characteristics with a definite peak or local failure curve of many forms depending on the method of test. Several rigorous attempts have been made to study the stress-strain behavior of soils (1, 2).

Clay soils comprise very fine plate-shaped particles surrounded by both adsorbed and free water. The geological processes common to the formation of a clay stratum can result in a preferred orientation of these particles as well as laminations and stratifications due to different rates of deposition. Changes near the ground surface resulting from desiccation and weathering can cause fissuring and cracking to considerable depths. From all the processes involved most clays possess, in situ, a system of shear stresses. The sampling and preparation of natural clays for laboratory testing invariably cause some damage to the arrangement of the clay particles and alteration of the stress system. The replacement of the estimated in-place field stress system in the laboratory specimen and the simulation of the additional stress changes that result during field loading cause deformations that are partly irrecoverable.

The immediate displacements of a clay stratum, both at ground surface and depth, may be important and under certain circumstances they can have a decisive control on design and construction. In many cases reliable prediction of ground movement is difficult and in such cases a valid approach is to measure the resulting field movements and compare them with computations based on laboratory test information. A site near Sarnia, Ontario, provided such an opportunity. Comprehensive deformability data for the firm-to-stiff clay deposit, obtained by laboratory triaxial testing, were complemented by several sets of field movements. This paper presents some of the test in-

Paper sponsored by Committee on Soil and Rock Properties and presented at the 47th Annual Meeting.

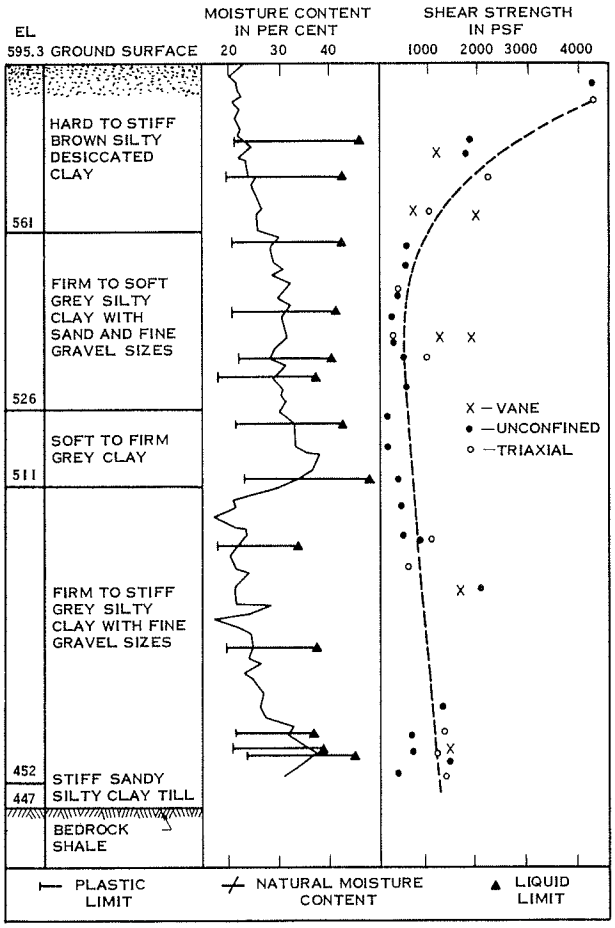

Figure 1. Geological profile.

formation obtained from this site. The data refer to natural clays from a large site where testing was predominantly commercial, and therefore the results are of a practical nature.

GEOTECHNICAL PROPERTIES OF THE CLAY

The site investigation for Ontario Hydro's 2000-megawatt generating station near Sarnia, Ontario, where the overburden consists of lightly overconsolidated "glacial-lake" clays, provided a large number of 2-in. and 2.5-in. Shelby-tube samples recovered from augered boreholes. To obtain less disturbed samples, piston techniques were used and during excavation works several 1-ft cube samples were recovered. A general description of the soil strata is contained in a recent paper (3) and details of the variability of the engineering properties will be reported eslewhere (4).

A detailed geological profile for a sampled borehole is shown in Figure 1. The desiccated surface crust has resulted in a hardening of the upper clay layers as reflected in the strength profile on the right. Extensive data indicate that the clays forming this profile are of the same geological origin (5) and that the differences in engineering property are a function chiefly of the natural water content (4).

While the clay is geologically very uniform it does exhibit definite laminations and stratifications in places (3, 4) and near the ground surface it is severely fractured by surface drying. Thus there is a definite sequence of layers of clay, macroscopically homogeneous, which constitute the profile. It is known that the in-place stress system existing within this mass of clay is heterogeneous and indeterminate. From this brief summary of the general soil conditions prevailing, it is evident that the mass behavior of the in-place clay is very different from that of a small laboratory test specimen. Throughout the following report, this limitation must be kept in mind, because it provides an understanding of the differences in behavior of natural clays and the extremely idealized versions that are assumed for test data interpretation and subsequent deformation distribution computation.

THE LABORATORY-DETERMINED MODULUS OF DEFORMATION

Unconsolidated undrained triaxial compression tests, run at an axial deformation of 0.05 in. per min, provided values of the modulus of deformation (secant value), E, determined from the reload part of the stress/strain curve. (These values refer to a stress level of about half the undrained strength of the test specimens.) The modulus values, E, are graphed against the undrained shear strength, C, and Figure 2 shows that the

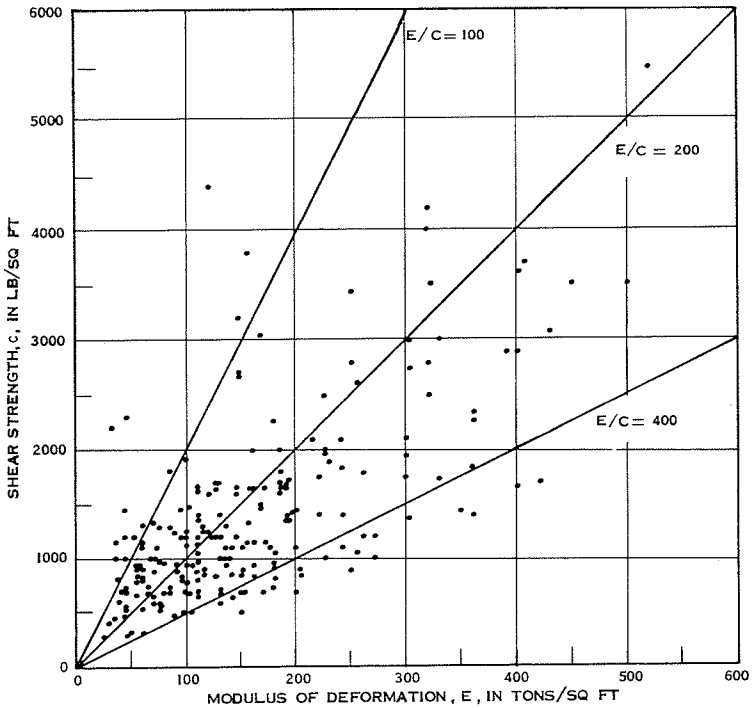

Figure 2. Relation of modulus of deformation, E, to undrained shear strength, C.

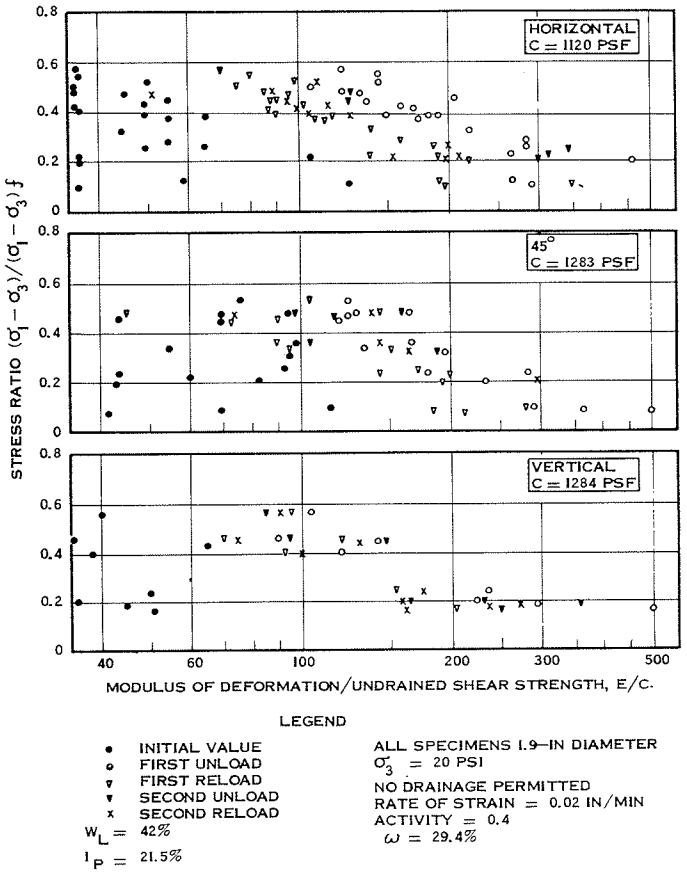

Figure 3. Modulus of deformation values for unconsolidated undrained triaxial specimens loaded at 0, 45, and 90° to the in situ vertical direction at constant strain loading.

data fall in the range 100 < E/C < 400, approximately. This information refers to specimens from the whole site. There are several disadvantages to the above system of modulus determination. Included are the strain-rate effect and the effective stress-loading system. To explore these factors in some detail, additional testing was performed on 1.9-in. specimens cut from 1-ft cubes of clay obtained at the 40-ft level in the side of a deep excavation. The testing comprised constant strain and constant stress methods of loading. In all tests, the top and bottom platens were lubricated with silicone grease to reduce the effect of end friction restraint on the specimen.

Constant Strain Tests

Samples were tested with the direction of the applied major principal stress inclined at 0, 45, and 90 deg to the in situ vertical direction, the load being cycled at stress levels between approximately 0.2 and 0.5 of the ultimate strength. An axial deformation rate of 0.02 in. per min was used and no drainage was permitted. Values of the secant modulus of deformation divided by undrained strength, E/C, are graphed against factor of safety of the specimen to failure in Figure 3. (Absolute values of E may be obtained from Figure 3 and subsequent Figures as values of c are quoted.) Several trends are evident: with increase in stress level, the modulus value decreased; the initial load modulus values were smallest while the unload values were greatest; and the moduli value for specimens tested with their axes horizontal were slightly greater than for specimens with their axes parallel to the in situ vertical. There was little difference between the 45° inclined and the horizontal specimens It was also found that the undrained strength measured with the direction of loading horizontal was slightly greater than the strength when loaded in the vertical direction (6).

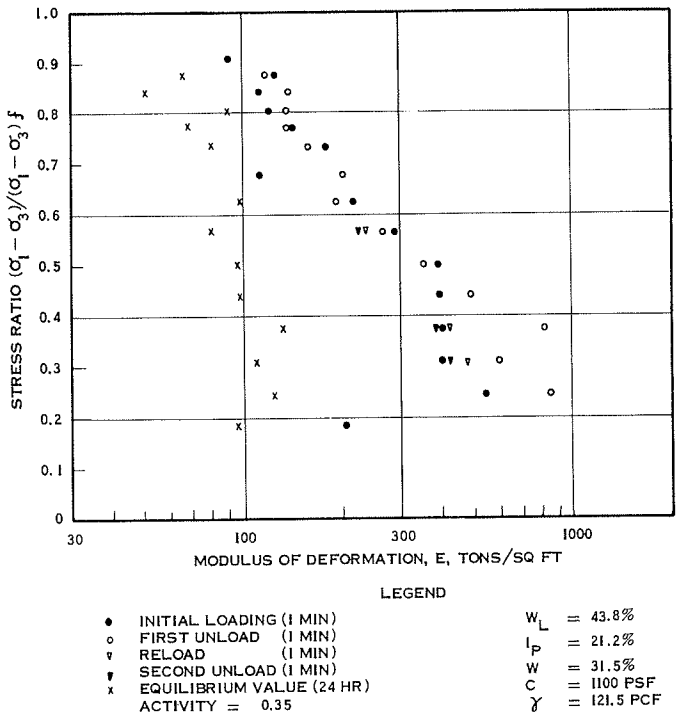

Figure 4. Modulus of deformation values for unconsolidated undrained triaxial specimen at constant stress loading.

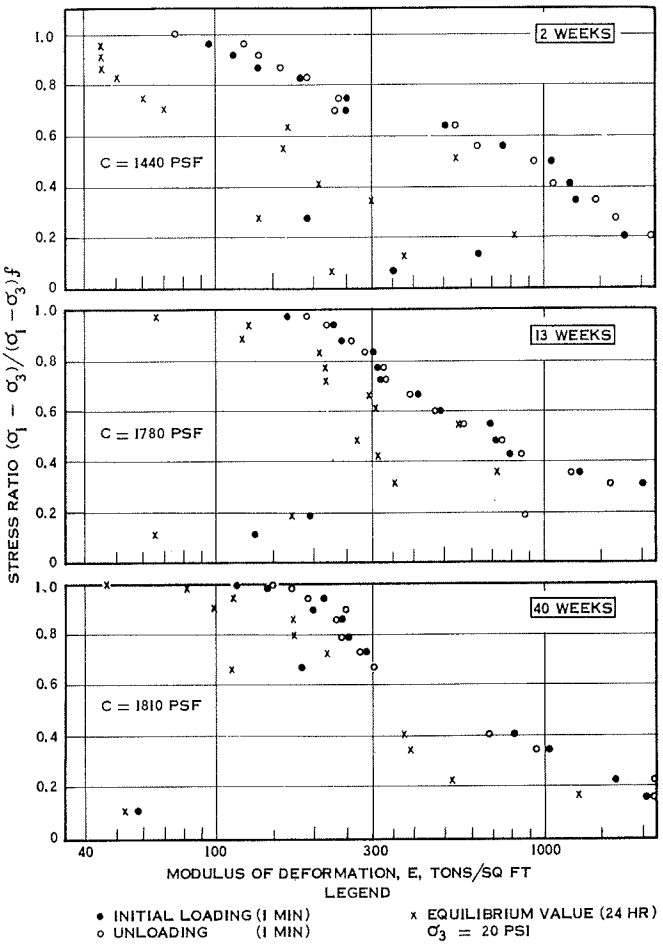

Figure 5. Modulus of deformation values for consolidated undrained triaxial specimens at 2, 13, and 40-week ages at constant stress loading.

Constant Stress Tests

Three variables were investigated: time of loading, isotropic consolidation, and stress level. All specimens were cut from a 1-ft cube of soil with their axes parallel to the in situ vertical. Loading was by deadweight to a hanger; generally each load increment was about 6 percent of the failure load and was maintained for a 24-hr period.

Two specimens were tested under unconsolidated undrained conditions with an applied cell pressure of 20 psi. Values of the modulus of deformation are graphed against stress level in Figure 4 for one test.

Three other "identical" specimens were consolidated by an isotropic effective stress of 20 psi with a back pressure of 40 psi. (In the present context, "identical" refers to specimens cut from adjacent parts of the cube sample. There are slight differences in plasticity, gradation, and natural water content.) Periods of consolidation of 2, 13, and 40 weeks ensued prior to the start of the load test. During this time the laboratory temperature was 68 ± 2 F. The drainage comprised a $\frac{3}{8}$-in. stone recessed in the top loading platen. Thus it was possible to use enlarged and lubricated end platens in all tests. The loading tests were similar to the unconsolidated undrained tests with a reload cycle at the start of each load increment. Values of the modulus of deformation are shown in Figure 5. Several trends emerged: the undrained shear strength increased

with the period of consolidation, i. e., age; the initial loading and unloading moduli values were of the same order of magnitude; the moduli values decreased with stress level; and there was no significant difference between the modulus of deformation and the age of the specimen.

FIELD DEFORMATION MEASUREMENTS

In-Place Plate Bearing Tests

A number of in situ plate loading tests were performed against the walls of test trenches cut at several depths in the side of a deep excavation. The 9-in. diameter by 1-in. thick plate was stiffened by the 6-in. diameter loading strut, which contained the hydraulic loading jack. Reaction for loading was obtained from the opposite wall of the test trench. The loading plates penetrated the clay surface at 0.15 in. per min, giving a time to failure in the order of 10 min. The load was cycled at several stress levels. By use of the simplification that the vertical clay face is equivalent to an elastic half-space and that the clay is homogeneous, unfissured, and isotropic, the penetration of the rigid plate was used to estimate the modulus of deformation of the clay. A summary of the moduli values computed from the plate tests is given in Table 1.

Many criticisms may be directed to the method of test and its analytical interpretation, and the unconditional use of elastic theory has been queried recently (7). Accepting the limitations, it is seen from the data in Table 1 that the moduli values during loading are less than during unloading, but there is a wide range in value, suggesting that some of the deformation readings are in error.

In-Place Ground Movements

Complementary to the small-scale laboratory test program, simple field measurements were made to record in-place ground movements resulting from load changes in the clay mass. The work comprised the monitoring of vertical and horizontal movements at several convenient ground positions. Data typical of the movements recorded are presented.

TABLE 1

MODULUS OF DEFORMATION VALUES FOR IN-PLACE HORIZONTAL PLATE BEARING TESTS

Depth (ft)	q/q_f	C (psf)	North Side $\frac{E}{c}$ Load	North Side $\frac{E}{c}$ Unload	South Side $\frac{E}{c}$ Load	South Side $\frac{E}{c}$ Unload	Thickness of Surface Crust (ft)
8	0.36	1800	100	320	85	170	
	0.48		290	910	240	980	15
	0.66		520	420	430	420	
8	0.28	2340	160	190	140	210	
	0.37		275	195	285	230	
	0.59		150	145	155	190	15
	0.75		165	195	170	210	
19	0.23	4040	220	150	170	230	
	0.40		300	1120	380	1600	
	0.52		300	530	630	430	25
	0.71		320	600	240	520	
34	0.18	2010	340	—	100	1170	
	0.32		740	2400	—	—	
	0.46		940	740	690	630	
	0.51		1100	610	860	600	25
	0.76		330	570	170	510	
	0.86		500	—	380	500	

Note: The test was carried out within 6 hr of trench excavation. All values are secant values and refer to 1-min load readings. q = applied plate pressure; q_f = ultimate bearing capacity.

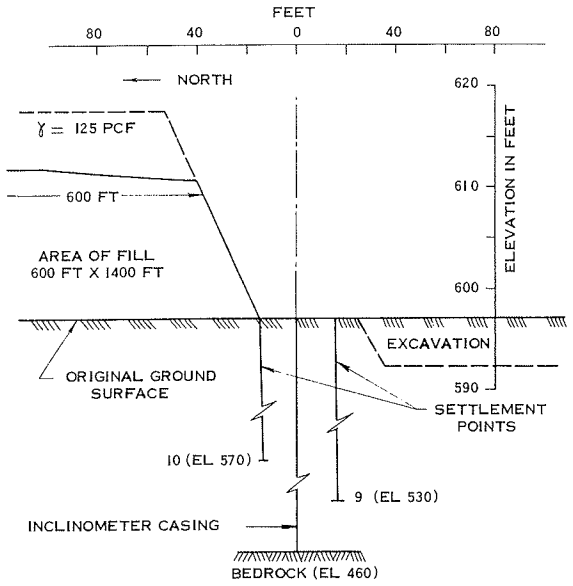

Figure 6. Profile through test fill and heave installation (solid line, profile 6/65; dashed line, profile 7/65).

Advantage was taken of a spoil area, and both lateral and vertical soil movements due to construction were measured. Two heave gages, similar in design to those reported by Bozozuk (8), were installed near the toe of the fill and their elevation determined to 0.001 ft by precise level prior and subsequent to fill placement. A profile through the fill, parallel to the heave gages, is shown in Figure 6. Also included are details of the heave gage positions and bedrock. The soil profile (Fig. 1) is near the heave gage installation and may be taken to be representative of the soils beneath the test fill. A slope indicator tube was installed midway between settlement gages 9 and 10 (Fig. 6) and anchored into bedrock. The space around the tube was filled with a medium sand placed by pouring through water. The slope of the casing was determined after

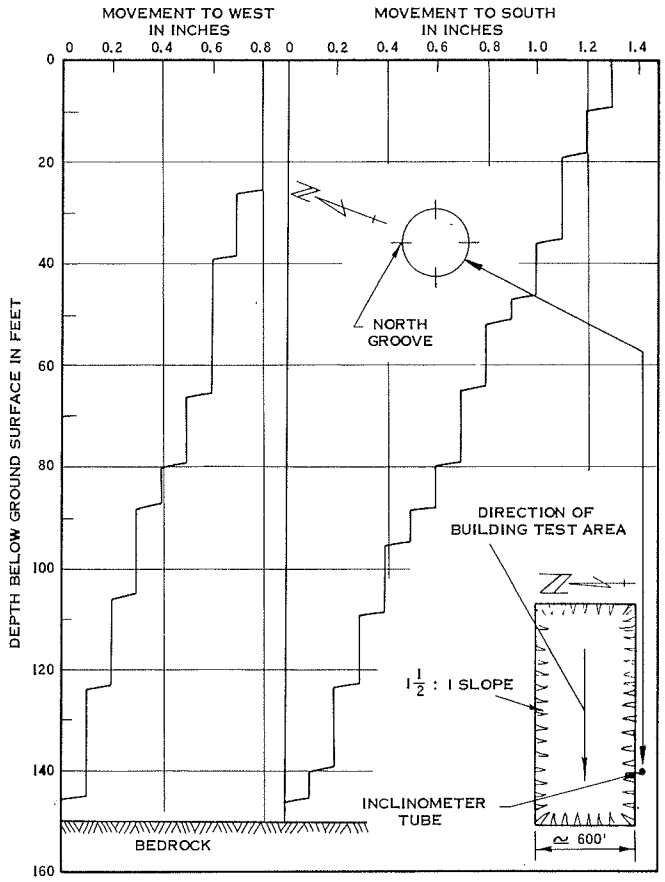

Figure 7. Lateral ground movement profiles adjacent to test fill.

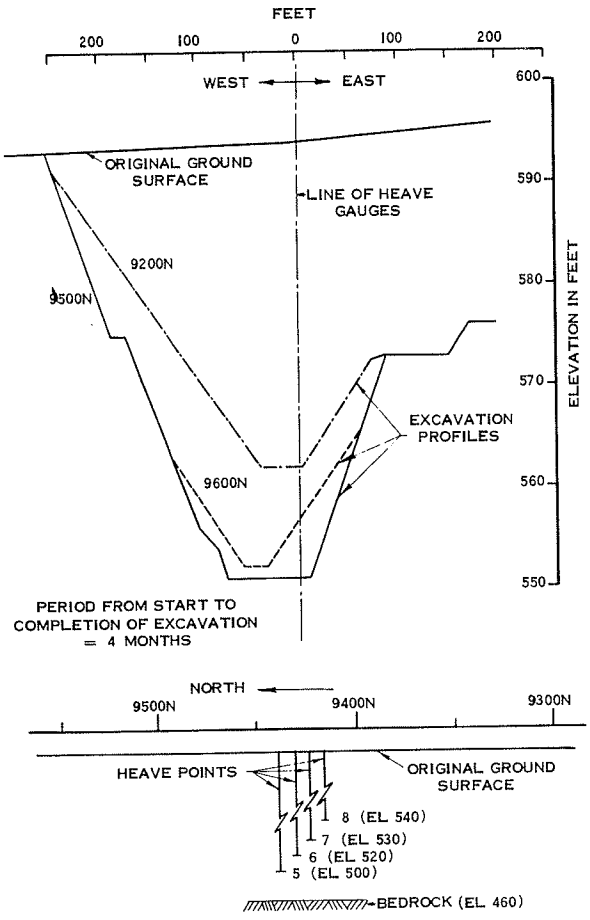

Figure 8. Profiles through excavation and heave points.

installation by use of a Wilson slope indicator series 200B instrument (9). Similar readings were taken subsequent to completion of the test fill construction. Subtraction of the deflection components for any particular depth gives the lateral components of clay movement in perpendicular directions. A profile showing the lateral ground movements resulting from the placement of the fill is shown in Figure 7. The movement away from the side of the test fill is about twice the magnitude of the movement parallel to the side of the fill. This observation is compatible with the order of fill placement, which proceeded from east to west.

A large excavation up to 45 ft deep was instrumented, with four heave gages at different depths below final grade. Profiles normal and parallel to the heave gages, both before and after excavation, are shown in Figure 8. This excavation was dug during a period of 4 months. Prior to the start of construction, the water table was about elevation 585, some 15 ft below ground surface. With excavation, the water level in the clay was lowered, but detailed readings were not taken in the vicinity of the heave points in the deep excavation. Adjacent to the test fill, four Geonor-type piezometers recorded slight increases in water pressure during fill placement.

TABLE 2

MODULUS OF DEFORMATION VALUES DETERMINED FROM FIELD DATA

Heave Gage No.	Observed Movement (ft)		Modulus of Deformation (tons/sq ft)		Remarks
	Settlement	Heave	Loading	Unloading	
5		—		—	Impossible to locate gage due to obstruction in hole.
6		0.076		1100	For details of layout see Fig. 8.
7		0.089		1265	Readings taken about 2 weeks after completion of excavation.
8		0.118		1320	
9	0.054		276		For details of layout see Fig. 6.
10	0.022		850		Readings taken at end of construction.

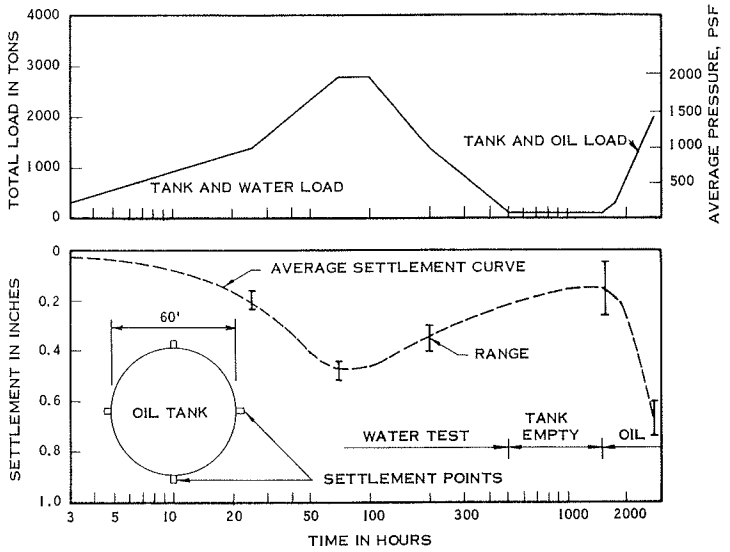

Figure 9. Oil tank load settlement data.

The vertical ground movements were translated into average moduli of deformation as follows: From the geometry of the excavation or the test fill, with respect to the heave gauge, the change in vertical stress was estimated by influence charts according to Osterberg (10). Assuming that the clay is elastic and disregarding the influence of the initial anisotropic stress system acting, the average modulus of deformation (E_{av}) for the clay between the heave gage and bedrock is

$$E_{av} = \sum \frac{\sigma v \cdot dh}{\Delta}$$

where Δ is the vertical movement of the heave gage, and σ_v is the vertical stress change in the element of height dh.

Values of the computed moduli of deformation are given in Table 2. Also included are the heaves measured and other pertinent details.

The test loading of a 60-ft diameter steel oil storage tank provided immediate settlement data during the load and unload sequence. Settlements were taken by geodetic leveling procedures to four peripheral settlement points with respect to a rock bench mark. The tank, of welded-steel construction, rested on a 5-ft thick granular pad. Details of the test load program along with the settlement data are shown in Figure 9. Values of the estimated modulus of deformation are shown in Figure 10(F).

COMPARISON OF LABORATORY-DETERMINED AND FIELD-INFERRED MODULI

Close agreement between laboratory-determined and field-inferred moduli of deformation is unlikely, except in special cases. The following sources of disagreement are believed to be important: (a) limitations of stress distribution theory, (b) inexact knowledge of the initial in-place effective stress system in the clay mass, (c) damage caused to small specimens during recovery from the ground and during setting-up for testing, and (d) the variability of the clay mass.

Bearing in mind these factors, and referring to the test data previously presented, one finds a very large range in modulus value. Generally the field-inferred moduli are larger than the corresponding laboratory values. The range of laboratory values was wide and depended on the sequence of loading, the applied stress level, and consolidation. To isolate some of the variables present and reduce the data to a generalized

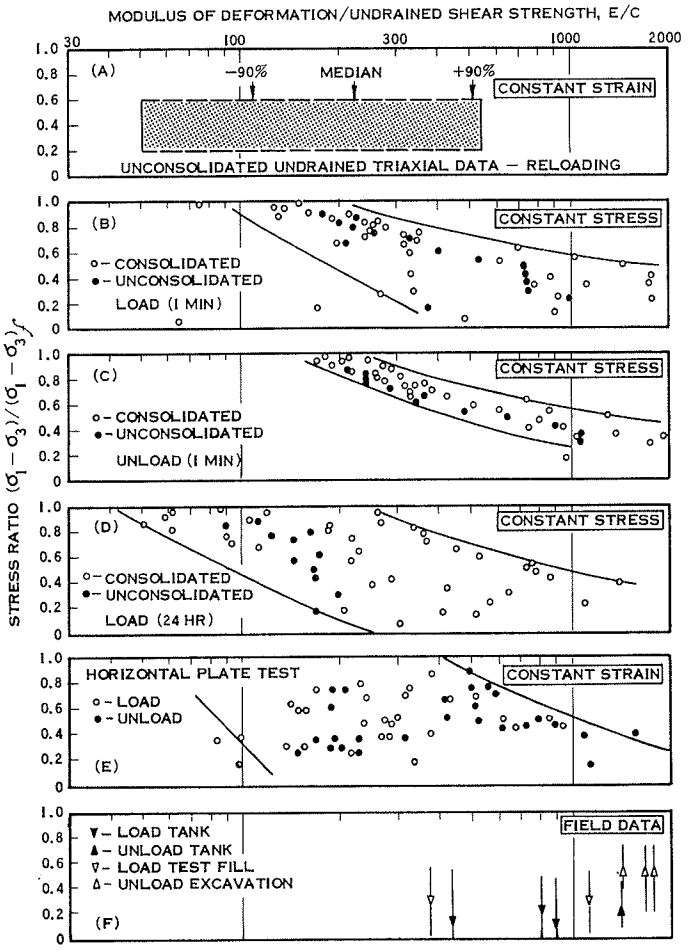

Figure 10. Comparison of field and laboratory-determined moduli.

form, the bulk of the test data was recompiled (Fig. 10). Six dimensionless plots of E/C against stress ratio are shown. (It should be noted that the data in Figure 10A refer to specimens from Shelby-tube samples, while the data in Figures 10B, C, and D refer to specimens trimmed from 12-in. cubes of soil carefully cut from the side of a deep excavation.) Figure 10A shows the routine test information obtained from over 200 unconsolidated undrained triaxial specimens reloaded once at a stress ratio about 0.5 ± 0.1. The median value and ± 90 percent range are indicated. Figures 10B, C, and D present the constant stress test information, showing the initial load values (Fig. 10B), the unloading data (Fig. 10C), and the 24-hr data (Fig. 10D). Upper and lower-bound envelopes have been drawn. The unconsolidated data are distributed throughout the consolidated data. Figure 10E shows the plate load test results. The lower graph (Fig. 10F) presents the field results obtained by taking an average undrained strength of 1500 psf for the soil profile. The stress ratio has been estimated from stability considerations and is approximate. The field data fall in two blocks, the loading results and the unloading results, with unload moduli somewhat larger than the load values. Comparison of the field data with the laboratory data shows the field results to be near the upper-limit laboratory results. Generally the constant stress tests are in better agreement with the field measurements than the constant strain tests. The importance of stress level is clearly evident when comparing test results.

It is believed that the elastic-plastic behavior of clay can account for the large range of modulus value determined by laboratory testing. On initial loading both elastic and plastic deformations occur. With increase in stress level the plastic component of deformation increases. Therefore modulus values determined by loading to high stress levels are less than those for loading to lower stress levels. Unloading causes a near-elastic rebound which gives a high modulus value. On reload the deformations are less than during initial loading but greater than the unload values. The marked reduction in modulus value obtained from the 24-hr reading shows creep to be significant. It is considered that the stress-controlled tests (1min reading) measure a near-elastic movement, particularly at low stress levels.

CONCLUSION

The summary of the field and laboratory-determined moduli shown in Figure 10 shows the laboratory triaxial test to underestimate the in-place modulus required for computing immediate ground movements. Several trends emerge—

1. Constant stress testing provides moduli values greater than constant strain testing, and the former are in better agreement with mass behavior than the latter.
2. Moduli determined from the loading and unloading part of the stress/strain relationship are different, the unloading value being the larger. Data inferred from the field movements show a similar trend.
3. The applied stress level had a marked influence, the modulus decreasing with stress ratio increase. This is believed to be due to the elastic-plastic behavior of soils.

ACKNOWLEDGMENT

Thanks are due to the Project Design and Construction Departments of the Generation Projects Division of the Hydro Electric Power Commission for their assistance with field installation and recording of data. The oil tank instrumentation was performed by the Applied Mechanics Section of the Structural Research Division.

REFERENCES

1. Rowe, P. W. The Stress-Dilatancy Relation for Static Equilibrium of an Assembly of Particles in Contact. Proc. Royal Soc. (London), Series A, Vol. 269, pp. 500-527, 1962.
2. Roscoe, K. H., Scoffield, A., and Wroth, C. P. On the Yielding of Soils. Geotechnique, Institution of Civil Engineers, London, Vol. 8, No.1, pp. 22-53,1958.
3. Hanna, T. H. Engineering Properties of Glacial-Lake Clays Near Sarnia, Ontario. Ontario Hydro Res. Quart., Vol. 18, No. 3, 1966.
4. Hanna, T. H., and Adams, J. I. Variation of the Engineering Properties of a Glacial-Lake Clay. (In preparation.)
5. Wu, T. H. Geotechnical Properties of Glacial Lake Clays. Jour. Soil Mech. and Found. Div., ASCE, Vol. 84, No. SM3, Proc. paper 1732, 1958.
6. Hanna, T. H. Discussion of Shear Strength Properties of Two Stratified Clays by Kwan Yee Lo and Victor Milligan. Jour. Soil Mech. and Found. Div., ASCE, Vol. 93, No. SM3, pp. 183-188, 1967.
7. Hanna, T. H. Discussion of The Elastic Properties of a Dense Glacial Till Deposit by E. J. Klohn. Canad. Geotech. Jour., Vol. 2, No. 2, pp. 129-131, 1965.
8. Bozozuk, M. The Modulus of Elasticity of Leda Clay From Field Measurements. Canad. Geotech. Jour., Vol. 1, No. 1, pp. 43-51, 1963.
9. Wilson, S. D., and Hancock, C. W. Horizontal Displacements of Clay Foundations. Proc. First Pan-American Conf. on Soil Mech. and Found. Eng., Mexico City, 1959.
10. Osterberg, J. O. Influence Values for Vertical Stresses in a Semi-Infinite Mass Due to an Embankment Loading. Proc. Fourth Internat. Conf. on Soil Mech. and Found. Eng., Vol. 1, pp. 393-394, London, 1957.

Comparison of Laboratory and Field Values Of c_v for Boston Blue Clay

LESLIE G. BROMWELL and T. WILLIAM LAMBE,
Massachusetts Institute of Technology

Laboratory values of c_{vs} (the coefficient of consolidation for swelling) for Boston blue clay are compared with the value back-figured from piezometer observations at a large building excavation. The field value is shown to be six times larger than the average laboratory value. Possible reasons for the large discrepancy between the laboratory and field values are sample disturbance, errors in laboratory test procedures, errors in field measurements, and three-dimensional consolidation effects. Of these four items, errors in laboratory test procedures, particularly the difficulty of measuring c_{vs} from oedometer tests, can contribute significantly to the discrepancy. In addition, it is shown that three-dimensional consolidation effects can account for the differences between laboratory and field values.

•SETTLEMENT predictions, although one of the most common tasks of the soil engineer, are subject to very large errors. Estimating rate of settlement is generally even more hazardous than estimating total settlement. This paper compares the laboratory value of c_{vs} (the coefficient of consolidation for swelling) for Boston blue clay with the value back-figured from piezometer observations at a large building excavation. The field data were taken under a program known as FERMIT (Foundation Evaluation and Research, M.I.T.), which is sponsored by the M.I.T. Office of Physical Plant. The building under study is the Julius A. Stratton Building, the M.I.T. Student Center.

DESCRIPTION OF FOUNDATION AND SUBSOILS

The M.I.T. Student Center is a five-story reinforced concrete frame structure. It was constructed on the west side of the campus during 1963-64. The location is shown in Figure 1. The building has a floating foundation and rests on a 3 to 10-ft thick concrete mat constructed on a sand-gravel layer.

Figure 2 shows the average soil profile at the site. The Boston blue clay, which is 60 to 75 ft thick in this area, is overconsolidated at the top (OCR~ 6). The amount of overconsolidation decreases with depth, and the bottom half of the clay is normally consolidated.

The results of extensive soil tests on the clay have been reported by Ladd and Luscher (1). The soil parameter of interest to this paper is the coefficient of consolidation for swelling, c_{vs}. Values of c_{vs} are shown in Figure 2 and are summarized in Table 1. Also given in Table 1 are values of c_{vc}, the coefficient of consolidation for compression. The values in Table 1 are averages of values computed by both the log time and the square root of time-fitting methods from 40 tests.

The average value of c_{vs} for the first stress decrement from the maximum past pressure, $\bar{\sigma}_{vm}$, is $60 \pm 30 \times 10^{-4}$ cm^2/sec. In addition, c_{vs} decreases with increasing OCR. For an OCR = 4, the average value of $c_{vs} = 30 \pm 10 \times 10^{-4}$ cm^2/sec. Thus, the upper layer of Boston blue clay, which is overconsolidated, should have a lower value of c_{vs}

Paper sponsored by Committee on Soil and Rock Properties and presented at the 47th Annual Meeting.

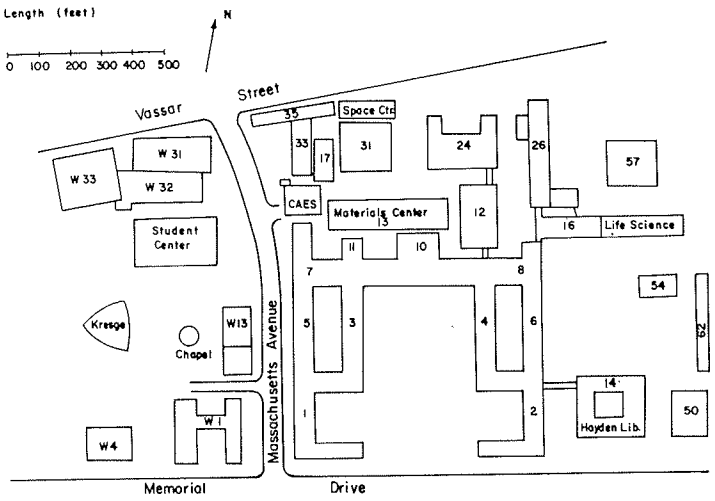

Figure 1. Plan of central M.I.T. campus.

than the normally consolidated clay. This variability in laboratory values of c_{VS} has not been considered in the analysis of the field data. The point is, however, that the large variability of laboratory values will in itself preclude the possibility of accurate rate predictions based on a few laboratory tests.

CONSTRUCTION HISTORY

A plan view of the foundation excavation is shown in Figure 3. The excavation was made in two stages:

1. Stage 1, from Elev. +22 to Elev. +15, during the period September 21-30, 1963. No dewatering was required during this excavation.
2. Stage 2, from Elev. +15 to Elev. +7.5, during the period October 7-16, 1963. Steady pumping from a well-point system located in the sand-gravel layer above the clay began on October 4 and continued throughout the stage 2 excavation.

The total vertical stress release from the excavation (Elev. +22 to Elev. +7.5) was about 0.82 kg/cm^2. The foundation mat, which constitutes about one-third of the structural dead load, was poured in four sections between November 23, 1963, and February 15, 1964.

TABLE 1

SUMMARY OF COEFFICIENT OF CONSOLIDATION DATA FOR BOSTON BLUE CLAY[a]

Coefficient	c_v, 10^{-4}cm^2/sec
1. Compression, c_{vc}, at $\bar{\sigma}_{vo}$	
Overconsolidated	40 ± 20
Normally consolidated	20 ± 10
2. Swelling, c_{vs}	
From $\bar{\sigma}_{vm}$ to $\frac{1}{2}\bar{\sigma}_{vm}$	60 ± 30
From $\frac{1}{2}\bar{\sigma}_{vm}$ to $\frac{1}{4}\bar{\sigma}_{vm}$	30 ± 10
From $\frac{1}{4}\bar{\sigma}_{vm}$ to $\frac{1}{8}$ or $\frac{1}{16}\bar{\sigma}_{vm}$	20 ± 10

[a]From Ladd and Luscher (1).

FOUNDATION INSTRUMENTATION

The foundation instrumentation at the Student Center included eight piezometers (Casagrande type), six heave roads, and a permanent benchmark. The locations of these instruments are shown in Figure 3. Several additional heave and settlement points were installed during later stages of construction. An observation well is located 100 ft north of the site.

CALCULATION OF FIELD c_{VS}

The measured pore pressures from piezometers 1 through 4 have been

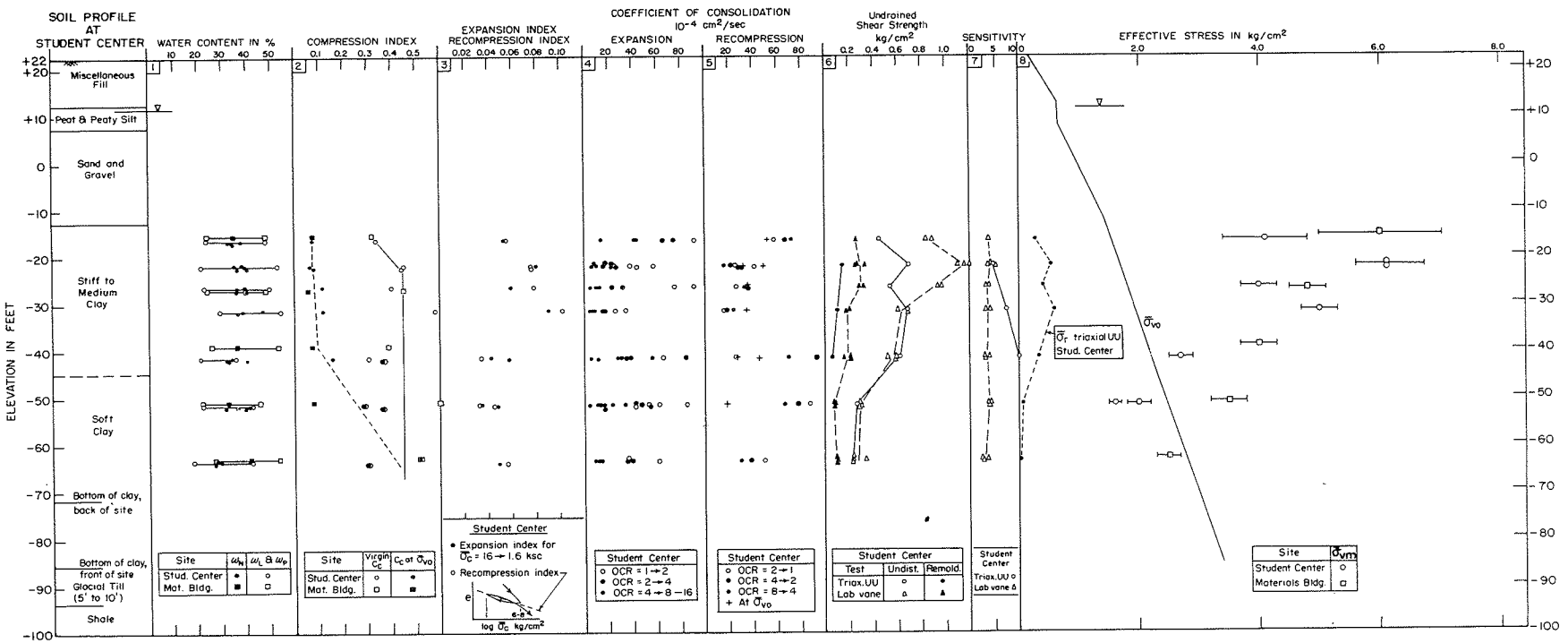

Figure 2. Typical soil test data for M.I.T. campus.

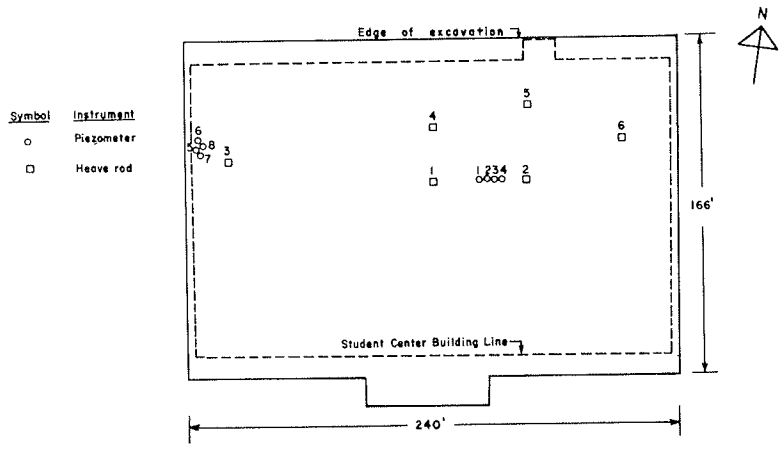

Figure 3. Dimensions of excavation.

used to compute a field value of c_{VS}. Figure 4 shows the location of these instruments in the clay layer. Figure 5 shows the measurements of pore pressures and vertical movements during foundation construction.

Figure 6 shows a plot of the measured negative excess pore pressures in the clay layer 15 and 105 days after excavation. The excavation and the dewatering were assumed to have occurred on October 7, the middle of the actual excavation period.

Also shown in Figure 6 are values of the initial excess pore pressures (t = 0) obtained by extrapolating the measured pore pressures at the end of excavation back to the middle of the excavation period. The values of initial excess pore pressure are quite close to $\Delta\sigma_V$, the change in vertical stress computed from elastic theory with $\nu = 1/2$.

Knowing the initial pore pressures at t = 0, and the equilibrium pore pressures at $t = \infty$, the measured values of pore pressure at any intermediate time can be used to compute a point value of U_Z, the percent consolidation. [The equilibrium pore pressures were taken as those resulting from steady state upward seepage due to pumping. The water table actually varied somewhat during excavation (as shown by the well-point data in Fig. 5). The average head drop in the sand-gravel layer due to pumping was -13 ft for t = 15 days and -10 ft for t = 105 days.] Using standard one-dimensional solutions (3), the time factor, T_S, can then be obtained. The time factor is related to the coefficient of consolidation by the following equation:

$$c_{VS} = \frac{T_S H^2}{t}$$

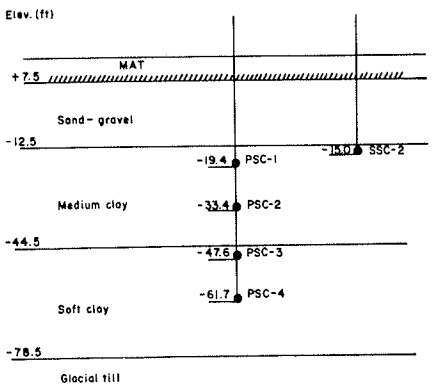

Figure 4. Location of piezometers.

The effect of errors in the assumed initial pore pressure distribution can be minimized by computing c_{VS} using the following equation:

$$c_{VS} = \frac{T_{S_2} - T_{S_1}}{t_2 - t_1} H^2$$

where T_{S_2} and T_{S_1} are the time factors at times t_2 and t_1, respectively.

This procedure led to an average field value of $c_{VS} = 350 \pm 50 \times 10^{-4}$ cm^2/sec. The agreement between the theoretical isochrone computed

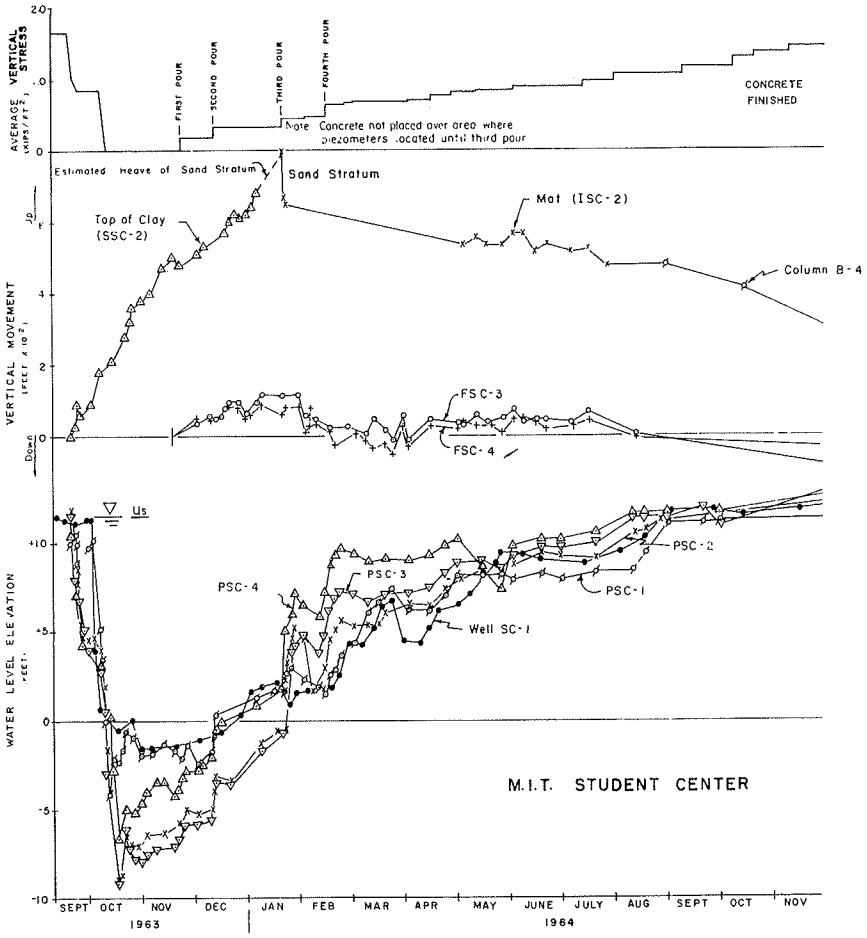

Figure 5. Pore pressures and vertical movements.

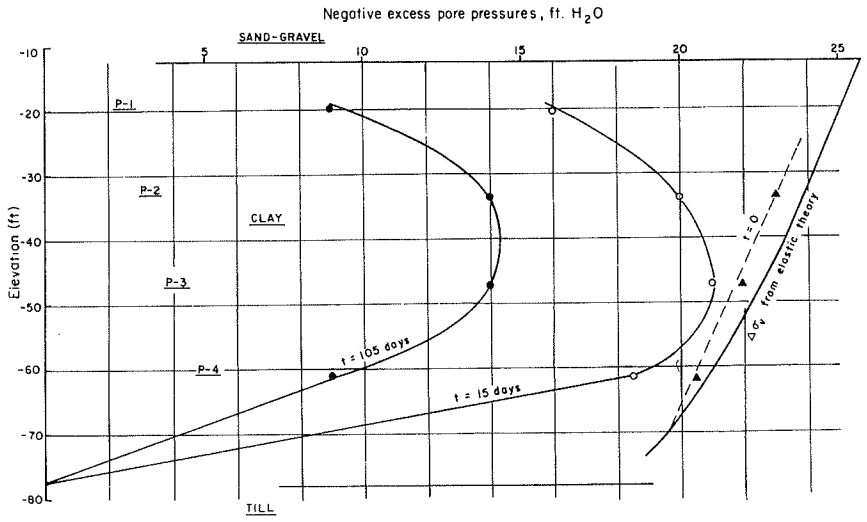

Figure 6. Measured pore pressures at 15 and 105 days.

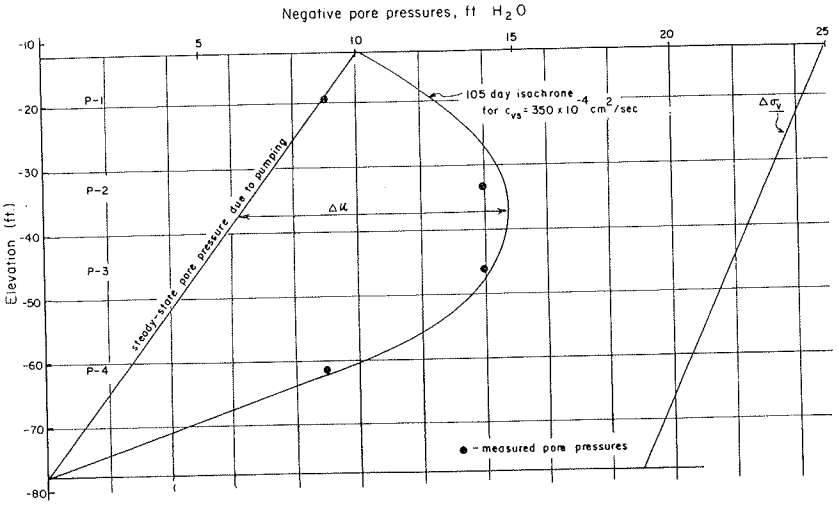

Figure 7. Measured and computed pore pressures after 105 days.

using this value of c_{vs} and the measured pore pressures at t = 105 days is shown in Figure 7. The agreement is quite good for the lower three piezometers. The top piezometer is much more sensitive to errors in the assumed steady-state pore pressures, which is probably why it does not show good agreement. The apparent field value of c_{vs} is about 6 times the average laboratory value. The remainder of the paper will discuss possible reasons for this discrepancy.

POSSIBLE CAUSES OF DISCREPANCY BETWEEN LAB AND FIELD VALUES

Possible reasons for the large difference between the average lab value of c_{vs} (60×10^{-4}) and the value back-figured from field data (350×10^{-4}) include the following:

1. Sample disturbance,
2. Laboratory test procedures,
3. Errors in field measurements, and
4. Use of one-dimensional consolidation theory.

Effect of Sample Disturbance

Disturbed soil samples give lower values of c_v. Taylor (2) showed a 40-fold decrease in c_v after remolding a sample of Boston blue clay. Sample disturbance is undoubtedly responsible for some of the scatter in c_v values shown in Figure 2.

A value of c_v corrected for disturbance can be obtained by estimating the effect of disturbance on k and a_v. The major change is the decrease in k resulting from the lower void ratio at any given consolidation pressure. A plot of e vs k can be used to estimate the magnitude of this effect. A corrected compression curve (4) can be used to obtain a better value of a_v. The new values of k and a_v can then be used to recompute an undisturbed c_v:

$$(c_v)_u = (c_v)_d \frac{k_u}{k_d} \frac{(a_v)_d}{(a_v)_u}$$

where subscript u refers to undisturbed conditions and subscript d refers to the disturbed laboratory sample.

Calculations using this procedure indicated that the effect of sample disturbance on the lab values of c_v is within the range of experimental error given in Table 1.

Laboratory Test Procedures

Lambe (5) discussed the differences in stress paths between laboratory tests and actual field conditions. In order to predict field behavior accurately, laboratory tests should in general follow the field stress path as closely as possible. However, this procedure will not, in general, provide accurate c_v data. For example, Lambe (6) described another M.I.T. building excavation (Center for Advanced Engineering Study), located across Massachusetts Avenue from the Student Center (see Fig. 1), where an oedometer test that duplicated the field vertical stress release gave a value of $c_{vs} = 3 \times 10^{-4}$ cm^2/sec. This value is a factor of 100 less than the value back-figured from field data.

Standard oedometer tests use a stress-increment ratio ($\Delta\bar{\sigma}/\bar{\sigma}$) of one. It has been shown that for smaller values of stress-increment ratio the Terzaghi consolidation theory does not apply (2, 7). However, the actual value of $\Delta\bar{\sigma}/\bar{\sigma}$ in the field is frequently less than one, and it varies with depth. A technique for correcting laboratory data to take this effect into account is not currently available. Hence, it is necessary to use a stress-increment ratio of one in laboratory tests in order to obtain c_v values that appear reasonable.

Another factor that influences the laboratory value of c_v is the curve-fitting method used. The $\sqrt{t}$ fitting method generally gives a value of c_v about 50 percent higher than the log t method for Boston blue clay (1). Values from the two methods were generally averaged to give the c_v values used in this paper.

The calculation of c_{vs} from oedometer tests is frequently difficult, because swelling curves tend to deviate much more from the theoretical time curves than do compression curves. Perhaps an equally valid procedure would be to calculate c_{vs} from measured values of c_{vc}, a_{vc}, and a_{vs}. If all of the values are chosen at the same average void ratio, then it can be assumed that k is the same for both compression and swelling without introducing a significant error. Then c_{vs} can be calculated as follows:

$$c_{vs} = c_{vc}\left(\frac{a_{vc}}{a_{vs}}\right)$$

Application of this procedure to the laboratory data on Boston blue clay yields an average value of $c_{vs} = 100 \pm 50 \times 10^{-4}$ cm^2/sec, almost two times higher than the average value calculated from time-swelling curves.

Errors in Field Measurements

The field value of c_{vs} relies on accurate piezometer data. The estimated accuracy of the measured pore pressures is ± 0.25 ft. The time lag for the piezometers is less than 24 hr for 90 percent equalization of pore pressure.

The assumed initial pore pressures may have been in error, although the distribution used is more likely to have underestimated the field c_{vs} than overestimated it.

Use of One-Dimensional Consolidation Theory

Most settlement problems are solved by use of the Terzaghi one-dimensional theory. Significant errors in rate of settlement predictions can result from this assumption. Rapid advances, using numerical methods, are being made in the application of three-dimensional consolidation theory to settlement problems. In the near future, the soil engineer may routinely use these three-dimensional analyses for settlement predictions. Solutions currently available can be used to estimate how much of the sixfold discrepancy between predicted and observed rates of pore pressure dissipation at the Student Center can be attributed to three-dimensional effects.

The importance of two- or three-dimensional drainage will increase as (a) the ratio of horizontal permeability to vertical permeability increases (k_h/k_v), and (b) the ratio of vertical drainage path to radius of loaded area increases (H/a).

The field permeability of Boston blue clay, measured by falling-head tests on piezometers, is 2-3 $\times 10^{-7}$ cm/sec, which is about 6 to 8 times greater than the vertical permeability measured on laboratory samples. To some extent the measured field permeability probably reflects the existence of thin silt seams that act as drainage layers.

Davis and Poulos (8) recommend using an average value of permeability to calculate a three-dimensional c_v:

$$k_{av} = \sqrt[3]{k_h^2 \, k_v}$$

The resulting equation for computing $(c_{vs})_3$ from measured oedometer values of $(c_{vs})_1$ is

$$(c_{vs})_3 = \frac{1}{3} \left(\frac{1 + \nu}{1 - \nu} \right) \frac{k_{av}}{k_v} (c_{vs})_1$$

Assuming $\nu = 1/3$, $k_h = 6 \, k_v$, and $(c_{vs})_1 = 60 \times 10^{-4}$ cm^2/sec; this gives an estimated in situ $(c_{vs})_3 = 130 \times 10^{-4}$ cm^2/sec.

In actuality, the Student Center excavation would not at first glance appear to have significant three-dimensional effects. The vertical drainage path is 33 ft and the equivalent radius is 112 ft, giving a value of $H/a = 0.29$. However, curves given by Gibson et al (9) indicate that the rate of settlement, even with these dimensions, may be twice as fast as predicted by one-dimensional theory. This calculation assumes that $k_h = k_v$. When the effect of anisotropic permeability is added, an "equivalent" one-dimensional c_{vs} of about 250 $\times 10^{-4}$ cm^2/sec is obtained. Considering the assumptions required to obtain this result, the rather close agreement with the field value must be considered fortuitous. However, it does indicate that three-dimensional consolidation effects may be able to account for the large discrepancy between laboratory and field values of c_{vs} at the Student Center.

The preceding analysis was made for one foundation, and is not intended to imply that the results are generally applicable. However, the authors hope that numerous such analyses, combined with advances in three-dimensional consolidation theory and advances in field measurements of soil properties will lead to better techniques for making settlement predictions.

CONCLUSIONS

1. Field rates of excess pore pressure dissipation measured in Boston blue clay gave a value of c_{vs} for swelling of 350 $\times 10^{-4}$ cm^2/sec, using a one-dimensional analysis.
2. Although the discrepancy cannot be definitely attributed to any one cause, three-dimensional drainage seems the most likely reason. The difficulty of obtaining an accurate value of c_{vs} from laboratory time-swelling curves appears also to be an important factor.

ACKNOWLEDGMENTS

The success of the FERMIT program is the result of numerous individual contributions. In particular, A. A. Gass (10) and K. C. de Fries-Von Arnim (11) studied the Student Center project for their graduate theses. Other present and former members of the M.I.T. staff who had prominent roles are Harry M. Horn (formerly Assistant Professor of Civil Engineering), Charles C. Ladd, L. A. Wolfskill, U. Luscher (formerly Assistant Professor of Civil Engineering), R. S. Ladd, W. R. Beckett, and N. F. Braathen. The M.I.T. Office of Physical Plant has provided continuous support and encouragement for FERMIT. Philip A. Stoddard, Vice-President, and William R. Dickson, Assistant Director of Physical Plant, have been especially helpful.

REFERENCES

1. Ladd, C. C., and Luscher, U. Engineering Properties of the Soils Underlying the M.I.T. Campus. M.I.T. Dept. of Civil Engineering Res. Rept. R65-58, Dec. 1965.
2. Taylor, D. W. Research on Consolidation of Clays. M.I.T. Dept. of Civil Engineering, Serial 82, Aug. 1942.
3. Lambe, T. W., and Whitman, R. V. An Introduction to Soil Mechanics, Ch. 27. John Wiley and Sons, Inc., in press.
4. Schmertmann, J. H. The Undisturbed Consolidation Behavior of Clay. Trans. ASCE, Vol. 120, p. 1201-1233, 1955.
5. Lambe, T. William. Stress Path Method. Proc. ASCE, Jour. Soil Mech. and Found. Div., Vol. 93, No. SM6, p. 309-331, Nov. 1967.
6. Lambe, T. William. The Behavior of Foundations During Construction. Proc. ASCE, Jour. Soil Mech. and Found. Div., Vol. 94, No. SM1, p. 93-130, Jan. 1968.
7. Leonards, G. A., and Girault, P. A Study of the One-Dimensional Consolidation Test. Proc. Fifth Internat. Conf. on Soil Mech. and Found. Eng., Vol. 1, p. 213-218, Paris, 1961.
8. Davis, E. H., and Poulos, H. G. The Analysis of Settlement Under Three-Dimensional Conditions. Symposium on Soft Ground Engineering, Brisbane, 1965.
9. Gibson, R. E., Schiffman, R. L., and Pu, S. L. Plane Strain and Axially-Symmetric Consolidation of a Clay Layer of Limited Thickness. Univ. of Illinois at Chicago Circle, MATE Rept. 67-4.
10. Gass, A. A. Comparison of Theoretical and Observed Performance of the M.I.T. Student Center Foundations. M.S. thesis in Dept. of Civil Engineering, M.I.T., 1964.
11. De Fries, K. S. The Prediction of Heaves and Pore Pressures Induced by Excavations in Clay. Civil Engineers thesis in Dept. of Civil Engineering, M.I.T., 1967.

Discussion

ROBERT L. SCHIFFMAN, University of Illinois at Chicago Circle—The authors are to be congratulated on pointing out the many factors that contribute to the discrepancy between laboratory and field values of c_v. They have noted that one of the reasons for differences between laboratory and field values of the coefficient of consolidation is the three-dimensional consolidation effect. It is to this general point that this discussion is directed.

The coefficient of consolidation, c_v, is defined (12) as

$$c_v = \frac{k}{\gamma_w m} \tag{1}$$

where k is a coefficient of permeability, m is the compressibility, and γ_w is the unit weight of water. For c_v to be theoretically the same in both the field and the laboratory, one of two conditions must be satisfied. First, if c_v were a fundamental soil property, its value would be independent of the measurement conditions. If c_v is not a fundamental soil property, then the same value can be expected theoretically only if the k and m were of the same magnitude in the laboratory and in the field. That is, if the boundary conditions in both the field and the laboratory were the same, one could expect k and m to theoretically have the same values. On the other hand, different boundary conditions would provide different values for k and m.

In the conventional oedometer test, the value of the coefficient of permeability is restricted to the vertical component k_v. For a natural soil, consolidated in a triaxial

device, or in the field, there are at least two values of the coefficient of permeability: the vertical permeability, k_v, and the horizontal permeability, k_h. Unless the soil is isotropic with respect to permeability there are, due to this effect alone, two possible coefficients of consolidation:

$$c_v = \frac{k_v}{\gamma_w m} \tag{2a}$$

for vertical flow of water, and

$$c_h = \frac{k_h}{\gamma_w m} \tag{2b}$$

for lateral flow of water.

The compressibility, m, is a factor that depends on the geometry of the loading and the boundary conditions, independent of the permeability. To show this, consider the consolidation of a clay layer of thickness h when the loading extends indefinitely on the surface (9). The governing consolidation equation is

$$\frac{k}{\gamma_w} \frac{\partial^2 u}{\partial z^2} = - \frac{\partial e}{\partial t} \tag{3}$$

where k is the coefficient of permeability, u is the excess pore pressure, and e is the dilatation of the soil skeleton. The dilatation is defined as

$$e = e_{xx} + e_{yy} + e_{zz} \tag{4}$$

where e_{xx}, e_{yy}, and e_{zz} are the normal strains of the soil skeleton.

Assume that the soil skeleton is elastic. Then the effective stress-strain relations are

$$Ee_{xx} = \sigma'_{xx} - \nu(\sigma'_{yy} + \sigma'_{zz}) \tag{5a}$$

$$Ee_{yy} = \sigma'_{yy} - \nu(\sigma'_{xx} + \sigma'_{zz}) \tag{5b}$$

$$Ee_{zz} = \sigma'_{zz} - \nu(\sigma'_{xx} + \sigma'_{yy}) \tag{5c}$$

where σ'_{xx}, σ'_{yy}, and σ'_{zz} are the normal effective stress components, and E and ν are Young's modulus and Poisson's ratio, respectively, of the soil skeleton.

The oedometer provides axially symmetric compression with frictionless sides. Thus, $\sigma'_{rr} = \sigma'_{zz}$. The stress-strain relations are

$$Ee_{rr} = (1 - \nu)\sigma'_{rr} - \nu\sigma'_{zz} \tag{6a}$$

and

$$Ee_{zz} = \sigma'_{zz} - 2\nu\sigma'_{rr} \tag{6b}$$

Since the lateral strain $e_{rr} = 0$, then

$$\sigma'_{rr} = \frac{\nu}{1 - \nu} \sigma'_{zz} \tag{7}$$

The dilatation, e, is equal to the vertical strain, e_{zz}, in the oedometer. Thus from Eqs. 6b and 7

$$e = \frac{(1 - 2\nu)\ (1 + \nu)}{E(1 - \nu)}\ \sigma'_{zz} \tag{8}$$

From the effective stress principle

$$\sigma_{zz} = \sigma'_{zz} + u \tag{9}$$

where σ_{zz} is the vertical total stress. Substituting the effective stress Eq. 9 into Eq. 8 and then into Eq. 3 results in

$$c_o\ \frac{\partial^2 u}{\partial z^2} = \frac{\partial u}{\partial t} \tag{10a}$$

where

$$c_o = \frac{kE\,(1 - \nu)}{\gamma_w(1 - 2\nu)\ (1 + \nu)} \tag{10b}$$

if the applied load intensity is time-independent. The coefficient c_o is the coefficient of consolidation for the oedometer.

The solution to Eq. 10a is of the form

$$u = u_o F\left(\frac{c_o t}{h^2},\ \frac{z}{h}\right) \tag{11a}$$

where the initial excess pore pressure, u_o, is

$$u_o = \sigma_{zz} \tag{11b}$$

The vertical strain is

$$e_{zz} = \frac{(1 - 2\nu)\ (1 + \nu)}{E(1 - \nu)}\ \sigma_{zz}\left[1 - F\left(\frac{c_o t}{h^2},\ \frac{z}{h}\right)\right] \tag{12}$$

and the settlement, ρ, is

$$e_{zz} = \frac{\partial \rho}{\partial z} \tag{13}$$

Then

$$\rho(t) = \frac{(1 - 2\nu)\ (1 + \nu)}{E\ (1 - \nu)}\ \sigma_{zz} \int_o^h (1 - F)dz \tag{14}$$

The degree of consolidation, U, is defined as

$$U = \frac{\rho\,(t)}{\rho(\infty)} \tag{15}$$

which becomes

$$U(t) = 1 - \frac{1}{h} \int_o^h F dz \tag{16}$$

Consider the consolidation under plane strain conditions. This is achieved by extending the width of a strip load indefinitely. Plane strain conditions are maintained in that the strain in the y direction is zero, or $e_{yy} = 0$. Then

$$\sigma'_{yy} = \nu(\sigma'_{xx} + \sigma'_{zz}) \tag{17}$$

The effective stress-strain relations become

$$Ee_{xx} = (1 - \nu^2)\sigma'_{xx} - \nu(1 + \nu)\sigma'_{zz} \tag{18a}$$

$$Ee_{zz} = (1 - \nu^2)\sigma'_{zz} - \nu(1 + \nu)\sigma'_{xx} \tag{18b}$$

The dilatation is

$$e = \frac{(1 + \nu)\ (1 - 2\nu)}{E}\ (\sigma'_{xx} + \sigma'_{zz}) \tag{19}$$

or, using the effective stress equation,

$$e = \frac{(1 + \nu)\ (1 - 2\nu)}{E}\ (\sigma_{xx} + \sigma_{zz} - 2u) \tag{20}$$

It can be shown that when the surface loading extends infinitely in all directions the total stress components are independent of time if the surface loading is static. Thus, substituting Eq. 20 into Eq. 3 results in

$$c_p \frac{\partial^2 u}{\partial z^2} = \frac{\partial u}{\partial t} \tag{21a}$$

where

$$c_p = \frac{kE}{2\gamma_w(1 - 2\nu)\ (1 + \nu)} \tag{21b}$$

The solution to Eq. 21a is

$$u = u_o F\left(\frac{c_p t}{h^2},\ \frac{z}{h}\right) \tag{22}$$

where the initial excess pore pressure, u_o, is

$$u_o = \left[\frac{\sigma_{xx} + \sigma_{yy} + \sigma_{zz}}{3}\right]_{\nu\, =\, 1/2} \tag{23}$$

Assume that, under plane strain, the clay layer rests on a frictionless base. Then the lateral total stress, σ_{xx}, is zero. Thus,

$$u_o = \frac{\sigma_{zz}}{2} \tag{24}$$

and

$$u = \frac{\sigma_{zz}}{2}\ F\left(\frac{c_p t}{h^2},\ \frac{z}{h}\right) \tag{25}$$

The consolidation settlement of the surface is

$$\rho(t) - \rho(0) = \frac{2(1 - 2\nu)\ (1 + \nu)}{E} \int_0^h \left[\frac{\sigma_{zz}}{2} - u\right] dz \tag{26}$$

and the degree of consolidation, $\overline{U}$, is defined as

$$\overline{U}(t) = \frac{\rho(t) - \rho(0)}{\rho(\infty) - \rho(0)} \tag{27}$$

Thus,

$$\overline{U}(t) = 1 - \frac{1}{h} \int_0^h F dz \tag{28}$$

Consider the consolidation of a layer under an axially symmetric loading. The effective stress-strain relations are given by Eqs. 6a and 6b. The dilatation is then

$$Ee = (1 - 2\nu)\ (\sigma_{zz} + 2\sigma_{rr} - 3u) \tag{29}$$

In this case, the load of indefinite extent is achieved by expanding the radius of a circular load to infinity. Thus Eq. 3 takes the form

$$c_r \frac{\partial^2 u}{\partial z^2} = \frac{\partial u}{\partial t} \tag{30a}$$

where

$$c_r = \frac{kE}{3\gamma_w (1 - 2\nu)} \tag{30b}$$

The solution is,

$$u = u_o F \left(\frac{c_r t}{h^2},\ \frac{z}{h}\right) \tag{31}$$

For a smooth-based layer the lateral stress, σ_{rr}, is zero. Then the initial excess pore pressure, u_o, is

$$u_o = \frac{\sigma_{zz}}{3} \tag{32}$$

Thus the consolidation settlement of the surface is

$$\rho(t) - \rho(0) = \frac{3(1 - 2\nu)}{E} \int_0^h \left[\frac{\sigma_{zz}}{3} - u\right] dz \tag{33}$$

The degree of consolidation, $\overline{U}$, is then

$$\overline{U}(t) = 1 - \frac{1}{h} \int_0^h F dz \tag{34}$$

Since Eqs. 16, 28, and 34 are identical in form, the relationships between the degrees of consolidation for the three cases considered follow from the relationship

between c_o, c_p, and c_r. That is, the time factor for a given degree of consolidation can be adjusted for case to case by a simple ratio of coefficients, or

$$\frac{T_o}{T_p} = \frac{c_o}{c_p} \tag{35a}$$

or

$$\frac{T_o}{T_r} = \frac{c_o}{c_r} \tag{35b}$$

in which

$$T_o = \frac{c_o t}{h^2} \tag{36a}$$

$$T_p = \frac{c_p t}{h^2} \tag{36b}$$

$$T_r = \frac{c_r t}{h^2} \tag{36c}$$

where T_o, T_p, and T_r are the time factors at the same degree of consolidation for the oedometer, the smooth-based layer under plane strain loading, and the smooth-based layer under an axially symmetrical loading, respectively. In the latter two cases, the load is extended to infinity in all directions.

Thus, for Poisson's ratio, ν, at zero,

$$T_p = \frac{T_o}{2} \tag{37a}$$

$$T_r = \frac{T_o}{3} \tag{37b}$$

The only time when these factors would be equal is the special case when the soil skeleton is incompressible ($\nu = 0.5$).

The foregoing analysis is based on a "one-dimensional" loading which extends indefinitely in all directions. The effect of a three-dimensional loading is given in Table 2. These results are taken from the solution of the three-dimensional consolidation problem for a clay layer of limited thickness (9). The surface is loaded by a uniform circular load of radius a. The layer, of thickness h, is assumed to have a frictionless base. The values in Table 2 are the oedometer time factors, T_o, for the given degree of consolidation, $\bar{U}$, Poisson's ratio, ν, and geometric ratio, a/h. The degree of consolidation, $\bar{U}$, has been calculated at the center of the load. The last values in the table are the time factors, T_o, for the usual one-dimensional theory (12).

TABLE 2

TIME FACTORS FOR AXIALLY SYMMETRIC CONSOLIDATION OF A SMOOTH-BASED LAYER

a/h	μ	$\bar{U} = 0.5$	$\bar{U} = 0.9$
0.1	0	2.0×10^{-3}	4.0×10^{-2}
	0.2	1.1×10^{-3}	2.4×10^{-2}
	0.4	3.4×10^{-4}	7.5×10^{-3}
1.0	0	1.5×10^{-1}	8.0×10^{-1}
	0.2	8.0×10^{-2}	4.7×10^{-1}
	0.4	2.4×10^{-2}	1.6×10^{-1}
10	0	4.5×10^{-1}	1.6
	0.2	2.5×10^{-1}	1.0
	0.4	8.5×10^{-2}	3.4×10^{-1}
∞	0	5.9×10^{-1}	2.5
	0.2	3.9×10^{-1}	1.7
	0.4	2.5×10^{-1}	1.1
	0.5	2.0×10^{-1}	8.5×10^{-1}

The field evaluation of the coefficient of consolidation depends on the theoretical

value of the time factor for a particular degree of consolidation. This value is a function of the geometric ratio, a/h. The time factor, T_O, for 50 percent consolidation and Poisson's ratio of 0.4 can vary by a factor of approximately 250 for a geometric ratio change of 100 (Table 2). For 90 percent consolidation the factor is approximately 45 for a geometric ratio change of 100. Thus, as expected, the higher the degree of consolidation, the closer the time factors. As pointed out by the authors, the three-dimensional effect will seriously influence the basis for evaluating the coefficient of consolidation.

This shows two of the many factors involved in the evaluation of the coefficient of consolidation. The first of these concerns the definition of this coefficient. It is seen that the coefficient of consolidation depends on the anisotropy of permeability and the definition of compressibility. This latter property depends on the nature of the surface loading and the boundary conditions of the clay layer. This means that the coefficient of consolidation is not a fundamental soil property. As such, values measured under different conditions will be different.

The second factor is the three-dimensional effect. That is, the curve-fitting at a specific degree of consolidation will have to be based on different time factors that depend on the effective stress-strain properties, the type of loading, the boundary conditions of the clay, and the load width to layer-thickness ratio.

All in all, even with perfect sampling, perfect field measurements, and perfect testing, there is no reason to expect that the coefficient of consolidation determined in the field and in the laboratory will be the same. In fact, they should be different.

Reference

12. Terzaghi, K. Die Berechnung der Durchlassigkeitsziffer des Tones aus dem Verlauf der Hydrodynamischen Spannungser-scheinungen. Akademie des Wissenschaften in Wein, Sitzungsberichte, Mathematish-naturwissenschaftliche Klasse, Part IIa, 132, No. 3/4, p. 125-138, 1923.

Consolidation Properties of an Organic Clay Determined from Field Observations

T. J. SCHMIDT, Delaware State Highway Department, and
J. P. GOULD, Mueser, Rutledge, Wentworth, and Johnston, New York, N.Y.

A program of observations of settlement and pore water pressures was undertaken in a soft organic silty clay for control of construction of a section of the Christina River Interchange of Delaware Interstate Routes I-95, I-495, and I-295 near Wilmington, Delaware. The roadway embankment was stabilized by use of vertical sand drains plus surcharge. Values of compression index and coefficient of consolidation computed from field observations were compared with laboratory test data. Undisturbed samples obtained at a later time when primary consolidation was largely complete were utilized to evaluate the gain in strength of the organic clay stratum. Conditions disclosed by field observations agreed reasonably well with those assumed for design.

•SOFT and compressible organic clay adjacent to the original course of the Christina River was stabilized by use of vertical sand drains plus surcharge in construction of the Delaware Interstate Highway routes south of Wilmington, Delaware. Numerous piezometers and settlement plates were installed early in the filling operations for control of construction and to determine when the surcharge loading had served its intended purpose. The observations permitted an evaluation of in situ properties of the organic clay, which could be compared to laboratory test values and design assumptions. The design, construction, observation program, and the results obtained are summarized herein. The stabilization was planned under contract with the Delaware State Highway Department by Moran, Proctor, Mueser, and Rutledge (now Mueser, Rutledge, Wentworth, and Johnston) of New York, engaged in a joint venture with J. E. Greiner Company of Baltimore for design of the Christina River Interchange.

SUBSOIL CHARACTERISTICS

The subsoil to be stabilized is a soft-to-medium dark gray organic silty clay with scattered vegetal matter. It is classified as OH material in the Unified Soil System with liquid limits between 65 and 100 and plasticity index about 8 points below the A-line. It is fairly typical of estuarine deposits formed in the lower reaches of slow-flowing streams on the Atlantic coastal plain. It was probably laid down in post-Pleistocene times as a result of the drowning of the stream valley by a 25- to 35-ft rise in sea level from a postglacial low water stage about 6,000 years ago. Before construction the surface of the deposit was several feet above sea level, and the material appears to have been overconsolidated by about 750 lb/sq ft in excess of overburden pressure. This was probably caused by a temporary low sea level stage at some time since deposition. There is no evidence of the existence of a greater height of overburden in the past. The surface material is not notably stiffened by desiccation but contains a concentration of vegetal matter in some locations. It is underlain by compact to very compact Pleistocene sands, followed by cretaceous coastal plain sediments.

The boring exploration program for design included recovery of a large number of 3-in. undisturbed samples obtained with a fixed-piston device, plus use of the Swedish

Paper sponsored by Committee on Soil and Rock Properties and presented at the 47th Annual Meeting.

foil sampler and vane shear equipment. The average initial properties of the organic silty clay, determined from field and laboratory tests, are listed in Table 1. Consolidation tests on the best quality undisturbed samples showed a drastic decrease in c_v values in a ratio of at least 5 to 1 between the recompression and virgin compression ranges of pressures. Shear strengths generally increased linearly with depth. The division of strength values at 7 ft depth in Table 1 is merely a convenience for analysis.

DESIGN

Stabilization was planned for sand drain plus surcharge in three separate sections, totaling 2 mi in length, where the highway embankment was to overlie a considerable thickness of organic soils. The two sections with the greatest thickness of organics, averaging 25.5 ft, controlled the overall stabilization requirements. Sand drains were 16-in. diameter, spaced at 7 ft center to center in triangular array, driven by displacement methods through 3 ft of sand drainage blanket and 1-ft working mat to the underlying Pleistocene sands. The average total height of fill required was 14 to 15 ft, measured from original ground surface to the bottom of the pavement base course. The average nominal height of fill plus surcharge chosen for design was 24.5 ft, including about 10 ft of surcharge without considering settlement.

A total surcharge loading period of not less than 400 days was computed as necessary at the least favorable cross section to eliminate primary consolidation plus one cycle of secondary compression under the final roadway embankment plus pavement. This required completion of an average of about 90 percent of primary consolidation under full surcharge, expressed in terms of effective stress transfer, or about 95 percent in terms of void ratio decrease or settlement. A vertical coefficient of consolidation of 0.03 sq ft/day was selected as a reasonably conservative value for design from the results of 21 consolidation tests, performed in the conventional manner with vertical double drainage. The selection disregarded the much higher coefficients exhibited in the recompression range of loading, but was somewhat larger than the lowest coefficients obtained at the highest applied pressures. This number was utilized in design without considering a possible higher horizontal coefficient or the effect of disturbance and smear due to driving drains, factors which were considered to be roughly balancing in their effect.

Based on an average initial shear strength of 350 lb/sq ft, stabilizing berms were designed to provide a safety factor of not less than 1.25 against shear failure during construction, including a conservatively selected gain in strength during placing of the fill. The berms ranged from about 120 to 200 ft in width and 9 to 18 ft in thickness. The rate of filling in sand drain sections was limited in the construction specifications to a maximum of 1 ft of height of fill placed per week in order to conform to the rate of gain of shear strength required for stability.

TABLE 1

IN SITU PRECONSTRUCTION PROPERTIES OF ORGANIC SILTY CLAY STRATUM

Index Properties
Unified soil classification: OH
Natural water content = 84%
Liquid limit = 84
Plastic limit = 46
Plasticity index = 32
Specific gravity = 2.61
Void ratio = 2.2
Dry unit weight = 51 pcf
Saturated unit weight = 94 pcf
Initial degree of saturation range = 97 to 100%
Consolidation Characteristics
Average effective overburden pressure for complete submergence = 400 psf
Probable average preconsolidation = 1150 psf
Overconsolidation = 750 psf in excess of submerged overburden pressure
Average virgin compression index, C_c = 0.95
Typical coefficient of consolidation in virgin compression range, c_v = 0.03 sq ft/day = 3×10^{-4} cm^2/sec
Typical coefficient of consolidation in recompression range = 0.2 sq ft/day = 2×10^{-3} cm^2/sec
Shear Strength Characteristics
In situ shear strength = 250 psf in upper 7 ft, 400 psf below 7 ft depth
Average shear strength for design = 350 psf
Angle of shearing resistance from drained shear tests = 27°
Angle of shearing resistance for consolidated undrained shear above the preconsolidation stress = 16°
Sensitivity = 3 to 4

CONSTRUCTION

Construction operations began with placement of sand blanket and temporary settlement plates. Sand drainage blanket material was pumped at an average rate of 350 cu yd/hr by a stationary dredge from a collection sump

pit which was filled by borrow excavated in the dry. The 11 percent passing the No. 200 sieve in the dry borrow was reduced to an average of 1.5 percent in the hydraulic placing operations. The contractor elected to make the 1-ft working mat of the same material as the sand drainage blanket. Vertical sand drains were installed from the working mat using a 16-in. outside diameter closed-end mandrel driven by a Vulcan OR hammer. A total of 24,300 separate vertical drains were placed amounting to 700,000 lineal ft of drains, averaging 29 ft per drain. As driving of sand drains progressed, collector pipes were laid and drainage windrows were installed within the blanket at right angles to the collector pipes. Fill material for the roadway embankment ranged from a coarse-to-fine sand with some gravel to a sandy silt, placed at an average field moisture content of 10.7 percent in 8-in. lifts and compacted by vibratory sheepsfoot rollers to an average dry density of 120.4 lb/cu ft.

Certain stabilizing berms were placed hydraulically and consisted of disposal material obtained by dredging unsuitable soils in other embankment areas. Elsewhere, berms were placed in the dry by truck dumping. During the first winter of construction, 1962-63, filling was suspended when it had reached an average of about two-thirds of the final total height. The construction sequence is summarized as follows:

1. Sand blanket placed—February, May, and June 1962;
2. Sand drains driven—April to September 1962;
3. Embankment fill placement started—July to October 1962;
4. Winter suspension—December 1962 to April 1963;
5. Fill complete to the top of surcharge—May to August 1963;
6. Surcharge removal commenced—February 1965.

OBSERVATION PROGRAM

A total of 43 Casagrande-type porous-stone piezometers were installed at 17 locations during the initial stages of construction with 97 settlement plates of various types. Piezometers were placed in boreholes made from the working mat after driving sand drains. Piezometers were positioned within the compressible stratum on a vertical line midway between drains in groups of three to a boring, located at center and quarter points of the thickness of layer. Stones were sealed from each other by bentonite. Observations of pore water pressures did not commence until at least several weeks following driving of sand drains in the immediate vicinity. Certain individual piezometers or observation wells were added in the upper sand blanket material and in the underlying compact Pleistocene sands.

Some settlement plates were placed on top of the sand blanket and attached to the riser pipe that carried piezometer plastic tubing through the fill. Other settlement plates were installed at or near the base of the sand blanket so that generally a complete record of movement is available from the beginning of filling operations.

Piezometers serve the dual purpose of controlling the rate at which height of fill increased and of determining progress of consolidation prior to removing surcharge. Although the piezometers functioned satisfactorily in the first 8 months, many of the lower and middle piezometers were rendered inoperative when the surface settlement exceeded about 2 ft and the differential settlement between surface and piezometer stone was about 1 ft. In planning for instrumentation on future contracts, it is hoped to avoid this condition by placing one piezometer per borehole, leaving casing around the plastic tubing lines, and by employing a double-tubing Casagrande piezometer of the type recently used successfully by the Port of New York Authority in similar compressible soils.

During May and June 1964, 11 replacement piezometers were installed at six locations at the center of the organic stratum as substitutes for those damaged at critical locations, placed midway between drains and one space removed from the original piezometers. Undisturbed samples were obtained in the borings for the replacement piezometers and particular attention was paid to recovering samples precisely at the piezometer elevation.

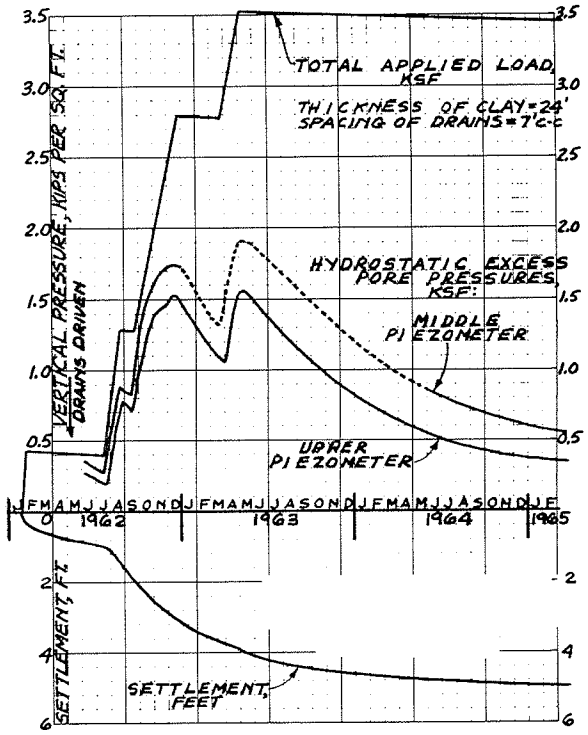

Figure 1. Loads, pore pressures, and settlements—piezometers 2 and 2A.

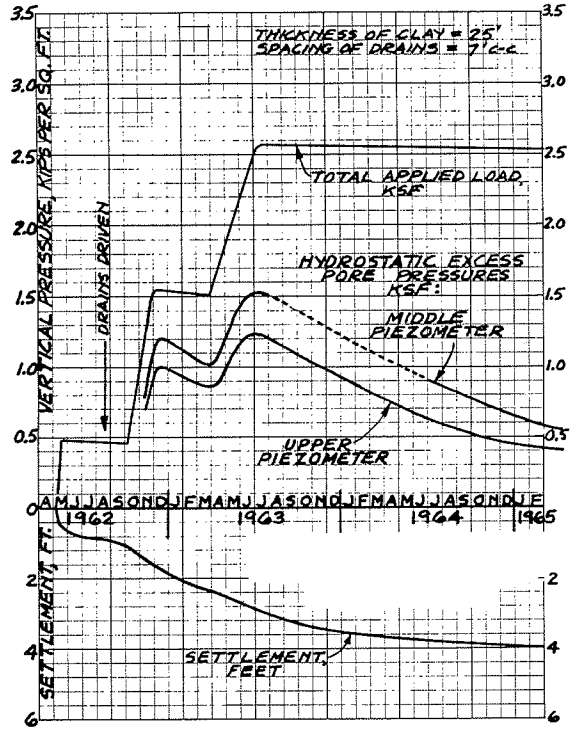

Figure 2. Loads, pore pressures, and settlements—piezometers 11 and 11A.

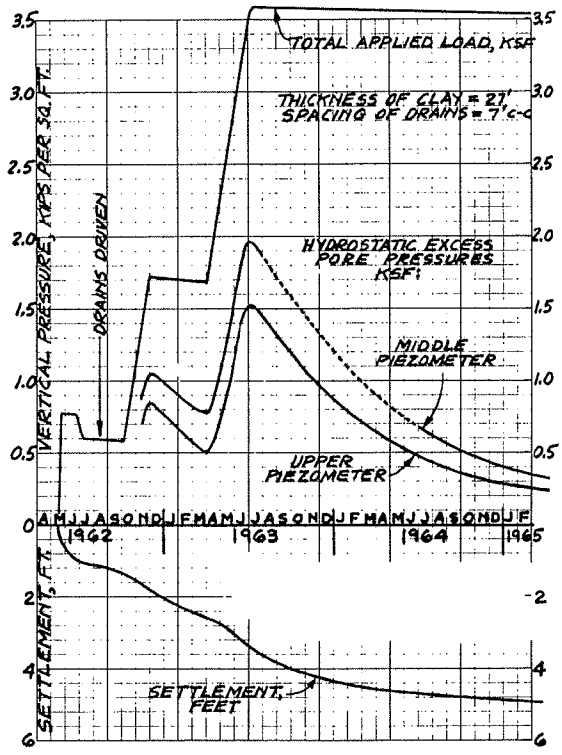

Figure 3. Loads, pore pressures, and settlements—piezometers 13 and 13A.

SUMMARY OF FIELD OBSERVATIONS

Three sets of piezometer and settlement observations taken at locations of thick organic clay and relatively high pore pressures are shown in Figures 1, 2, and 3. Piezometer readings are plotted as kips per square foot of hydrostatic excess pore water pressures, compared to the total applied pressure of fill including sand blanket, permanent fill, and surcharge. The dashed section of the pore pressure record is that interval when middle and lower piezometers were inoperative and the record is interpolated to June or July 1964 when the replacement piezometers were under observation. The small decrease in applied load in periods following placing of fill is due to settlement of the base of fill below the upper water table.

The progress of primary consolidation taken at various dates in the stabilization program, in terms of settlement, effective stress increase, and void ratio decrease, is listed in Table 2. While the history of pore

TABLE 2

PROGRESS OF PRIMARY CONSOLIDATION DETERMINED FROM FIELD OBSERVATIONS

Property	Initial Conditions Jan. 1962	Completion of Fill May-July 1963	Final Sampling June 1964	Surcharge Removal Feb. 1965	100% Consolidation Under Surcharge
Thickness of clay stratum, ft	25.5	21.8	21.1	20.85	20.7
Measured settlement, ft	—	3.7	4.4	4.65	4.8 (Theoretical)
Decrease in void ratio	—	0.46	0.55	0.58	0.60
Void ratio	2.20	1.74	1.65	1.62	1.60
Total applied load, ksf	—	3.4	3.4±	3.4±	3.4±
Observed maximum hydrostatic excess, ksf	—	1.9	0.8	0.5	0.0
Average hydrostatic excess, ksf	—	1.1	0.4	0.25	0.0
Average percent primary consolidation, stress basis	—	68	88	93	100
Average percent primary consolidation, settlement basis	—	77	92	97	100

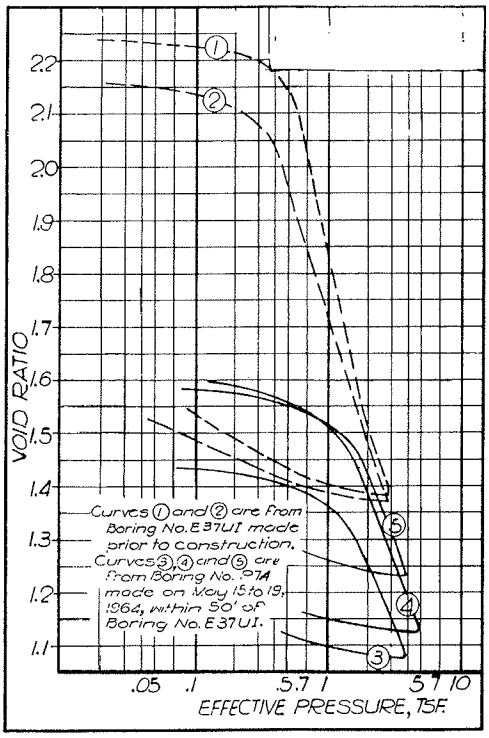

Figure 4. Consolidation curves, before construction and during stabilization.

pressure buildup varied with the sequence of load application, the maximum hydrostatic excess midway between drains and at midheight of the thick clay layer was fairly consistent at 55 to 60 percent of the total applied load at the completion of fill in May to July 1963. The average hydrostatic excess at this time was about 32 percent of total applied load, and completed primary consolidation averaged 68 percent of the ultimate under full surcharge, in terms of effective stress transfer. In a number of locations the pore pressures at the middle of the layer and at the lower quarter point were roughly equal, whereas pore pressures at the upper quarter point averaged about 0.3 kip/sq ft less than those measured lower in the layer. Pore pressures at the lower quarter points are not plotted in Figures 1, 2, and 3.

At the end of the 400-day minimum surcharge period in September 1964, the maximum hydrostatic excess averaged 0.7 kip/sq ft, about 21 percent of total applied pressure. The overall primary consolidation averaged about 89 percent of ultimate, in terms of effective stress transfer. In February 1965 the maximum hydrostatic excess was 0.5 kip/sq ft, about 16 percent of total applied pressure, and consolidation averaged about 93 percent of the ultimate. The amount of load to be removed in excavation of the surcharge after settlement averaged about 0.9 kip/sq ft, and it was determined that surcharge could be removed at any time after November 1964. Surcharge removal commenced in February 1965 and subsequent measured settlements have been insignificant. The numerous alignment stakes indicated that horizontal movements during construction did not exceed several tenths of a foot and were everywhere within tolerable limits.

No complete information was obtained as to the maximum pore water pressures developed by displacement driving of sand drains. Readings taken at certain piezometers several weeks after driving of drains indicated that the pore pressures built up by displacement stresses amounted to no more than about 6 to 8 ft of water or 400 to 500 lb/sq ft, midway between drains, and that the excess pressures had dissipated in about one month after driving. These relatively low pressures could be explained by the presence of free gas in the organic soils. The gas content is indicated by the large immediate settlement after placing the sand blanket. In any case, the average weight of overburden and fill in excess of original groundwater pressures was about 0.8 kip/sq ft at the time of drain driving and the maximum pore pressures caused by displacement probably were limited by this weight.

FINAL LABORATORY TESTING PROGRAM

Thin-tube undisturbed samples were obtained by fixed-piston sampler in each of the borings made for the six replacement piezometers installed in June 1964. Twelve consolidation tests and 51 unconfined compression tests were performed on these samples to compare with tests for the design investigation and with field performance data. A comparison of typical consolidation tests performed on samples before construction and on samples of June 1964 is shown in Figure 4. It can be seen that the tests on samples

TABLE 3

INCREASE IN SHEAR STRENGTH DURING SAND DRAIN STABILIZATION

Condition	Effective Vertical Stress, psf	Average Test Value of Shear Strength, psf	Ratio of Strength to Effective Vertical Stress, c/p
Initial conditions, Jan. 1962	400	350	Not Valid
Preconsolidation conditions, Jan. 1962	1150	350	0.30
Final sampling, June 1964	3200	920	0.29
Increase over preconsolidation condition, Jan. 1962 to June 1964	2050	570	0.28

of June 1964 exhibit void ratio-pressure curves which continue the trend established in the range of virgin compression by the preconstruction testing. The original test curves were concave upward in the manner expected of good quality undisturbed samples.

The average moisture content of the June 1964 samples equaled 62 percent, compared with 84 percent for the preconstruction test samples. This decrease in moisture content is consistent with a decrease in void ratio of 0.55, computed from the average settlement of 4.4 ft observed in June 1964 (Table 2).

Shear strengths obtained from the 51 unconfined compression tests of June 1964 ranged from 750 to 1250 lb/sq ft and averaged 920. This meant that consolidation to June 1964 had provided a strength increase of 570 lb/sq ft beyond the preconstruction strength of 350. The average effective stress at the strength test sample locations in June 1964 was interpreted as 3200 lb/sq ft from the pore pressure observations. This amounted to an increase of 280 lb/sq ft over the initial overburden pressure, or 2050 lb/sq ft above the preconsolidation stress. The original ratio of strength to vertical pressure (c/p ratio) and the final and incremental ratios are given in Table 3. All values equal approximately 0.3. By contrast, the c/p ratio obtained by analysis of slides in similar Atlantic Coast estuarine materials, where the ground spreads and horizontal pressures are lower than at-rest values, is typically about 0.25. The combined effect of disturbance and high pore pressures ordinarily produced by displacement driving would be expected to greatly decrease shear strength around the drains, at least in the early stages of the consolidation process. However, the damage to strength appears to be compensated by compression at high effective stress.

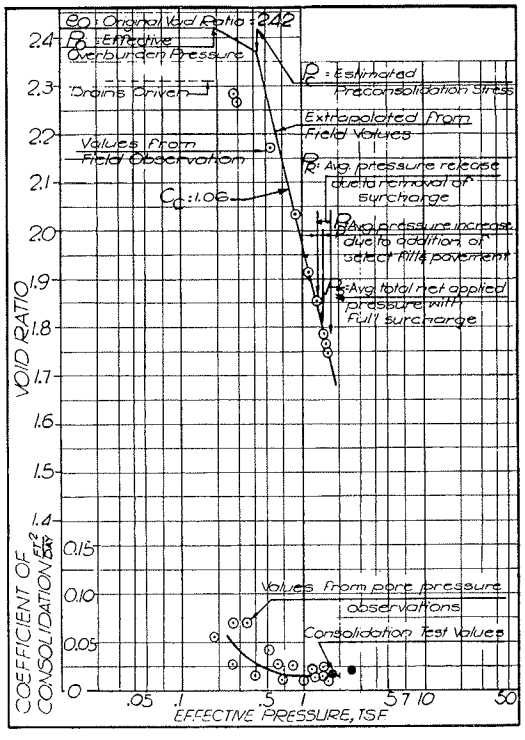

Figure 5. Comparison of field and laboratory data, piezometers P2 and P2A.

CONSOLIDATION CHARACTERISTICS

Figures 5 through 10 compare the laboratory consolidation tests of June 1964 at the six replacement piezometer locations with consolidation properties determined from field observations at the same locations.

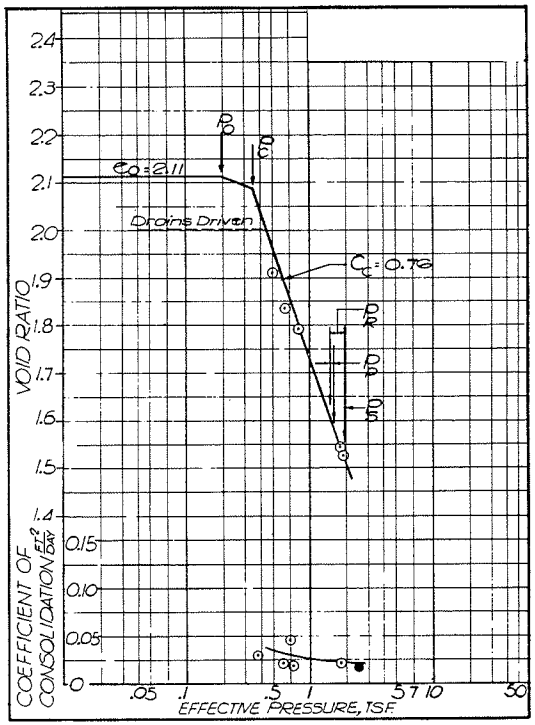

Figure 6. Comparison of field and laboratory data, piezometers P5 and P5A.

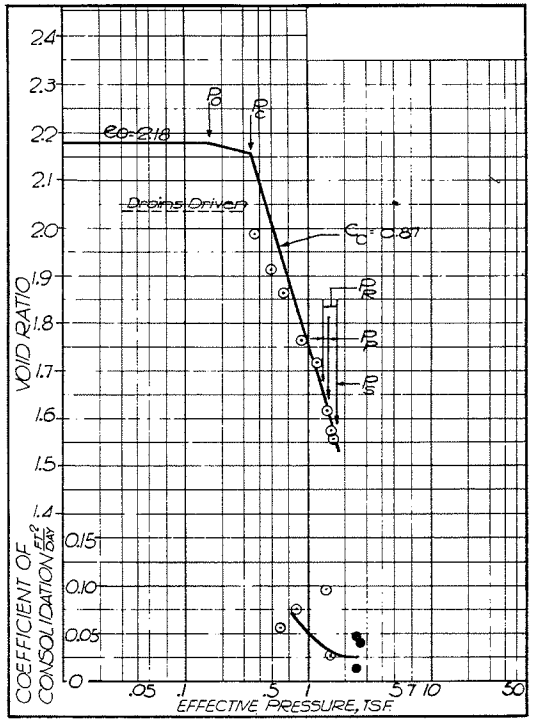

Figure 7. Comparison of field and laboratory data, piezometers P7 and P7A.

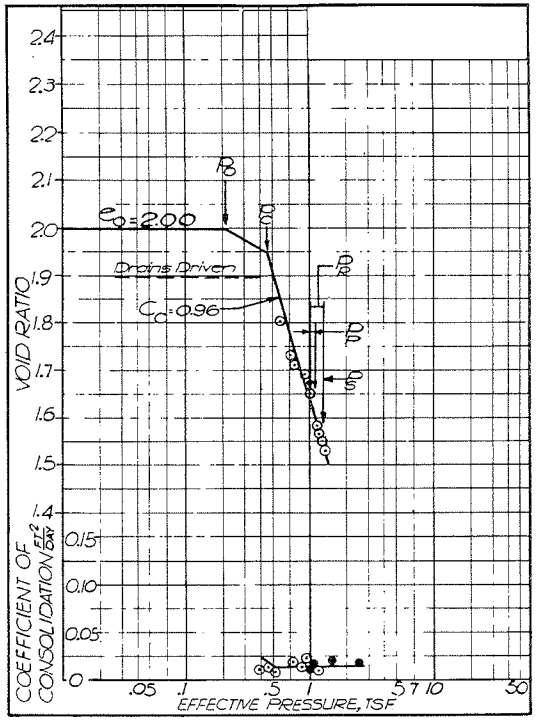

Figure 8. Comparison of field and laboratory data, piezometers P11 and P11A.

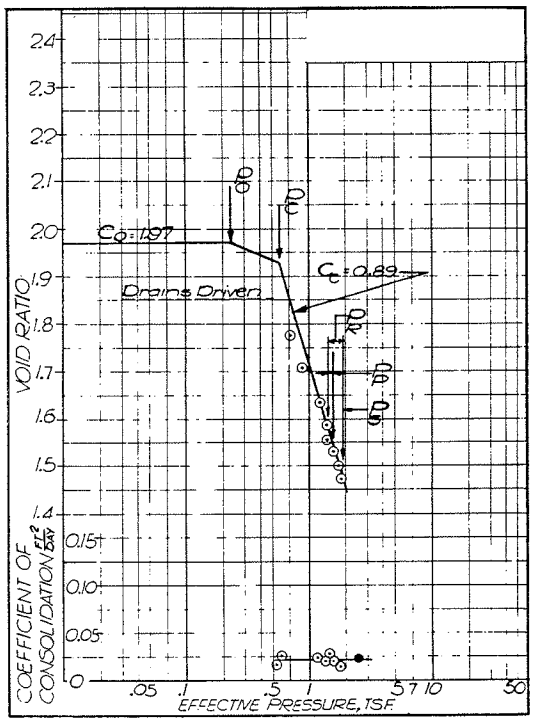

Figure 9. Comparison of field and laboratory data, piezometers P13 and P13A.

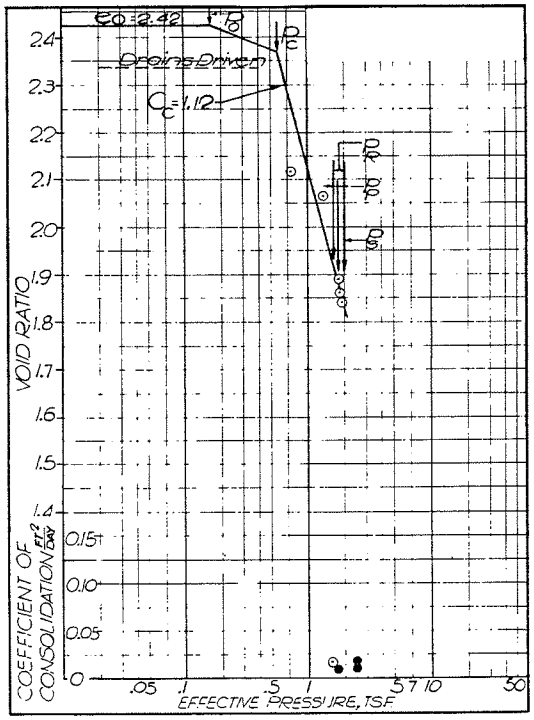

Figure 10. Comparison of field and laboratory data, piezometers P15 and P15A.

In the lower panel of each Figure the coefficient of consolidation computed from observed pore pressure dissipation is plotted with values computed from the June 1964 tests in the higher pressure ranges. Field values, indicated by open circles, are point values computed for individual piezometers from the decrease in excess pore pressure during periods of constant load, assuming radial drainage to sand drains and ignoring smear and disturbance. The laboratory test values, indicated by solid circles, were obtained from conventional tests with vertical double drainage.

In certain locations, where pore pressures could be evaluated in the recompression range of loading, field values show a marked reduction of consolidation coefficient from the recompression to the virgin compression range. However, this difference is not as great as in the original laboratory tests, where the ratio of c_v values was at least 5 to 1. At the higher pressure range, field c_v and laboratory test values correspond fairly well, varying from 0.013 to 0.025 sq ft/day and averaging 0.017 sq ft/day. These are to be compared with the c_v of 0.03 sq ft/day assumed for design as an average throughout the entire pressure range. The difference is undoubtedly due in part to disturbance caused by displacement driving.

The upper panels in Figures 5 through 10 represent a reconstruction of the field compression curve, derived in the following manner: The observed hydrostatic excess pressures were plotted in profile on the vertical line at the piezometer locations for a series of dates during the observation program. The average pore pressure on this line midway between drains was corrected to reflect lower pore pressures near the drains. The average effective stress at this date was obtained by subtracting the average pore pressure from overburden plus applied load. The void ratio at corresponding dates was obtained by subtracting the void ratio decrement, computed from observed settlements, from the original average test value of void ratio at this location. The corresponding void ratio vs effective pressure points are plotted as open circles. The straight line for virgin compression is extrapolated backward from the circled values at higher pressures, ignoring the concave upward shape of the laboratory test curve. The straight line segment in the recompression range is estimated from the laboratory tests, extending from initial overburden pressure to intersect the virgin slope at the apparent preconsolidation stress.

As a further check the estimated ultimate primary settlement was obtained by extrapolating the field log time vs settlement curves and verified by the square root of time method. The corresponding void ratio when plotted against the average total net applied pressure with full surcharge load gives a point that is in very close agreement with the field compression curve.

It can be seen that the circled field values fall below the extrapolated virgin compression straight line at lower pressures in the manner of disturbed laboratory consolidation test curves. The reconstructed C_c values range from 0.76 to 1.12 and the average slope of the straight-line virgin compression line equals 0.94, compared to the design value of 0.95. Such a close agreement must be considered fortuitous, based on the chance similarity of materials utilized in the comparison. It appears that although disturbance in sand drain driving lowers the equilibrium void ratio for the initial loading, it does not significantly alter the void ratio reached at much higher pressures.

Various stress conditions are indicated on the reconstructed field compression curves in Figures 5 through 10, as follows:

P_o = initial effective overburden;

P_c = preconsolidation stress;

P_s = load under full surcharge;

P_R = load decrement on removal of surcharge; and

P_p = load increment on addition of base course and pavement.

CONCLUSIONS

This study is intended to provide a comparison between laboratory design values and soil properties determined from field observations relative to primary consolidation of

a soft organic clay. The raw measurements from field observation programs, which are presented merely as time curves of settlement or pore pressures, are only of passing interest in that form. Utility for future designs requires an analysis of observations to derive from them parameters of significance to the design problem.

1. The evidence indicates that the effect of displacement driving of sand drains in this particular case is less than has frequently been reported, probably because of the cushioning effect of free gas within this organic soil.
2. The value of the c/p ratio deduced from the strength increase during stabilization equals about 0.3 compared to the ratio of 0.25 which has been evidenced in shear failures of similar estuarine deposits. Evidently the inevitable damage to strength by displacement driving has been compensated by compression at high effective stress.
3. The final total settlement can be computed with reasonable accuracy from conventional tests on undisturbed samples in the situation where loading extends far into the virgin compression range. Displacement driving of drains appears to have increased the amount of settlement in the early stages of load transfer without altering the final equilibrium void ratio under high loads. The increased early settlements may result from a combination of driving disturbance, gas contained in the organic soil, and a higher c_v value in the recompression range of loading. Whatever the cause, a c_v value computed from this rapid early settlement record cannot be utilized alone to extrapolate rates of consolidation and times for surcharge removal.
4. Disturbance by displacement driving appears to reduce substantially the high c_v values in the recompression range determined from laboratory tests. However, the c_v values under larger loads well within the virgin compression range appear to be little altered by this field condition.
5. At the present state of knowledge, a precise sand drain design employing a carefully determined ratio of vertical and horizontal coefficients of consolidation with an allowance for smear or disturbance is difficult to justify for organic soils of the type tested here and for conventional methods of installation. The procedure utilized in this design, wherein an average vertical coefficient of consolidation is utilized with no allowance for smear, appears appropriate. However, the c_v value must be selected conservatively, generally disregarding in the selection the higher coefficients given in the recompression range by better quality laboratory tests.

In Situ Permeabilities for Determining Rates of Consolidation

WILLIAM G. WEBER, JR., W. G. Weber and Associates, Inc., Sacramento, Calif.

This paper presents the use of an in situ permeability test to predict the rate of consolidation of foundation soils. The test method is described and the method of calculation presented. The sources of error in performing the test are discussed. The in situ permeability is used to estimate the rate of settlement on several projects. The rate of settlement as estimated using the in situ permeability agreed with the rate measured by settlement platforms. Using the data from the consolidation tests, the rate of settlement frequently varied from the measured rate of settlement. This relationship was found to exist in a wide range of foundation soil types.

•THE rate of consolidation of foundation soils is a difficult item to estimate during the design of embankments. However, the effectiveness of sand drains, the required height of overloads, and the duration of overloads are determined from the rate of consolidation. Thus, for design studies of embankments constructed upon yielding foundations, a reasonable estimate of the rate of consolidation becomes necessary.

A common method of determining the rate of consolidation is by the use of the data from the consolidation test. The rate may be estimated from the time consolidation curves using the relation that the time is a function of the square of the drainage path. In the work at the California Division of Highways this has proved to be an approximation at best. Another method is to determine the time for a given percent of consolidation to occur, and to determine from this test data the value of the coefficient of consolidation, C_V. This involves comparing a theoretical time with a measured time in the consolidation test. However, when the void ratio, e, coefficient of compressibility, a_V, and permeability, k, are known the coefficient of consolidation, C_V, can be calculated directly. The e and a_V are readily determined with a reasonable degree of accuracy in the consolidation test. However, the permeability is difficult to determine in the laboratory. As a result, the California Division of Highways in 1953 undertook a study of the various methods of determining the in situ permeability of soils in conjunction with an evaluation of the effectiveness of sand drains. A method was developed using a piezometer as a variable head permeameter (1). This new test method showed promise, although the techniques used were very crude at the time.

Work was continued with the piezometer method on several construction projects where settlement and pore pressures were being observed. The techniques of performing these tests were improved. The results indicated that the piezometer method could be used in a wide range of soil types. The piezometers would serve a dual function—measurement of permeability and measurement of excess hydrostatic pressures during construction. A report was received from the U. S. Army Corps of Engineers (2) that confirmed the theoretical work concerning the use of piezometers to determine in situ permeabilities.

PIEZOMETER TEST

The test is performed using nonmetallic, porous tube type piezometers. The installation of these devices by the California Division of Highways has been described else-

Paper sponsored by Committee on Soil and Rock Properties and presented at the 47th Annual Meeting.

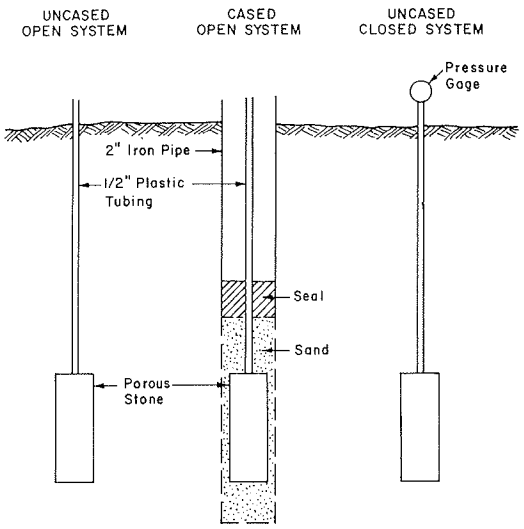

Figure 1. Schematic of piezometer installations.

where (1). The piezometers consist of the porous stone, with or without sand filter, placed in the soil mass. A ½-in. plastic tube is connected to the porous stone and extends vertically to the ground surface. A schematic of the piezometer installation is shown in Figure 1. The test is normally conducted using the open-type system; however, it can be conducted using the closed-type system.

In conducting the test using the open piezometer system, the water level in the plastic tubing is lowered about 5 ft. This is accomplished by means of a hand vacuum pump connected to a ¼-in. plastic tube placed inside the ½-in. plastic tubing. The depth to the water level is then measured at various time intervals (see Fig. 2). The pressure head at a given time interval is then divided by the amount of the total reduction in head (H/H_0). The time interval is plotted against the logarithm of the head ratio. Typical examples of the field data are shown in Figure 3. From these data the basic time lag, the time for H/H_0 to equal 0.37, is determined.

It may be noted that these time lag curves do not always form a straight line through the zero time and 1.00 H/H_0 point. This is primarily due to air in the soil or piezometer system. By lowering the water level in the ½-in. plastic tubing, the pressure is reduced and the air expands, partially escaping. This is one of the reasons for the use of the rising head test instead of the falling head test, in which water is introduced into the system to increase the head. The correction for the air is made by parallel shifting of the straight line portion so as to pass through the zero time and H/H_0 equals unity point. This parallel shifting of the curve assumes that the air has not affected the volume of water passing through the porous stone, which is approximately true when small amounts of air are present. This restricts the use of this test to saturated soils.

These time lag curves are the basis for calculating the permeability of the soil surrounding the piezometer. There are three physical dimensions that must be known to calculate the permeability: the length of the permeameter, its diameter, and the diameter of the standpipe. These variables can all be measured with reasonable accuracy. Using the following equation the horizontal permeability can be calculated (4):

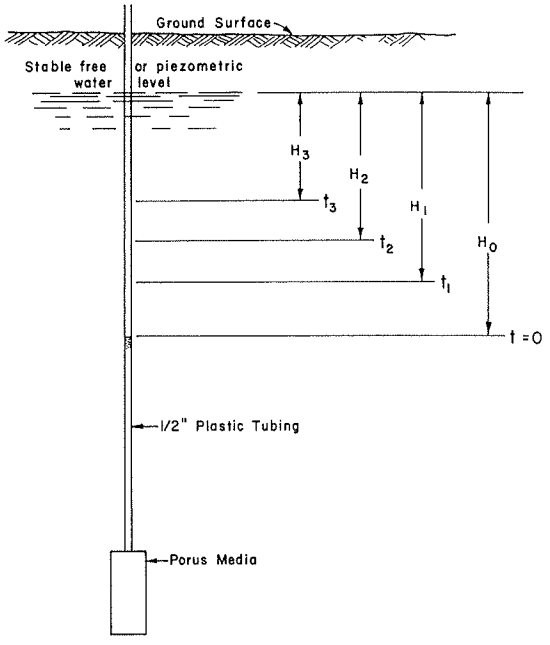

Figure 2. Open piezometer system, indicating water levels at various time intervals.

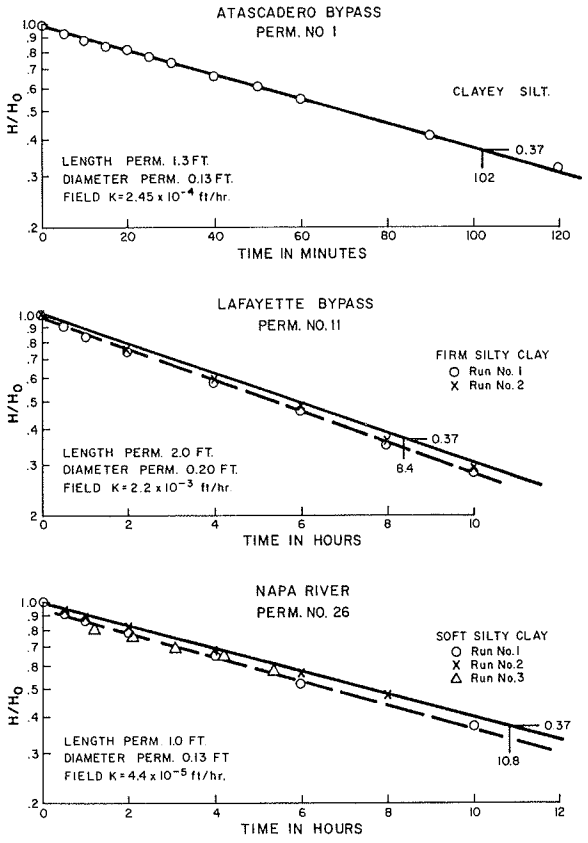

Figure 3. Typical field time lag curves.

$$K_h = \frac{d^2 \ln\left[\frac{mL}{D} + \sqrt{1 + \left(\frac{mL}{D}\right)^2}\right]}{8\,LT}$$

where

K_h = permeability in the horizontal direction,
d = diameter of standpipe,
L = length of permeameter,
D = diameter of permeameter,
ln = natural logarithm,
m = square root of the ratio of horizontal to vertical permeabilities (assume m = 1 for first approximation), and
T = basic time lag.

A correction factor, m, is used to correct the horizontal permeability where the vertical permeability is not the same. This correction factor is generally small. However, concern existed over the effect on the factor m of using different lengths of permeameters. Figure 4 shows one set of data on varying the lengths of the permeameter in a uniform soil. As was expected the basic time lag was decreased from 18.6 to 5.4 hr by lengthening the permeameter; however, only a minor change in permeability resulted. This was found to occur in every instance where variable length permeameters were used in uniform soils. The standard size permeameter now being used is $1\frac{1}{2}$ in. in diameter and $\frac{1}{2}$ to 2 ft in length with a $\frac{1}{2}$-in. OD plastic tubing as the riser.

Factors Affecting the Test

The factors affecting the test were studied on several projects with widely varying soil conditions. It was found that the test was only valid in saturated soils. However, this presented no major problem because the settlement in nonsaturated soils would generally occur during the loading of the embankment.

The range of soil permeabilities successfully measured varied from 10^{-2} to 10^{-6} ft per hour. This range of permeabilities adequately covers the normal range encountered in California soils. Thus, the same test could be used in all soils by simply varying the length of the porous medium from $\frac{1}{2}$ to 2 feet. The time to perform the test could thus be held to one day for all soils. Also the same installation could be later used to measure piezometer pressures developed when the embankments were constructed.

It is frequently necessary to conduct permeability tests on tidal flat soils. Considerable concern existed about the effects of the tide on the results. At three locations near the ocean, a series of tests was performed to evaluate this tidal effect. At two locations a soft silty clay existed and at the other a soft clayey silt existed. At all locations the tide had no effect on the excess hydrostatic pressures or the permeability data as long as the tide was below the elevation of the ground surface. However, when the tide was above the ground elevation a measurable effect on both of these readings

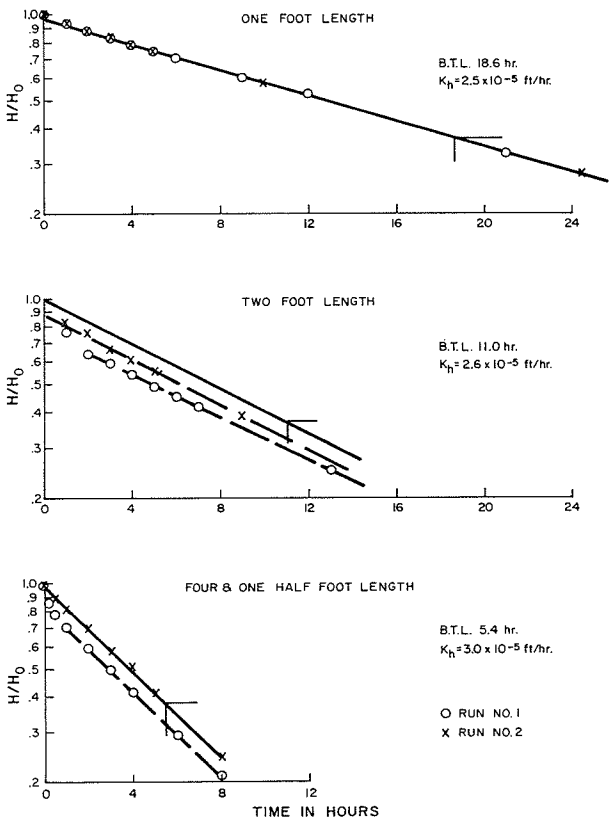

Figure 4. Comparison of various lengths of permeameter.

TABLE 1

SUMMARY OF SOURCES OF ERROR IN DETERMINING BASIC TIME LAG AND EXCESS HYDROSTATIC PRESSURE[a]

Type of Error	Preventable	Precautions and Remarks
Stress adjustment time lag	No	Allow time for soil stress adjustment to take place—usually 3 to 5 days—to minimize effect.
General instrument and installation errors	Yes	Careful workmanship.
Seepage—between soil and conduit	No	No known prevention. Study soil conditions existing at location and use judgment as to best method of installation. Note conditions on log to aid future evaluation of results.
Seepage—between conduit and plastic tubing	Yes	Careful check of bentonite seal.
Gas in lines	Yes	No difficulty in open systems. Use double lines in closed systems.
Gas in porous medium and soil	No	No known prevention. Note on test if suspected that gas exists in porous medium or soil. Careful workmanship will reduce this item.
Internal clogging of porous medium	Yes	Use only clear, clean water in installations. Keep corks on tubing in open systems.
External clogging of porous medium	No	Keep pressure head differences small at all times so as to reduce water flow across porous medium.

[a]From Weber (3).

was noted. These soils had a permeability of 10^{-4} ft per hour or less. It is obvious that at a somewhat higher permeability the tide will have some effect on the readings. The distance between the installation and the tidal waters would also have some effect. These installations had at least 100 ft between the test locations and the tidal waters. Thus, permeabilities can be obtained in tidal flats when proper care is taken.

A summary of common sources of error is given in Table 1, with indications as to how they can be minimized. A discussion of many of the causes of errors in the permeability determination is also included in Hvorslev (2). Most of these errors can be minimized by care in conducting the test, and in making the piezometer installation.

COMPARISON OF RATES OF SETTLEMENT

The primary purpose of this study was to improve the reliability of the estimated rate of consolidation. A comparison of the theoretical rates calculated by the time consolidation curves and the in situ permeability methods with the measured rates would indicate the reliability of the two theoretical methods. The two theoretical methods will be presented and then several comparisons of actual project records will be given.

Time Consolidation Method

The time consolidation method is the normal way of estimating the rate of settlement in the California Division of Highways. The time consolidation curves are plotted for the various loadings. After correcting for the zero and 100 percent consolidation points, the 50 percent consolidation point is determined. From this the time for 50 percent consolidation is determined. Using this time and the corresponding theoretical time factor, a C_V is calculated. This C_V is then used to calculate the times in days for various percentages of consolidation to occur, using the time factors as presented by Taylor (4).

Permeability Method

When the rate of settlement is calculated by the permeability method the e and a_V are obtained from the pressure void ratio curves. From this data a C_V is calculated by the following equation:

$$C_V = \frac{K(1 + e)}{a_V \gamma_W}$$

where

C_V = coefficient of consolidation,
K = in situ permeability,
e = initial void ratio,
a_V = coefficient of compressibility, and
γ_W = unit weight of water.

Using this C_V the time in days for various percent consolidations are calculated as in the previous method. In this method, the C_V is calculated from measured test data.

PISMO OVERHEAD

Sand drains and surcharges were used to accelerate the settlement of a yielding foundation soil under an approach fill to a bridge on the Pismo Overhead project. Settlement and excess hydrostatic pressure data were obtained in both the sand drain and non-sand drain areas. A comparison in the non-sand drain area will be presented.

The foundation soil on this project is a heterogeneous mixture of sedimentary deposits. The top 8 ft is a loose, fine-to-medium sand, to a sandy silt, that is pervious and moderately compressible. Because this layer was above the water table the settlement was assumed to occur as the loading was applied. This sand is underlain by a 5-ft layer of wet, soft silty clay to clayey silt that is somewhat pervious and fairly compressible. A 6-ft layer of wet, compact, sand and gravel underlies the silty clay.

TABLE 2

COMPARISON OF PERMEABILITIES AT PISMO OVERHEAD AS DETERMINED FROM CONSOLIDATION TEST AND FROM PIEZOMETERS

Elevation	Soil Type	Permeabilities in ft/hr	
		Piezometer	Consolidation Test
10	Damp, soft, sandy loam Damp, loose, sand		
0	(Original ground) wet, soft, sandy silt Wet, compact, sand and gravel	4.0×10^{-3}	8.1×10^{-7}
-10	Wet, soft, silty clay	3.2×10^{-5}	2.9×10^{-6} 1.8×10^{-6}
-20	Wet, soft, silty clay	1.3×10^{-6}	9.1×10^{-7}
-30			
-40	Wet, compact, sand and gravel		

This sand and gravel layer is free draining and for the settlement studies was considered incompressible and continuous. The sand and gravel layer is underlain by 28 ft of soft, silty clay that is impervious and compressible. This silty clay layer contributes the major subsidence after construction. The silty clay layer is underlain by a wet, compact, sand and gravel layer that appears to be extensive.

A soil profile and the permeabilities obtained are shown in Table 2. The in situ permeabilities indicate that the soil is more permeable than the permeability calculated from the consolidation test. This is especially noted in the upper soil layers. In the lower compressible layer there is only a minor difference in permeabilities.

A 30-ft fill above original ground, with a 5-ft overload, was constructed. The construction rate was about 3 ft of fill per week. The surcharge remained in place about 180 days.

The comparison of the measured and theoretical rates of settlements of the original ground are shown in Figure 5. The consolidation test data indicate a slower rate of settlement than that indicated using the in situ permeability data. This is mainly due to the differences in indicated permeabilities in the upper foundation soil layers. The measured settlements are within reasonable agreement with the settlement indicated by

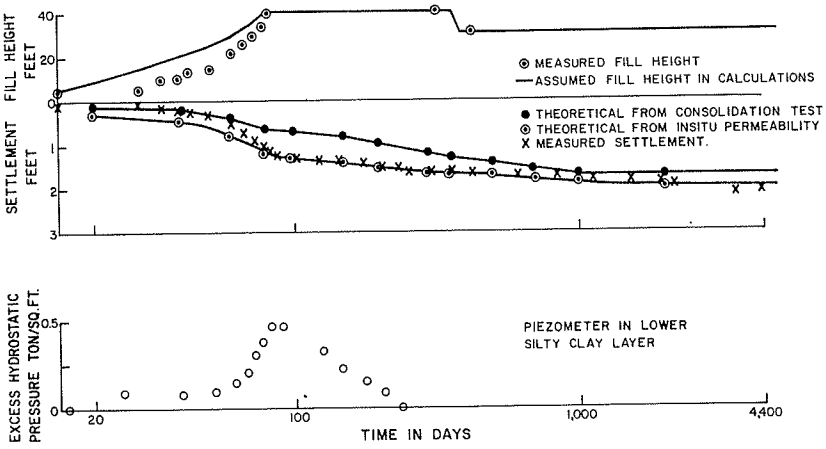

Figure 5. Rate of settlement comparison, Pismo Overhead.

the in situ permeabilities. During construction the measured settlements followed the rate indicated by the in situ permeabilities, then continued at a slower rate than indicated by either method after construction.

One piezometer was placed in the center of the upper sandy silt layer. This piezometer indicated only minor (less than 0.1 ton per sq ft) excess hydrostatic pressure (EHP) during loading and returned to zero about 30 days after loading ceased. Two piezometers were placed in the lower silty clay layer. One piezometer was placed near the upper quarter depth of the layer (Fig. 5). This piezometer indicated about 0.5 ton per sq ft EHP upon completion of loading and decreased to zero EHP in about 200 days. The piezometer in the center of the lower silty clay layer indicated about 0.7 ton per sq ft EHP when loading was completed and ceased to function about 60 days later, when it indicated about 0.5 ton per sq ft EHP. The piezometers indicated that the primary consolidation was completed when the surcharge was removed.

LAFAYETTE BYPASS

A portion of the Lafayette Bypass passes through a valley consisting of soft-to-firm silty clays. A small stream, a county road, and an E.B.M.U.D. pipeline was crossed by means of a bridge on the west side of the valley. The east approach to the bridge consisted of a 40-ft fill over approximately 55 ft of compressible foundation soils. A 9-ft surcharge was used to accelerate the settlement of the fill. Settlement platforms and piezometers were installed to measure the consolidation of the foundation soils.

The foundation soil consisted of three compressible layers underlain by a compact sand. The top layer was about 5 to 10 ft in thickness and consisted of a damp sandy, clayey silt. As this layer was above the water table, instantaneous settlement with loading was assumed.

The center layer is about 20 ft thick, consisting of a damp, soft-to-firm silty clay with varying amounts of sand and gravel; it is below the water table. Using the piezometers as permeability tubes, an average permeability of 3.0×10^{-5} ft/hr was obtained. Using the consolidation time curves from the consolidation test, an average permeability of 6.5×10^{-6} ft/hr was obtained. In calculating the rate of settlement, this layer was assumed to drain upward into the sandy clayey silt layer. This layer contributed a major portion of the longtime settlement.

The lower compressible layer is a damp firm silty clay, with varying amounts of sand, about 30 ft thick. The firm silty clay is underlain by a compact sand to clayey sand that was assumed to be free draining and incompressible. Using the piezometers as permeability tubes, an average permeability of 2.0×10^{-3} ft/hr was obtained for this silty clay layer. Using the consolidation time curves from the consolidation test, an average permeability of 4.7×10^{-5} ft/hr was determined. In calculating the rate of settlement this layer was assumed to drain downward. The major difference in the theoretical rates of consolidation during construction was due to this layer.

The theoretical and measured settlements of original ground at one location are shown in Figure 6. The theoretical settlement using the in situ permeabilities indicates a rapid settlement during loading with no further settlement after the surcharge is removed. The theoretical settlement obtained using the consolidation test data indicates about 20 percent of the consolidation would be expected at the completion of loading and about 70 percent when the surcharge was removed. The measured settlements indicated that the settlement was completed shortly after completion of loading.

Two piezometers were used, one in the center of each compressible layer. The piezometer in the upper silty clay layer indicated about 1.0 ton per sq ft EHP at completion of loading and ceased to function shortly thereafter. Piezometers at other locations in this layer indicated a slow decrease in EHP after loading. The piezometer in the lower silty clay layer indicated a EHP of 0.75 ton per sq ft when loading was completed and had reduced to about 0.3 ton per sq ft when the surcharge was removed. The piezometers on this project indicated that primary consolidation was nearing completion when the surcharge was removed.

The estimated settlement on this project was about twice the measured settlement. This was due to a failure to consider the preconsolidation of the lower silty clay layer.

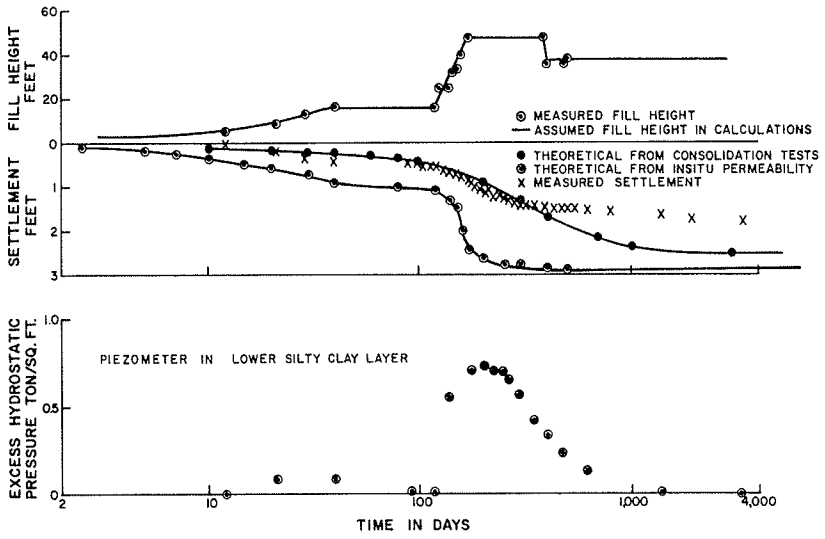

Figure 6. Rate of settlement comparison, Lafayette Bypass.

Generally no significant EHP developed in this layer until 25 to 30 ft of fill was in place (Fig. 6).

ATASCADERO BYPASS

The Atascadero Bypass consisted of about 5 miles of freeway through gently rolling hills. At many of the valleys, cattle or creek crossings, or similar structures were built into the fills. Surcharges were used on many of the fills to eliminate long-term settlements.

The location was a small alluvial valley through which an intermittent stream flows. The fill across this valley contained a culvert for this stream and a cattle crossing, which were constructed by the imperfect trench backfill method. The foundation soil consisted of 19 ft of a sandy silt and was underlain by 12 ft of sandy silty clay. The water table was 2 to 3 ft below the ground surface. The entire area is underlain by a pervious, incompressible silty sand with sandstone fragments. For the settlement calculations it was assumed that the top layer drained to the surface and the lower layer drained to the underlying silty sand layer; also that all settlement above the water table took place during loading.

The permeabilities indicated by the piezometers were generally much higher than those indicated by the time consolidation data. The in situ permeability obtained was 2.1×10^{-1} ft per hour and from the consolidation test data it was 4.6×10^{-6} ft per hour in the lower sandy silty clay layer. In the upper sandy clayey silt layer both methods of determining the permeability indicated a permeability of about 10^{-2} ft per hour. It was thought that the reason for the discrepancy in the lower sandy silty clay layer was that the finer grain portions of the material were tested in the consolidation test while the in situ permeameter tested a larger representative sample. This resulted in the in situ permeability indicating complete settlement as loading occurred. The settlement indicated using the consolidation test data was that about 50 percent of the settlement would occur during loading and about 300 days would be required for completion of the primary settlement (see Fig. 7). This was typical of the results obtained at several locations on this project.

The measured settlements of original ground indicate that the settlement occurred during loading. The piezometer in the lower sandy silty clay layer did not indicate a significant excess hydrostatic pressure during loading. A piezometer placed in the

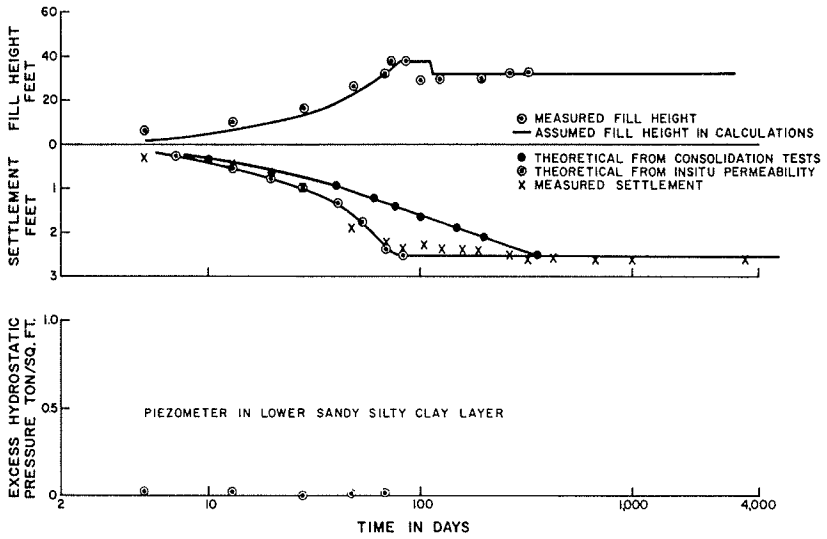

Figure 7. Rate of settlement comparison, Atascadero Bypass.

lower portion of the sandy clayey silt layer was destroyed when the fill was approaching 20 ft in height, and did not indicate a measurable excess hydrostatic pressure during the time it was functioning. At all of the locations studied on this project the in situ permeabilities indicated rates of settlement that were in agreement with the measured rates of settlement and excess hydrostatic pressure readings.

LA TRIANON

The realignment of the existing highway near Blue Lake in northern California required the construction of a fill in excess of 40 ft in height. During the design of this fill it was determined that the foundation soil had insufficient strength to support this height of fill under normal construction procedures. In situ permeameters were installed to determine the anticipated rate of consolidation using various foundation treatments. Whereas the previous in situ permeabilities were determined at the start of construction, the permeabilities were obtained during the design stage on this project and were used to estimate the rate of settlement during construction. Sand drains on 15-ft centers without an overload were used to construct a stable fill.

The foundation soil for the fill consisted of an old slide that blocked the westward drainage of Blue Lake. The material consisted of soft plastic silty clay with fragmented Franciscan sandstone and sand to a depth of 40 ft. The material was extremely heterogeneous and only the finer grain portions of the soil could be tested in the laboratory.

A summary of the permeabilities obtained is given in Table 3. The permeabilities from the consolidation test data were all in the range of 1×10^{-5} to 3×10^{-6} ft per hour. The in situ permeabilities were in the range of 2×10^{-2} to 7×10^{-4} ft per hour. The in situ permeabilities were obtained using a 5-ft long permeameter while the consolidation tests contained a 1-in. high sample. It was felt that this was the reason for the differences in permeability.

The estimated rates of settlement, using Barron's work (5), are shown in Figure 8.

TABLE 3

COMPARISON OF PERMEABILITIES–LA TRIANON

In Situ Permeability, ft/hr	Permeability From Consolidation Test, ft/hr
1.8×10^{-3}	3.2×10^{-6}
5.0×10^{-4}	3.3×10^{-5}
2.3×10^{-2}	1.9×10^{-5}
7.2×10^{-4}	1.4×10^{-5}

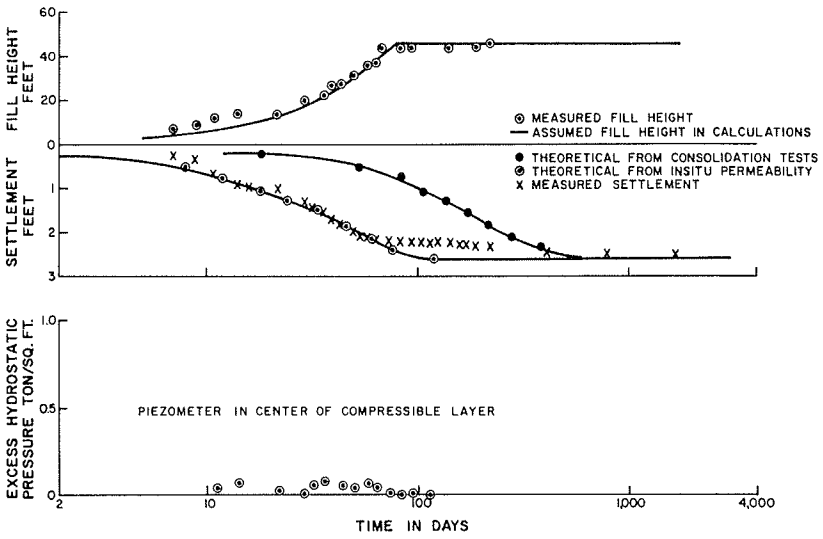

Figure 8. Rate of settlement comparison, La Trianon.

Using the in situ permeabilities it was estimated that 90 percent of the settlement would occur during loading. Using the data from the consolidation tests it was indicated that 20 percent of the settlement would occur during loading. An average of 6.5×10^{-3} ft per hour was used for the in situ permeability and 9.6×10^{-5} ft per hour for the permeability from the consolidation tests. The measured settlements indicated that all of the primary settlement occurred during loading. The piezometers showed only minor increases in excess hydrostatic pressures, indicating that primary consolidation was occurring during loading. The long-term settlement readings indicate minor secondary consolidation is now occurring. The embankment was stable at all times.

NAPA RIVER

The west approach to the Napa River bridge at Mare Island was constructed on 60 to 65 ft of soft silty clay (San Francisco Bay mud) underlain by a stiff silty clay. This fill was constructed as an experimental section with both sand drain and non-sand drain sections. The permeabilities of this foundation soil were determined by both the consolidation tests and by in situ permeabilities (see Table 4). The average in situ permeability was 6.8×10^{-5} ft per hour and the average permeability from the consolidation test data was 2.9×10^{-5} ft per hour. For a report on this project, see Weber (6).

TABLE 4

COMPARISON OF PERMEABILITIES—NAPA RIVER

Depth, ft	In Situ Permeability, ft/hr	Permeability From Consolidation Test, ft/hr
10	8.4×10^{-5}	3.9×10^{-5}
20	5.0×10^{-5}	4.0×10^{-5}
30	5.1×10^{-5}	2.2×10^{-5}
10	11.3×10^{-5}	3.4×10^{-5}
20	4.9×10^{-5}	1.7×10^{-5}
30	4.6×10^{-5}	4.9×10^{-5}
10	10.8×10^{-5}	2.5×10^{-5}
20	7.3×10^{-5}	2.2×10^{-5}
30	3.9×10^{-5}	1.4×10^{-5}

The method used in analysis of the permeabilities and coefficient of consolidation obtained from the consolidation test data is shown in Figure 9. The k and C_v were calculated for various loadings in the consolidation test. These values were then plotted against the logarithm of the average pressure as

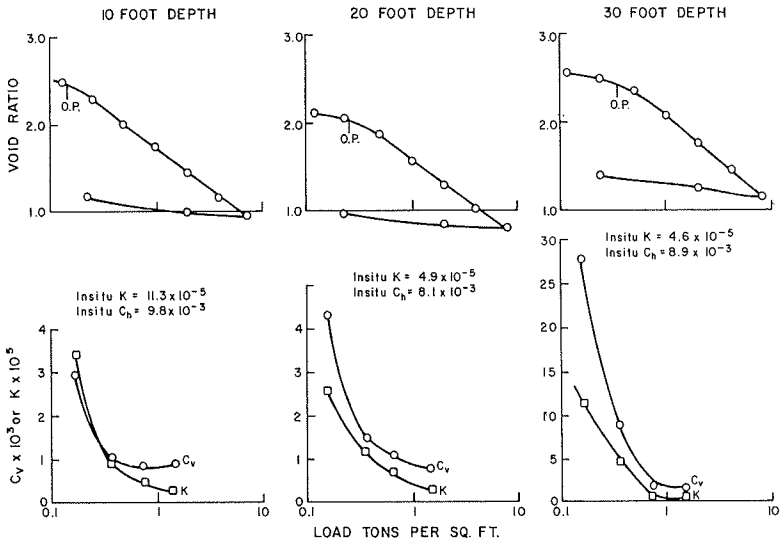

Figure 9. Determination of permeability from consolidation test, Napa River.

shown in Figure 9. The k and C_V at the existing pressure were used to obtain the values to compare with the in situ permeameter values. This procedure was the same for all permeability studies that were conducted.

Using the in situ permeabilities, there tended to be a decrease in permeability with depth (see Table 4). This is as would be expected in a normally consolidated uniform soil deposit. The piezometers installed prior to construction indicated that no EHP existed in this soil. The permeabilities from the consolidation test data are of a random nature. During the design of this project the average in situ permeability was used to estimate the rates of consolidation for the various foundation soil treatments.

The theoretical rates of consolidation for the 15-ft height of embankment and non-sand drain section are shown in Figure 10. The rate of settlement determined from the

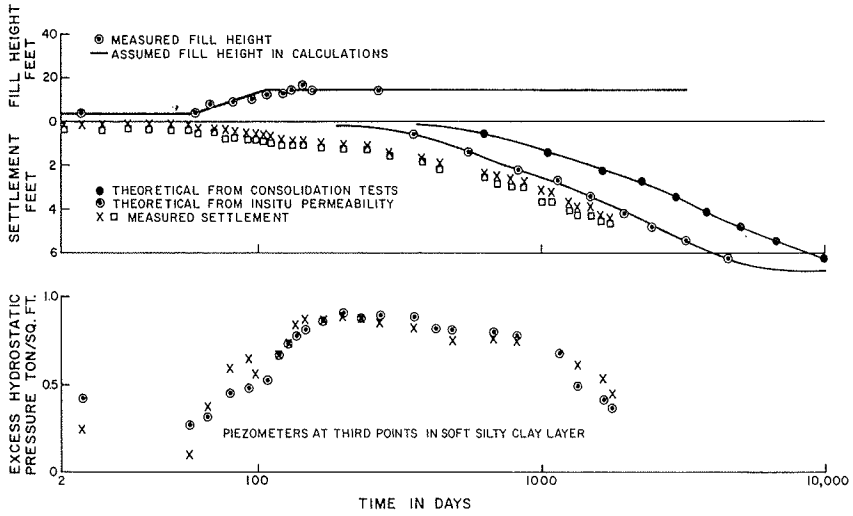

Figure 10. Rate of settlement comparison, Napa River.

consolidation data indicated that it would require about twice the time indicated by the in situ permeability data. As there was a thin peat and/or sand layer between the soft silty clay and stiff silty clay, double drainage was assumed. The measured settlement at two points in this test section are shown in Figure 10. The measured settlements occurred at about one-half the time as indicated by the rate determined by means of the in situ permeability. This non-sand drain section was 150 ft in length with sand drain sections on each end. It was felt that these adjacent sand drain sections may have contributed to the acceleration of the measured rate of settlement. The excess hydrostatic pressure readings of two piezometers, at about the third points of the soft silty clay layer thickness, are shown in Figure 10. The excess hydrostatic pressures are in reasonable agreement with the measured settlement data. Typical examples of the variation of EHP with depth are given by Weber (6). Attempts were made to correlate the settlements as determined by the piezometers with the measured settlements. The measured settlements at the example cited were in reasonable agreement with the settlements as determined by the piezometers. At many locations the measured settlements were greater than the settlements determined by the EHP readings due to plastic flow of the soft foundation soil. In the sand drain areas the rates of settlement were affected by the method of placement of the sand drains and do not directly compare with either theoretical solution for rates of settlement (6).

GENERAL DISCUSSION

The in situ permeameters measure primarily the horizontal permeabilities of the foundation soils. Generally, they indicate a larger permeability than the data from the consolidation tests. There was originally considerable concern that the in situ permeabilities would indicate too rapid a rate of consolidation. However, the measured rates of settlement were generally in reasonable agreement with the settlement rate as determined by use of the in situ permeabilities. This would indicate that either considerable horizontal drainage was occurring in the foundation soils or that the in situ permeabilities were primarily affected by the vertical permeability of the foundation soil.

Comparative permeabilities have been obtained on a large number of projects with a wide variation of soil conditions. In every case the measured settlements have been in reasonable agreement with the rate determined by the in situ permeameter. Thus, a useful tool is available for estimating the rates of settlement with reasonable accuracy. The time required for surcharges to remain in place can be estimated with reasonable accuracy during design operations. On several projects, such as La Trianon, this has resulted in the successful elimination of overloads.

The volume of soil tested by the two methods varies greatly. The in situ permeameter tests from 1 to 3 cu ft of soil in-place. There is some disturbance of the soil mass in installing the permeameters, but it is not felt that this disturbance is large. The consolidation test is conducted upon a sample of soil with a volume of about 3 cu in. This soil sample must be removed from the foundation soil and generally has some disturbance during sampling operations. Also, further disturbance occurs when the sample is placed in the consolidometer and reloaded. Thus, a partially remolded sample of small volume is used in the consolidation test. It is felt that this disturbance and size of the sample account for the differences in permeability obtained by these two methods.

CONCLUSIONS

A simple, consistent test is available for determination of in situ permeabilities of foundation soils. This in situ permeameter will also serve as a piezometer during construction. The principal sources of error have been studied and techniques for performing the test developed.

The rates of settlement determined from this in situ permeability agree well with the measured settlements. Thus, a useful tool is available with which to estimate the amount and duration of time for overloads necessary to eliminate primary consolidation after completion of construction. The permeabilities can also be used for estimating the effectiveness of special foundation treatments, such as the use of sand drains.

ACKNOWLEDGMENTS

The research described in this paper was conducted by the California Division of Highways, Materials and Research Department, in cooperation with the U.S. Bureau of Public Roads. The Materials and Research Department was under the supervision of F. N. Hveem (retired) and J. L. Beaton. The work was performed by the Foundation Section under the direction of A. W. Root (retired) and Travis W. Smith.

REFERENCES

1. Weber, W. G. Measurement of Excess Hydrostatic Pressures in Soils. ASTM STP 254, 1959.
2. Hvorslev, M. J. Time Lag and Soil Permeability in Ground Water Observations. Waterways Experiment Station Bull. No. 36, 1951.
3. Weber, W. G. Discussion of Accuracy of Field Permeability Determinations. Unpublished memorandum to T. W. Smith, California Division of Highways, Materials and Research Department, Jan. 7, 1957.
4. Taylor, D. W. Fundamentals of Soil Mechanics. John Wiley and Sons, 1948.
5. Barron, R. A. Consolidation of Fine-Grained Soils by Drain Wells. ASCE Trans., Vol. 113, p. 718, 1948.
6. Weber, W. G. Experimental Sand Drain Fill at Napa River. Highway Research Record 133, p. 23-44, 1966.
7. Golder, H. Q., and Glass, A. A. Field Tests for Determining Permeability of Soil Strata. ASTM STP 322, 1962.

Soil Bearing Tests Using a Spherical Penetration Device

GHULAM S. BUTT, Pakistani Army Corps of Engineers; and
TURGUT DEMIREL and RICHARD L. HANDY, Department of Civil Engineering, Iowa State University

•ALTHOUGH widely used for evaluations of strengths of soils, present bearing capacity and static penetrometer tests tend to give nonlinear relationships between load and contact area. This is usually attributed to edge punching shear, which in turn is influenced by the perimeter-area ratio. The plate bearing test, for example, may be performed with different size of plates, and results corrected for the perimeter shear effect or extrapolated to an anticipated loading area. Alternately the bearing or penetration tests are standardized at a certain size and results are used in empirical correlations; the widely used California bearing ratio is one such test.

A review of Prandtl theory for bearing-type or punching shear failure in metals and the Brinnell hardness test for metals (6) suggested that a test might be devised to eliminate or reduce this dimensional aspect of bearing testing (2). If successful, such a test would give a bearing value independent of plate or penetrometer size that might be readily converted into existing evaluations such as CBR or plate bearing k, or that might be usable directly as a bearing capacity.

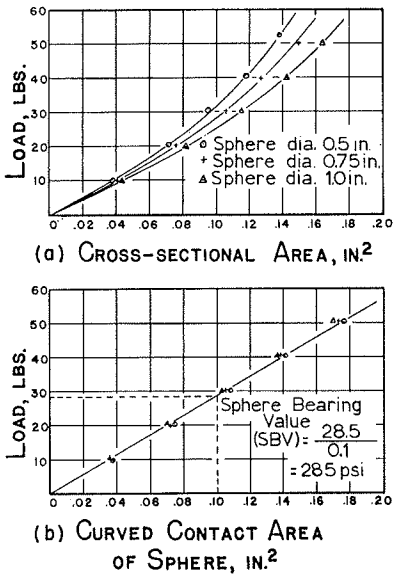

Figure 1. Relationship between load and areas of different sizes of spheres: (a) load vs cross-sectional area; (b) load vs curved contact area of sphere.

A specimen of loess silt was compacted at optimum moisture content with standard compactive effort in CBR molds. Three sizes of sphere diameters were used: 0.75 in., 0.562 in., and 0.50 in. On each specimen three tests were run, one with each sphere under similar conditions.

If the mean pressure is defined similar to the Meyers hardness number, i.e., Load/Cross Section Area of Indentation, the plot is curved as shown in Figure 1a. However, if mean pressure is defined similar to the Brinnell hardness number, i.e., Load/Contact Area, then the curve is one straight line regardless of sphere size, (Fig. 1b). For soils the pressure divided by contact area will be referred to as the Sphere Bearing Value (SBV), given here in psi; that is,

$$SBV = \frac{\text{Load}}{\text{Contact Area}} = \frac{W}{\pi Dh}$$

where W is load, D is diameter of the sphere, and h is penetration depth. (Because of the linear graph, SBV can also be expressed metrically.) Similar results were obtained by Demirel and Enustun in 1955 (2) and Tsytovitch in 1960 (10).

Paper sponsored by Committee on Soil and Rock Properties.

CLASSICAL BEARING CAPACITY THEORY

Classical bearing capacity theories in soil mechanics are modifications of theories of plastic deformation of metals. The shape of the deformation zone or the plastic flow zone plays an important role in interpretation of these theories for our purpose. It is essential to investigate the shape of the failure surfaces and determine their influence on the bearing capacity of the soil surface.

The problems of deformations of metals were studied by Prandtl (1920), Hencky (1923), Ishlinsky (1944), and others. A summary of their conclusions, without attempting a rigorous proof, is given below.

According to Prandtl and Hencky, when a load is first applied to a flat rectangular punch on metal, the shear stresses developed at the edge of the punch are very high. Consequently, even with a small applied load, these regions will be in a state of incipient plasticity. As the load on the punch increases, the material around the punch is in a state of plasticity and the indenter begins to penetrate. The failure zone is shaped like two wings and the zone is commonly known as the Prandtl failure zone. The applied load on the punch is assumed to cause a uniform normal pressure over the face of the punch and is given by $p = 5.14\ k$, where k is a constant for a metal.

This solution was adopted by Terzaghi (8) for determining the ultimate bearing capacity of continuous footings with a smooth base. The equation for this ultimate bearing capacity per unit of area is $q_o = 5.14\ C$ where C is the cohesion of the soil. The ultimate bearing capacity of soil is thus analogous to the mean pressure at in instant of full-scale plastic flow in metals.

In a similar manner Hencky and Ishlinsky have shown that the pressure needed by a circular punch to penetrate the surface of a metal equals 5.2 k to 6 k. Terzaghi modified this relation and gave the following empirical relation to determine the ultimate bearing capacity of a smooth circular footing on a purely cohesive soil: $q_o = 1.3\ (5.14\,C)$.

For deformation of metals by a spherical indenter, Ishlinsky (4, 6) determined that the mean pressure, i.e., the load divided by the cross-sectional area, has a value of about 2.66 Y, where Y is the constant yield stress of the material, analogous to the unconfined compressive strength of the soils.

MODEL INVESTIGATION OF THE DEFORMED ZONE UNDER A SPHERICAL PENETROMETER

In the theoretical treatments of bearing capacity the soil is assumed to be rigid until plastic, i.e., no significant strains occur until rupture occurs. It is also assumed that a boundary exists which encloses all material that is plastically deformed. Equations and calculations are therefore valid only to the extent that the two assumptions are approximately satisfied. Since these two assumptions are not strictly valid in soils, it is not surprising to find that the plastic theory does not provide a completely satisfactory explanation of the deformation pattern.

It was recognized that the penetration of a sphere is a three-dimensional problem where symmetry exists on any plane that includes the central axis. Deformations were examined in two planes, by contouring the surface of indented specimen, and photographing movements in a vertical section cut through the center of the indenter. For the first, specimens were molded in Proctor molds at standard Proctor compaction and various moisture contents, except that the sand was compacted dry. A line was inscribed on the surface of the specimen, and heights were measured at intervals of 1 cm along the inscribed line. A steel ball of 0.75 in. diameter was placed at the center and loaded with increments of 10 lb. After each test, the load and ball were removed and the heights remeasured to give the change in surface elevation. Any hair cracks that appeared on the surface were examined under a magnifying glass, and their lengths were measured with vernier calipers.

In the second technique, specimens were molded by static compaction in a heavy steel mold used for the ASTM soil-cement flexure beam test (1). A specimen 3 by 3 by $11\frac{1}{4}$ in. was transferred to an aluminum box of the same size having a detachable $\frac{3}{4}$-in. thick Plexiglas front. Before the front was attached, a grid was scratched on the face of the specimen and small ball bearings were embedded at the intersections. The Plexiglas

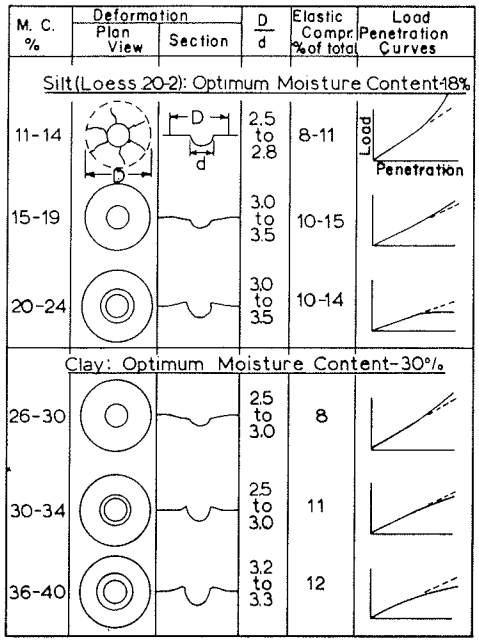

Figure 2. Deformation characteristics of silt and clay.

wall was then bolted in position to contact the specimen. A lubricated hemisphere was placed with its flat surface against the Plexiglas, in contact with the top of the specimen. The sphere was then loaded, and a series of 1-sec. time exposure photographs were taken at no load (for reference) and at various states during the process of deformation under each applied load. This technique was not highly sensitive, and a zone of small deformations could exist that might not be detected on the photographs.

Silt Deformation Analysis

Surface deformations in the silt were found to depend on moisture content, as shown in Figure 2. At a moisture content well below optimum no change of height of the specimen surface was observed except at the point of indentation, and radial hair cracks appeared on the surface of the specimen, their length increasing with increasing applied loads. The diameter of a hypothetical circle joining the extremities of these cracks was found to be 2.56 d to 2.80 d, where d is the diameter of the indentation. Elastic rebound amounted to 8 to 11 percent of the penetration. After penetration was about 15 percent of the sphere diameter, as the load increased the line curved upwards, indicating an increased resistance of soil to penetration, perhaps because of compaction.

At moisture contents between 15 and 19 percent and near optimum (18 percent) no radial cracks appeared, and the surface of the specimen around the indentation decreased in height. The area thus affected could be enclosed with a circle of diameter 3 to 3.5 times d. Close to the optimum moisture content, concentric rings of cracks appeared around the indentation, with new rings forming progressively outwards as the load increased. The slope of the load vs penetration curve was similar to that observed at lower moisture contents, and the elastic recovery ranged between 10 and 15 percent of total penetration of the sphere.

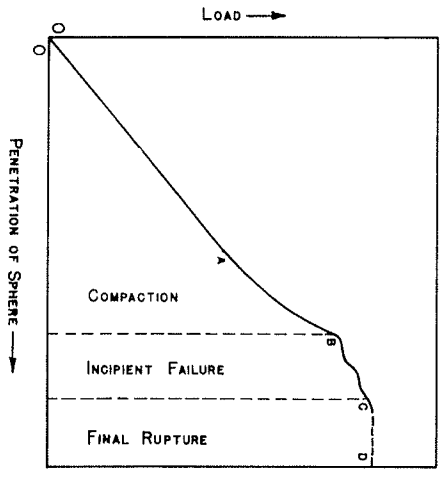

Figure 3. Stages of deformation process of soil.

At moisture contents well above optimum there was another change in deformation characteristics: the load vs penetration curves after the linear portion sloped downward, and a raised lip of soil formed around the sphere. The diameter of the raised surface was 2 to 3 times d.

Two silt specimens molded at optimum moisture content were subjected to very high loads. Initial load increments showed a straight-line relation which corresponds to 0-A in Figure 3. During the next increments the line curved upwards (A-B) showing the previously noted increased resistance of the soil to penetration. At still higher loads the curve was erratic (B-C), and finally the sphere suddenly disappeared below the surface. These stages are interpreted as representing states

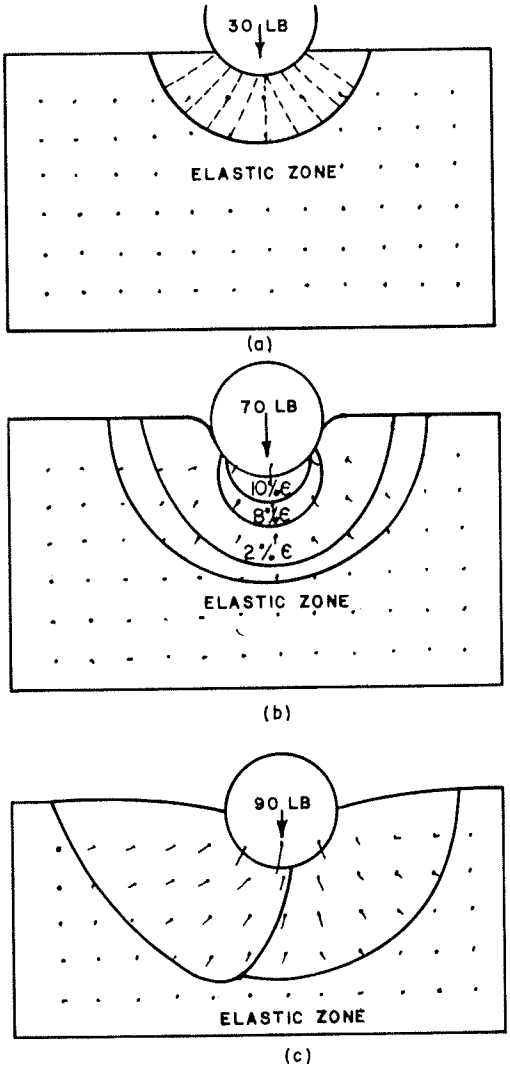

Figure 4. Stages of deformation in silt, showing (a) the flow lines, represented by dotted lines; (b) semicircular deformed area and strain contours; and (c) incipient failure conforming to one wing of a Prandtl deformation boundary.

of equilibrium compaction, incipient failure, and final rupture when shear strength of soil is completely exhausted.

Figure 4 shows the deformations in a vertical plane in loess molded at 16 percent moisture content. The deformed area of the grid is approximately semicircular with a center on the axis of the indenter following the Boussinesq pattern for major principal stresses. The dotted lines in Figure 4 are the flow lines, indicated by movements of the spheres during the time exposure photographs. The percent strain was measured and contoured; high-strain contours are nearly elliptical near the ball, merging gradually into an approximately circular plan at greater depths. The elastic-plastic boundary was sketched to enclose all detected movement.

In Figure 4c, an eccentric zone of compression has emerged, conforming to one wing of a Prandtl deformation boundary. We may assume that shear failure is incipient compounded with eccentric compression. In both Figure 4b and 4c the free surface of soil is depressed, and the ratio D/d is in close agreement with observations in the first series of tests. The ratio of curved area of the elastic-plastic boundary to sphere contact area ranged between 6.7 and 7.4.

Clay Deformation Analysis

The optimum moisture content of the clay at standard Proctor density is 30 percent, and specimens were molded with moisture content ranging from 26 to 40 percent. Specimens molded below 26 percent were discarded because of a honeycombed texture.

The clay surface geometry was almost identical to that observed in silt at ranges of moisture content around the optimum (Fig. 2). The ratio D/d is approximately 3. The load vs penetration curves at moisture contents below and close to optimum deviate very little from a straight line even at higher loads. Figure 5 shows deformations in a vertical plane in the clay sample molded at 30 percent moisture content. The pattern of deformation in Figure 5a is again radial, with a hemispherical elastic-plastic boundary. The ratio of this boundary area to sphere area is 6.6.

Figure 5 shows a failure pattern approximating Prandtl-type failure zones. However, below the failure zone a zone of radial compression extends in a somewhat hemispherical form, probably distorted by the confines of the box. There is also bulging of the free surface adjacent to the sphere.

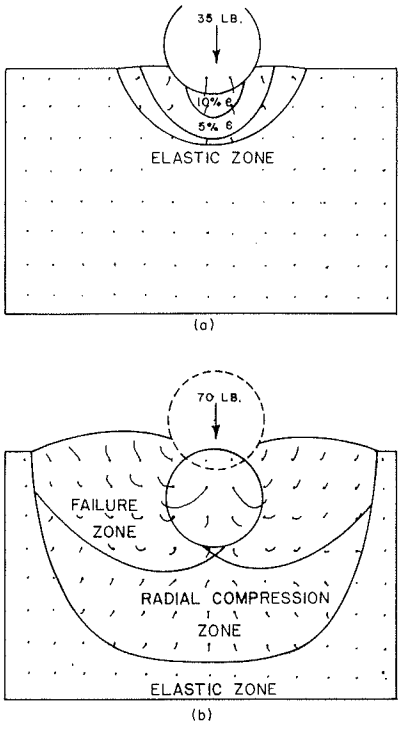

Figure 5. Stages of deformation in clay, showing (a) radial compression, and (b) Prandtl-type failure zones and radial compression zone extending up to the elastic zone.

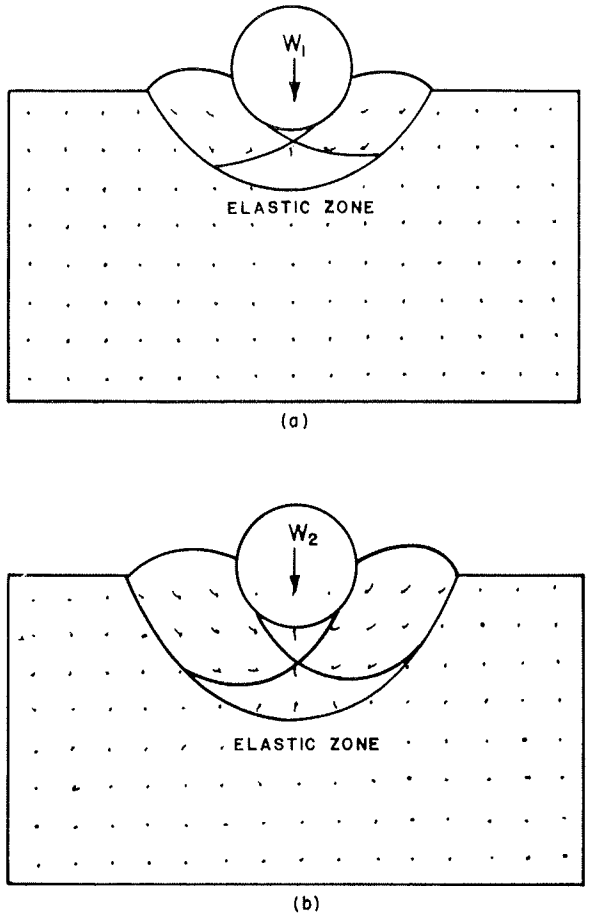

Figure 6. Deformation boundaries in sand with increasing applied loads. Rupture surfaces are curved and sliding takes place in a rotary motion.

Sand Deformation Analysis

Dry compacted sand was used in a series of tests. Because of weakness of the sand it was not possible to take an initial zero reading; therefore observations were entirely qualitative.

As seen in cross section, the sand particle movement initially was vertically downward. As settlement of the sphere increased, the soil was displaced laterally along slip surfaces. These slip surfaces curved upward to reach the free surface of soil around the sphere and form a mound, as seen in Figure 6. The rupture surfaces are curved, and sliding takes place in a rotary motion. Approximate failure planes and elastic-plastic boundaries are sketched in Figure 6. As in clay, there is a deep-rooted zone of compression underneath the shear surfaces.

Discussion

The experimental evidence indicates that penetration of a soil mass by a spherical penetrometer occurs in two stages: compression of soil, and rupture of soil by plastic flow combined with deep compression.

Compression—Prior to application of load on the soil surface the soil mass is in elastic equilibrium. When the load is applied on a sphere, there is a uniform radial displacement and compression of soil which causes a change in volume by densification. In permeable soil the decrease in volume is rapid and results in downward deflection of

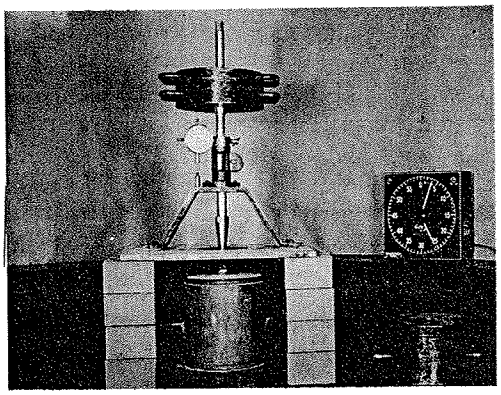

Figure 7. Spherical penetrometer used in laboratory investigations.

the surface of the specimen around the indenter. In turn, densification causes a decreased porosity and an increased resistance to penetration, whereas in theoretical treatments it is assumed that the material is incompressible and there is no volume change throughout the process of deformation.

The mechanism of deformation may be regarded as essentially compression of a set of concentric hemispherical shells except in a region very close to the sphere, where densification probably forms a cap of dead soil. Outside this cap, the irregularities of strain are rapidly smoothed out and an approximately uniform radial strain is produced.

Flow—The onset of plastic flow is preceded by irregular settlement under an increasing load. In some cases the curved rupture surface is eccentric. In most cases, because the sphere is centrally loaded, symmetrical doughnut-shaped rupture takes place beneath the sphere. In all the three soils tested, an inverted cone of soil was visible at this stage, the base of the cone being against the sphere. Initially the cone is short, but as the sphere penetrates deeper and the contact angle increases the cone becomes larger. The rupture surfaces and the flow lines are curved, rising up to a free surface of the soil.

At higher moisture contents the load vs penetration curve falls below the initial straight line, and a mound of soil appears around the sphere. It is reasonable to assume that at this stage the shear strength of soil is completely exhausted; the strains are large compared to stresses imposed, the deformation zone is in a state of plastic flow. The point at which slope of curve changes is the ultimate bearing capacity of soil.

The theoretical treatment also assumes that deformation is entirely within a boundary described by a rupture surface. It appears, from this investigation, that this boundary does not enclose the full plastic region, since there is a further zone in which the material is pseudo-elastically compressed. Here the compression and the plastic parts of the strain may be of comparable magnitude.

None of the plastic-elastic boundaries determined in the soil models correspond exactly to those of the theoretical models, a fact recognized by Terzaghi (8).

LABORATORY AND FIELD TESTS

The laboratory test device (Fig. 7) consists of a sphere, a loading frame, and a dial gage to measure the depth of penetration. Specimens were molded in CBR molds at different moisture contents and compactive energies. At least five tests were conducted on each sample to obtain load vs sphere contact area curves. The SBV is the slope of the line, and is expressed in psi.

One advantage of a linear load to area relationship is that fewer readings are needed to establish a line. To fully exploit this advantage and save time, a "one-shot" method was tried whereby only one load and its corresponding penetration was used to find the bearing value. The initial contact between the sphere and the soil was indicated by an electrical circuit.

Sphere bearing tests were performed on one face of the CBR specimens and CBR tests were performed on the opposite faces of the specimens. Triaxial compression tests, unconfined compressive strength tests, and direct shear tests were also performed to correlate with the SBV. The laboratory tests were performed on a loess silt, a montmorillonite clay, and a sand; their properties are given in Table 1.

Field tests were performed on a silty clay, a glacial till, and a sandy loam (Table 2). Since the soil in the field was heterogeneous and often had large pebbles, small diame-

TABLE 1
PROPERTIES OF SOILS TESTED IN THE LABORATORY

Property	Clay	Loess 20-2	Sand
Physical properties			
Liquid limit, %	88.8	30.8	—
Plastic limit, %	30.1	24.6	—
Plasticity index, %	58.7	6.2	NP
Specific gravity	2.74	2.71	—
Textural composition			
Gravel (2 mm)	—	—	
Sand (2-0.074 mm)	0.5	0.4	100
Silt (0.074-0.005 mm)	9.0	79.8	—
Clay (<0.005 mm)	90.5	19.8	—
Colloidal clay (<0.001 mm)	35.0	14.5	—
Field dry density, pcf	93.2	83.3	—
Field moisture content, %	33.0	17.0	—
Textural classification (BPR system)	Clay	Silty loam	Sand
AASHO-ASTM classification	A-7-6(20)	A-4(8)	A-1-a

ter spheres gave erratic values, and field penetrometers were made with 12 and 6-in. diameters. The loading device consisted of a hydraulic jack with 10,000-lb capacity, equipped with a gage graduated in increments of 200 lb. This was connected to the frame of a loaded truck with a ball swivel. Prior to testing, the top 6 in. or more of desiccated soil was removed from an area 3 by 3 ft and the area was leveled and smoothed with a hand trowel. The equipment was set up as shown in Figure 8. Five equal load increments were applied, and the penetration for each increment was recorded to give load vs contact area curves.

"One-shot" load tests were also performed in the field, and the values obtained were only slightly different from those obtained by the method described above. In no tests did total penetration exceed 15 percent of the diameter of the sphere, which is regarded as a limiting value for the load-contact area proportionality.

The field sphere bearing tests were correlated with the modulus of subgrade reaction obtained from the plate bearing tests with a 12-in. diameter plate and the ultimate bearing capacity of soil using values of C and φ obtained with the field bore-hole shear device (3) and triaxial compressive tests.

Correlation and Comparison Test Results

SBV vs CBR—One of the objectives of the investigation was to establish, if possible, a relationship between the SBV and the CBR.

TABLE 2
PROPERTIES OF SOILS—FIELD TESTS

Property	Silty Clay	Glacial Till	Sandy Loam
Physical properties			
Liquid limit	61.4	24.0	—
Plastic limit	26.1	15.0	NP
Plasticity index	35.3	9.0	—
In-place density, pcf	126.9	138.0	83.7
Dry density, pcf	99.5	125.8	78.8
Field moisture content, %	27.3	10.2	6.23
Textural composition			
Gravel (>2 mm)	—	4.2	8.6
Sand (2-0.074 mm)	24.0	42.9	66.4
Silt (0.074-0.005 mm)	24.6	28.7	14.9
Clay (<0.005 mm)	51.2	24.2	20.1
Colloidal clay (<0.001 mm)	44.1	17.5	9.3
AASHO-ASTM classification	A-7-6(20)	A-4(4)	A-2-4(0)

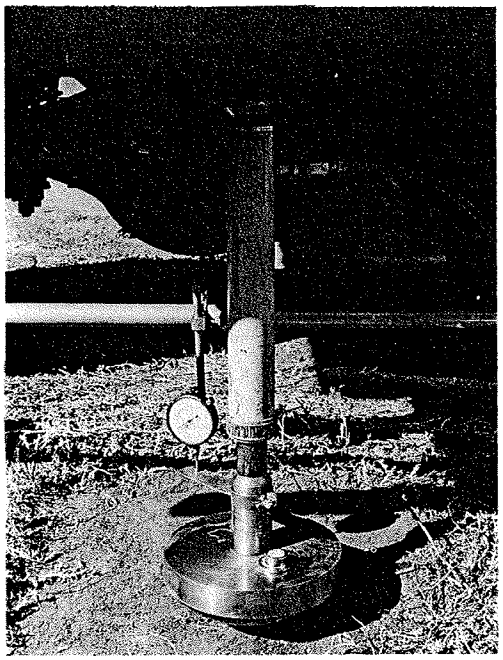

Figure 8. Field spherical penetrometer with 12-in. diameter.

Statistical analysis of the data gave a coefficient of variation of 0.142 (14.2 percent) for the CBR tests and 0.0767 (7.67 percent) for the sphere bearing tests, or about half. This indicates that an individual sphere bearing test is more reliable and reproducible than a CBR test. Consistency of the sphere bearing test was also observed in the field tests (Table 3).

All comparative CBR and SBV data are shown in Figure 9. Since most of the tests were on loess, a regression line and 95 percent confidence band were drawn for the loess tests, omitting those at very low moisture content (x's in Fig. 9) and those at very high moisture content (grouped near the origin). The tests on clay fell on or near the same regression line, but those on sand did not. Much of the width of the confidence band probably relates to the lower reproducibility of the CBR tests.

Apparently when the moisture content is low, soil under the sphere densifies and offers increased resistance to penetration—more so than under a flat piston—giving a higher SBV in relation to the CBR. At high moisture contents the CBR value is higher than the corresponding SBV, probably because of viscous resistance, since the CBR test utilizes a higher rate of shear.

In the case of the sand, all CBR tests were performed with a 10-lb surcharge on the specimen, whereas all the sphere bearing tests were performed without any surcharge. Since coehesionless sand does not develop any resistance to deformation unless it is confined and/or loaded over a large area, the sand CBR test values shown in Figure 9 are much higher than the corresponding SBV's. The SBV's of these tests are merely an indication of the bearing capacity without surcharge.

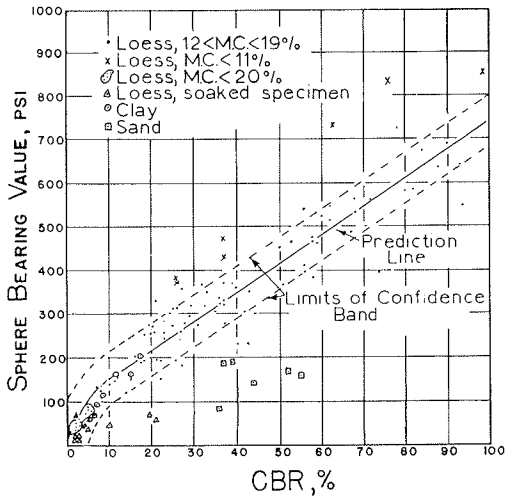

Figure 9. Relationship between the sphere bearing value and the CBR.

No relationship was found between the sphere bearing test data and the corresponding CBR ratings of the soaked specimens. The data, however, are also plotted in Figure 9. After a specimen had been soaked for four days, its surfaces became very soft and did not offer much resistance to penetration of the sphere.

To sum up, a correlation exists between the SBV and the unsoaked CBR of clay and silt compacted near the optimum moisture content, and may be expressed by the following prediction equation:

$$\text{CBR, \%} = \frac{1}{6.6}\,(\text{SBV} - 84)$$

The equation does not apply to sand, or wherever the soil moisture content is far from optimum.

TABLE 3

FIELD DATA: SBV, PLATE BEARING TEST, AND BORE-HOLE SHEAR TEST RESULTS

Test No.	Soil	In-Place Dry Density, pcf	Sphere Bearing Value, psi			Plate Bearing Test		Bore-Hole Shear Test	
			12 In.	6 In.	0.75 In.	$k = \sigma/0.5$, pci	Failure Stress[a], psi	C, psi	φ
Rest area—Hwy. 69									
1	Sandy loam	98.5	55	—	—	170	48	0.5	38
2	Sandy loam	98.5	86	—	—	260	49	1.0	38
3	Sandy loam	98.5	90	94	87	250	51	1.0	38
4	Sandy loam	98.5	85	70	82	220	61	1.0	38
5	Gravelly sandy loam	98.5	115	118	—	420	52	—	—
6	Gravelly sandy loam	98.5	108	118	—	300	40	—	—
7	Gravelly sandy loam	98.5	190	157	—	—	—	—	—[b]
			200	185					
Hwy. 35—Under construction									
8	Glacial till	130	118	—	—	400	51	2.1	32
9	Glacial till	130	150	150	—	450	—	2.1	32
			150	140					
			140						
10	Glacial till	130	150	175	103	360	51	2.1	32
				175					
11	Glacial till	130	120	120	—	440	59	2.1	32
12	Glacial till	130	175	175	181	560	37	3.5	32
				200					
13	Glacial till	130	203	300	—	600	67	3.5	32
				335					
14	Glacial till	130	200	250	—	550	75	3.5	32
				300					
15	Glacial till	130	175	175	—	450	42	3.5	32
			175	205					
16	Glacial till	130	170	175	—	—	—	3.5	32[c]
			170						
County road—north of Ames									
17	Silty clay	85	70	72	—	300	57	9.2	2
18	Silty clay	85	68	—	—	360	71	9.2	2
19	Silty clay	85	75	96	—	—	—	9.2	2
				96					
20	Silty clay	85	70	60	—	—	—	9.2	2[d]
			60	60					

[a]As shown in Figure 10.
[b]Direct shear test values from Shelby-tube samples were C = 4 psi and φ = 38.
[c]UCS = 46.6 psi.
[d]UCS = 25.7 psi.

Sphere Bearing Test vs Plate Bearing Test—Small loads on a circular plate cause a settlement approximately proportional to the applied load, as shown in Figure 10. However, as the load is increased, a point is reached beyond which the settlement increases

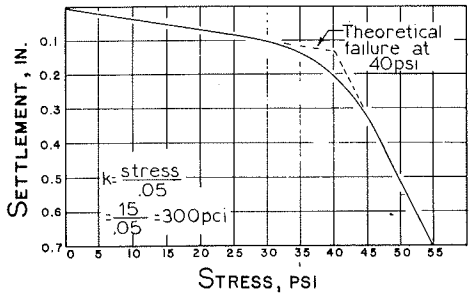

Figure 10. Stress-settlement curve of the plate bearing test.

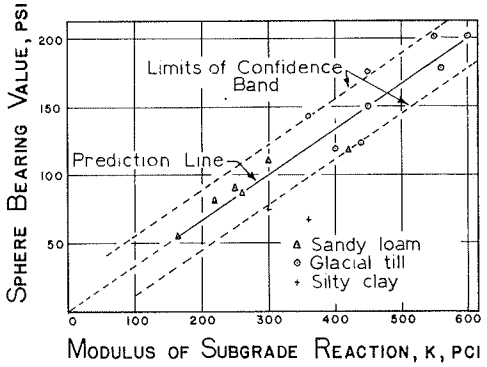

Figure 11. Relationship between SBV and k.

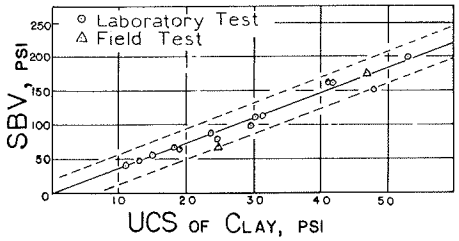

Figure 12. Relationship between SBV and UCS of clay.

much more rapidly. The initial straight-line part of the stress-deflection curve is attributed to pseudo-elastic distortion and compression of the soil, and the steep part is believed caused by shear failure. Between is a transition region of local cracking or partial failure. The intersection of two tangents, one drawn to the elastic branch of the curve and a second drawn to the steep branch, defines the theoretical point of soil failure, or the maximum load that the soil can carry (5, p. 538).

Rigid pavement designs for highways and airports are based on modulus of subgrade reaction k. Foundations are often designed on the failure-point criterion of plate bearing tests.

The numerical values of the sphere bearing test and the 12-in. circular plate tests performed in the field are given in Table 3. No correlation was found between the SBV and the plate bearing failure stress. The SBV's were much higher, probably because of the densification previously mentioned. At lower stresses an excellent linear relationship was found between SBV and the modulus of subgrade reaction k. The equation of the prediction line is

$$k = 3.0\,(SBV)$$

where k is the modulus of subgrade reaction of soil in psi/in. with a 12-in. diameter plate, and the sphere bearing value is in psi. The 95 percent confidence band and the prediction line are shown in Figure 11. In Table 3 the k values are far less reproducible than SBV, and tests repeated on the same soil give widely different values. As in the correlation with CBR, the width of the confidence band is due more to the variability of plate bearing test than the sphere bearing test.

TABLE 4

ULTIMATE BEARING CAPACITY OF SOIL BY TERZAGHI'S EQUATION FOR CIRCULAR FOOTINGS

Test No.	Soil Classification	C, psi	φ	γ, pcf	q_D, psi	SBV, psi
Field 1	Sandy loam	0.5	38	98.5	46.5	55
2	Sandy loam	1.0	38	98.5	88.0	86
3	Sandy loam	1.0	38	98.5	88.0	92
4	Sandy loam	1.0	38	98.5	88.0	80
7[a]	Sandy loam	4.0	38	98.5	340.0	183
8	Glacial till	2.1	32	130	120.0	118
9	Glacial till	2.1	32	130	120.0	146
10	Glacial till	2.1	32	130	120.0	167
11	Glacial till	2.1	32	130	120.0	120
12	Glacial till	3.5	32	130	197.0	183
13	Glacial till	3.5	32	130	197.0	203
14	Glacial till	3.5	32	130	197.0	200
15	Glacial till	3.5	32	130	197.0	175
16	Glacial till	3.5	32	130	197.0	172
17	Silty clay	9.2	2	85	69.4	71
18	Silty clay	9.2	2	85	69.4	68
19	Silty clay	9.2	2	85	69.4	89
20	Silty clay	9.2	2	85	69.4	65
Lab 178[b]	Clay	43.55	—	123	322	308
179[b]	Clay	47.8	—	116	362	346
180[b]	Clay	6.55	—	113	48.5	50

[a] C and φ values were obtained from Shelby-tube samples in lab by direct shear.
[b] C values were obtained from remolded specimens by direct shear; the remaining C and φ values were obtained in the field by the bore-hole shear device.

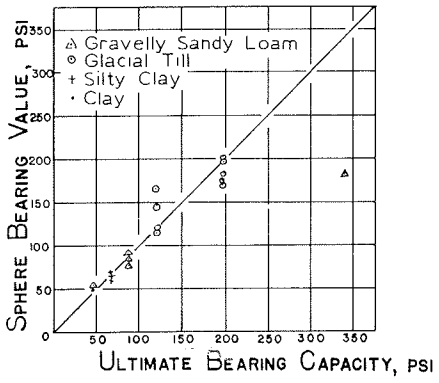

Figure 13. Relationship between the SBV and the ultimate bearing capacity of soil as determined by Terzaghi's equation for circular footings.

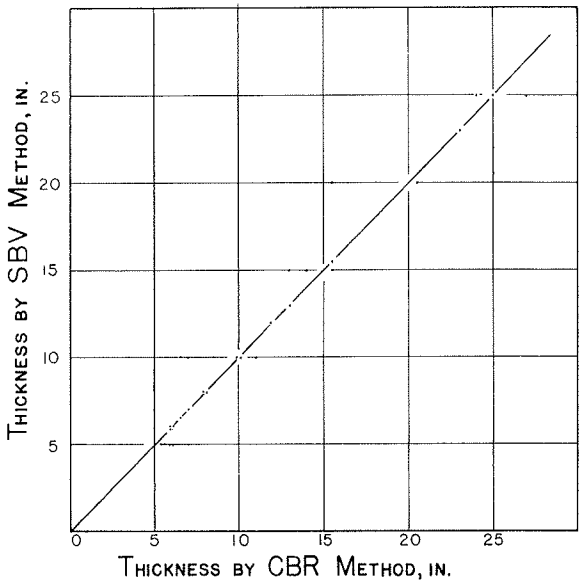

Figure 14. Relationship of pavement thickness for wheel load 9,000 lb by SBV and CBR curves.

Sphere Bearing Test vs Unconfined Compressive Strength—In cohesive soils a simple and direct determination of the ultimate bearing capacity of footings at the surface of cohesive soils has been worked out independently by Prandtl, Fellenius, and Terzaghi with fairly good agreement between their solutions. Taylor (7) has simplified their solutions in terms of unconfined compressive strength (UCS) as

$$q_u = 3.5 \text{ Unconfined Compressive Strength}$$

where q_u is the ultimate bearing capacity of circular or square footings.

In an earlier section it was shown that the mean pressure over the surface of a spherical indenter over the region of contact with metal has a value of about 3y, where y is the constant yield stress of the metal. Yield stress of the metals may be considered analogous to the unconfined compressive strength of soils. It was also observed that the shape and extent of deformation was remarkably similar to that described by Ishlinsky in the deformation of metals.

Figure 12 shows the SBV plotted against the unconfined compressive strength of clay. The regression line has the equation SBV = 3.66 UCS. The 95 percent confidence band is narrow and all the points fall within this band. For a $\varphi = 0$ soil the Terzaghi equation (discussed below) gives $q_D = 1.3\,C\,(5.7) = 7.4\,C = 3.7$ UCS, which is in excellent agreement with the observed regression values.

SBV and the Ultimate Bearing Capacity—Whereas the above equations are suitable for metals or cohesive soils, most soils also have an internal frictional component, which is included in Terzaghi's bearing capacity equation. Cohesion and φ's of the soils were measured in the field with the recently developed bore-hole shear test device (3), and ultimate bearing capacities were computed according to the equation developed by Terzaghi (9, p. 172) for circular foundations. The surcharge term was dropped from the equation because surcharge was essentially zero. To simplify the calculation, size of the footing, which has only a small effect on the bearing capacity of cohesive soils, was taken as 1 sq in. Calculated bearing values are given in Table 4 along with the SBV obtained at the test sites in three different soils. Three sets of laboratory data have also been included.

In Figure 13 the calculated bearing capacity is plotted against the sphere bearing value. A regression line may be sketched in at 45-deg, and all the points lie about this

line except for a gravelly-sandy loam. The C and φ values for this site were obtained from Shelby-tube samples by direct shear tests in the laboratory, and the value of C of 4 psi (Tables 3 and 4) appears too high. The data thus indicate that the sphere bearing value represents a reliable ultimate bearing capacity of soils with the exception of clean sands.

The correlation between SBV and theoretical bearing capacity is far better for the sphere than for the plate (Table 3), the plate bearing failure stresses for all except the weakest soil being too low. This may be partly due to the difficulty in drawing two meaningful tangents to a continuously curving line, or it may relate to densification under the sphere, as previously discussed. If the latter, the densification must be closer response to applied normal pressure, perhaps because of better drainage and lower pore pressures under the sphere than under the plate.

PAVEMENT DESIGN METHOD FROM THE SBV

The most common cause of pavement structural failure comes from increased deformation of the subgrade through repeated application of load, with consequent failure of the layers above. By application of Boussinesq theory one can derive an equation for pavement thickness Z (11)

$$Z = \left[\frac{P/p\pi}{\left(\frac{p}{p - SBV} \right)^{2/3} - 1} \right]^{1/2}$$

where P is load and p is the tire pressure.

Pavement thicknesses were calculated and compared to those from the CBR method assuming a wheel load of 9,000 lb and a uniform tire pressure of 75 psi. Pavement thicknesses were obtained by both the CBR and the SBV method for all the test data in this investigation, and a close correlation was found between the CBR design thickness and SBV design using a factor of safety of 5.5 (Fig. 14). Since the SBV test is faster (particularly the "one-shot" test) and gives better reproducibility, it might be considered for pavement design; the main limitation is in regard to clean, dry sand. This problem can be solved with further research. Also an advantage that might be exploited in future research is the adaptability of the SBV to repeated loading and the possibility for electrical monitoring of the sphere contact area.

CONCLUSIONS

1. Use of a spherical penetration test on a variety of cohesive soils gave linear plots of spherical contact area vs load. The slope of this plot is termed the sphere bearing value (SBV), dimensionally FL^{-2}, for example, psi. The sphere bearing value was found to be the same regardless of the size of the sphere, so long as the sphere is large enough to overcome inhomogeneities in the soil. An exception was clean sand, which gave nonlinear relationships, perhaps because of immediate plastic bearing capacity failure from lack of a surcharge.

2. Model tests indicated that with increasing loads, penetration of the sphere initially involves pseudo-elastic compression of cohesive soils followed by a plastic bearing capacity failure. The latter failure zone overlies zones of further compression. During the late stages of compaction and during shear failure the load-contact area plot became nonlinear after the penetration depth had exceeded 15 percent of the diameter of the sphere. The low-range load and contact area values are therefore used to determine the SBV.

3. The qualitative observation that the SBV test involves pseudo-elastic compaction was supported by a correlation between SBV and the modulus of subgrade reaction determined from the plate bearing test. A regression line indicated that $k = 3.0$ SBV, where k is in psi/in., using a 12-in. diameter plate, and the SBV is in psi.

4. The SBV also correlated with bearing capacity values such as CBR and plate bearing with several exceptions: The correlation to CBR did not hold for sands, or for silts

except near the optimum moisture content. The correlation to plate bearing failure stress did not hold for high bearing capacity soils, probably because of excess pore pressure in the plate test or imprecision in determination of the plate bearing failure point.

5. The SBV correlated closely with bearing capacities predicted from the Terzaghi equation using soil shear strength parameters C and φ obtained by use of the field borehole shear test. Plate bearing test data did not correlate nearly as well, probably for reasons mentioned in the previous conclusion.

6. A regression line gave SBV = 3.66 times unconfined compressive strength, which is very close to theoretical values.

7. An SBV flexible pavement design method based on an assumed Boussinesq vertical stress distribution and using a factor of safety of 5.5 gave pavement thicknesses comparable to those obtained by existing CBR methods.

8. Advantages of the SBV for bearing tests of soils exclusive of clean sands include

- Possibility for a more rapid "one-shot" test since the load-contact area relationship is a straight line.
- Lower coefficient of variation, i.e., better reproducibility of test results than in CBR and plate bearing testing of the same soils.
- Possibility for changing the sphere size to fit the soil or the loading equipment available with no change in SBV.
- Adaptability for repeated loading and electrical monitoring.

ACKNOWLEDGMENT

This research was done at the Engineering Research Institute, Iowa State University. The project was sponsored by the Iowa Highway Research Board, and was supported with funds from the Iowa State Highway Commission.

REFERENCES

1. Making and Curing Soil-Cement Compression and Flexural Test Specimens in the Laboratory. ASTM Standards Part 2, Designation D 1632-63, p. 476-485, 1966.
2. Demirel, T., and Enustun, B. V. Turkish Report on Soils. Perm. Internat. Assoc. Road Congress Repts. 10, 2, p. 1-14, 1955.
3. Handy, R. L., and Fox, N. S. A Soil Bore-Hole Direct-Shear Test Device. Highway Research News 27, p. 42-51, 1967.
4. Ishlinsky, A. J. Analysis of Spherical Indentation (translated title). Prikl. Matem. i Mekh. SSSR 8, No. 3, p. 233-253, 1944. Original available but not translated, cited in Tabor, D. The Hardness of Metals. The Clarendon Press, Oxford, England, p. 48, 1951.
5. Leonards, G. A., ed. Foundation Engineering. McGraw-Hill Book Co., Inc., 1962.
6. Tabor, D. The Hardness of Metals. The Clarendon Press, Oxford, England, 1951.
7. Taylor, D. W. Fundamentals of Soil Mechanies. John Wiley and Sons, Inc., 1948.
8. Terzaghi, K. Theoretical Soil Mechanics. John Wiley and Sons, Inc., 1948.
9. Terzaghi, K., and Peck, R. B. Soil Mechanics in Engineering Practice. John Wiley and Sons, Inc., 1949.
10. Tsytovitch, N. A. Bases and Foundations on Frozen Soil. HRB Special Report 58, p. 32-35, 1960.
11. Butt, G. S. Soil Bearing Tests Using a Spherical Penetration Device. Unpublished PhD thesis, Iowa State University, 1967.

Summary and Evaluation of Symposium Papers

E. C. W. A. GEUZE, Rensselaer Polytechnic Institute

COMPARISON OF FIELD AND LABORATORY MEASUREMENTS OF MODULUS OF DEFORMATION OF A CLAY

•AUTHORS Hanna and Adams performed triaxial tests to obtain the modulus of deformation and the shear strength of the clay. These tests were either stress controlled or rate of strain controlled, consolidated or unconsolidated, with loading intervals as short as 1 min or as long as 24 hr. The authors attach considerable importance to the ratio of the modulus of deformation and the undrained shear strength of the soil. The modulus of deformation is taken as the secant of the stress-strain curve between the strain values corresponding to the deviator stresses of about 0.2 and 0.5 of the undrained strength, both at loading and unloading.

The authors do not give reasons for their choice of these stress levels. Since the deformation modulus of clay soils has a unique significance only in the range of time-independent strains, the choice of the upper stress level seems questionable. In fact, the presence of a creep or viscous component is clearly demonstrated in the test series shown in Figure 4 of the paper, where controlled stress increments were maintained over 1 min and over 24 hr. In the short interval tests, the viscous component affected the deformations at loading to a much smaller extent than in the long interval tests. As a consequence a much smaller spread in E/C ratios and a greater similarity between consolidated and unconsolidated behavior appears. The limit of the stress range yielding mostly time-independent strains represents a strength of the soil that has no relationship with the conventional shear strength obtained from constant rate of strain or stress controlled triaxial tests where indefinitely increasing strains at constant stress deviators cause failure of the particle structure.

Interesting results were obtained with samples preconsolidated at 20 psi over periods of 2, 13, and 40 weeks. As a result of the compaction, the undrained shear strength increased from an unknown value to 1440 psf, 1780 psf, and 1810 psf. The moduli of deformation were obtained at loading and unloading intervals of 1 min. If the results can be considered to have been obtained from identical samples, the undrained strength increased to 0.5, 0.618, and 0.629 times the consolidation pressure. The results in the diagrams of Figure 5 are shown in terms of the ratios between the stress differences at the peak values of the major principal stress and the principal stress differences at failure. From the similarity between the 13-weeks and 40-weeks tests it can be concluded that the deformation moduli at the various stress levels are proportional to the principal stress differences at failure after the samples had been subjected to extended consolidation periods.

It is also of interest to note that flow affected the strength of the unconsolidated material to a greater extent than the preconsolidated material. Whereas the dots in the diagram of Figure 10B are interspersed with the circles in the band of points, they appear to be shifted to the left in Figure 10D.

The results obtained by the authors raise several questions. It does not follow from these results that the E/C ratio would present any advantage over the use of the modulus of deformation itself, particularly not when the interpretation of the in situ measurements can only yield the values of the moduli. For reasons mentioned before, correlations between the modulus and undrained strength cannot be expected because the choice

Paper sponsored by Committee on Soil and Rock Properties and presented at the 47th Annual Meeting.

of the maximum principal stress difference is too arbitrary. In clay soils the contributions of the elastic and of the viscous deformations do not depend on the limiting strength. Building materials other than clay soils may behave more consistently in terms of E/C ratios, because the structural bonds are less affected by short-term viscosity effects. The choice of a deformation modulus in cohesive soils therefore would necessarily be an arbitrary one.

A second point of controversial nature is the anisotropy of the soil. The authors suggest that in the upper portion of the clay medium a near-passive in situ state of stress could exist. Under these conditions the undrained, constant-volume method of triaxial testing will yield the value of the deformation modulus in axial direction only. The interpretation of the plate load tests will yield an intermediate value of the moduli, if a theory based on isotropic material properties is used. The interpretation of the field data cannot successfully be achieved if the anisotropic properties of the material are taken into account, and as a consequence certain discrepancies between these results and the laboratory and in situ test data can be expected.

FIELD AND LABORATORY STUDIES OF MODULUS OF ELASTICITY OF A CLAY TILL

Authors Soderman, Milligan, and Kim have performed field and laboratory studies of the properties of a clay till much along the same lines as the previous investigators. The reload modulus of deformation obtained from repeated cyclic loading between zero load and one-third of the expected maximum principal stress difference may have been affected by time-dependent strains to a smaller degree than those obtained from cyclic loading to one-half and to three-quarters of the expected maximum. The results shown in Figure 7 of the paper suggest little change in the reversible portions of the strains after four load cycles. The results shown in Figure 6 of the paper supply additional evidence of the negligible effect of the strain rate on the deformation modulus. A decrease of the deformation modulus with increasing principal stress ratio was found to occur regardless of the test type and mode of sampling. The authors attribute this decrease in modulus to a breakdown of the soil structure at increasing magnitudes of the shearing strains. This statement is of sufficient importance to cause a reconsideration of the value of the deformation modulus as a basis for predicting the deformations of a soil mass resulting from the application of loads. The elastic component of a clay soil under undrained conditions at increasing values of the stress deviator (1) shows a substantial decrease beyond the yield value of the shearing stress. The reason for this behavior is the occurrence of irreversible (viscous) strains increasing with time and with the magnitude of the shearing stress. It is therefore not possible to predict the magnitude of the deformations at values of the stress deviator exceeding the yield value of the clay without consideration of the irreversible, time-dependent strains. The actual breakdown of the soil structure takes place in the upper range of values of the stress deviator.

The plate tests yielded interesting information concerning the irreversible portions of the settlement at increasing plate loads (Fig. 3). Unfortunately the time effects are not shown in this diagram. The pore water pressure results suggest that at the load represented by the principal stress difference of about 17 psi the shearing stress at the point of measurement exceeded the yield value of the clay. It is doubtful, however, that the magnitude of the axial strain and of the principal stress difference in the diagram can be obtained by the simple application of the Boussinesq equation mentioned in the report, because of reasons discussed in the previous paper.

The authors are to be commended for the extensive research performed on the effects of sample size, modes of sampling, and types of testing on the test results. When the plate test results in Figure 13 are left out of consideration the comparison of results obtained with samples of different size may point not only to effects of sampling disturbance but also to the rate of equalization of pore pressures in the triaxial tests due to a nonuniform strain distribution in the samples. As could be expected, the consolidated undrained tests yielded higher values of the modulus than the unconsolidated undrained tests. Obviously, a comparison between these results is of little significance since they represent two different states of the material.

The authors did not find an acceptable correlation between modulus and undrained strength of the material. In view of the discussion on this point in the previous paper, this conclusion is noted without further comment.

COMPARISON OF LABORATORY AND FIELD VALUES OF c_v FOR BOSTON BLUE CLAY

Authors Bromwell and Lambe have studied the vertical displacements and the pore pressure changes in Boston blue clay due to two separate effects: the removal of a sand and gravel overburden to a depth of 14.5 ft, and the lowering of the water table in the sand and gravel deposit by about 12 ft.

During the first stage of the excavation about 7 ft were removed in 9 days. Four days later the well point system was put into operation and three days later another 7.5 ft were removed over a period of about 9 days. During the 38-day interval between the completion of the excavation and the pouring of concrete the water table was lowered from about 12 ft to about 13.5 ft.

The pore pressures in piezometers 2, 3, and 4, located in the lower two-thirds of the clay layer (Fig. 5) dropped by identical amounts during the first stage of the excavation. In their interpretation of the field data, however, the authors assumed that no dissipation of pore pressures had occured at the end of the second excavation period at the locations of piezometers 3 and 4. The initial excess pore pressure vs depth curve is based on this assumption. A shift of this curve in either direction obviously affects the value of the time factor in the early phase of pore pressure dissipation and, thereby, the magnitude of the coefficient of swelling c_{vs}.

When the effect of the anisotropic properties of the clay is taken into account, the simultaneous drop of the pore pressures at locations 2, 3, and 4 can be explained by making reasonable assumptions for the values of Poisson's ratios and assuming that the lateral strains are equal to zero. The immediate effect on the pore pressures was thus found to be in the order of one-half of the release of the vertical total stress during the first excavation period. It is interesting to note that at location 1, 7 ft below the top level of the clay, the pressure drop amounted to only a few feet as a result of the swelling which took place during the excavation period.

Subsequent to the first stage of the excavation the water table was lowered by about 12 ft. The authors do not specifically mention the magnitude of the resulting decrease of the pore pressure at the upper boundary of the clay layer. It is obvious, however, that it must be introduced to its full amount in the initial excess pore pressure. The second excavation involved the removal of 7.5 ft of sand and gravel amounting to a decrease of the vertical total stress of 0.42 kg/cm^2, a somewhat larger quantity than the decrease caused by the first excavation. If the effect of these stress releases on the pore pressures would be introduced at half their values and if the effect of lowering of the water table to its full extent would be introduced, the initial negative excess pore pressure at the upper boundary of the clay layer would be in the order of 25.5 ft and at the lower boundary in the order of 13. 5 ft. The fact that the authors arrive at similar assumptions for the initial negative excess pore pressures is fortuitous.

It would seem that the introduction of the immediate elastic effect and of the time-load diagram would substantially affect the magnitude of the swelling coefficient.

The laboratory testing procedure is of major importance among the factors the authors hold responsible for the discrepancy between laboratory and field values. They refer to Taylor, Leonards, and Girault in connection with the effect of the pressure-increment ratio on c_v values. It should, however, be emphasized that the swelling process of clay differs substantially from the compaction process. As a result the swelling curves do not follow the semilogarithmic linear law. However, it does not seem impossible to simulate the load-time program over a period as short as 2 months.

One can entirely agree with the conclusions concerning the importance of anisotropic permeability and the three-dimensional nature of the problem. Both factors tend to accelerate the swelling process. In my opinion, however, preference is to be given to the solution of the points discussed in the evaluation of the paper.

CONSOLIDATION PROPERTIES OF AN ORGANIC CLAY DETERMINED FROM FIELD OBSERVATIONS

Settlements and pore pressures were measured in a soft, organic silty clay deposit underlying a roadway embankment during and after construction. The deposit was stabilized by using vertical sand drains and by the application of a surcharge. Values of compression indexes and consolidation coefficients were computed from settlement and pore pressure measurements as a function of the time-load program. These values were compared with laboratory test data of undisturbed samples taken previous to construction. Samples taken at the time when primary consolidation was nearly completed were used to measure the gain in shear strength of the clay.

Authors Schmidt and Gould give particular attention to the effects of displacement driving of sand drains as evidenced by conclusion No. 1, the second part of conclusion No. 3, and conclusion No. 4. From these conclusions it would follow that the early settlements are ascribed to the driving disturbance and the gas contained in the organic soil. Both factors would contribute to an increase of the c_v values. Part of the rapid initial settlement may, however, also be due to the instantaneous deformation of the clay foundation as a whole, considering the ratio between the thickness of the layer and the width of the embankment. The driving disturbance should have been considerable in view of the ratio of 1 to 5 between the diameter of the drains and their distance center-to-center. It was found that the rather small pore pressures at mid-distance between the drains had dissipated after about one month. Since the first placement of the fill occurred a few months after the driving operations were completed the clay soil had already gone through primary consolidation by that time. It therefore does not seem likely that the rapid initial settlement would be the result of the increase in the compressibility of the clay due to the driving disturbance. The instantaneous deformation of the clay foundation as a whole seems a more plausible explanation. One of the consequences of the reconsolidation of the clay in lateral directions is the reversal of the field stress conditions. The authors conclude that the c_v value computed for the rapid early settlement records cannot be used to extrapolate the rate of consolidation to determine a time for surcharge removal. This conclusion is supported in part by the preceding discussion. If, however, a major part of the initial settlement could be accounted for by the instantaneous effect of deformation a better approximation of the rate of settlement during the early phase might be possible. One can agree with the principal conclusion that the present state of knowledge does not warrant an accurate design, utilizing a carefully determined ratio of the vertical and horizontal coefficients of consolidation, with an allowance for smear or disturbance. The fact that they obtained a more than satisfactory agreement between predicted and observed settlement behavior of the embankment by using a conservative value of the average vertical coefficient of consolidation suggests a reasonable similarity between the laboratory test procedures and in situ behavior.

The authors are to be commended for the comprehensive presentation of the results of their investigations.

IN SITU PERMEABILITIES FOR DETERMINING RATES OF CONSOLIDATION

Weber investigated the effect of in situ measured permeabilities on the agreement between observed and predicted settlements of embankments. Using the in situ k values and the a_v values from laboratory pressure vs void ratio curves, the author obtained a much closer agreement between predicted and actual time-settlement curves than by using c_v values obtained from laboratory consolidation tests. With the latter method deviations mostly occurred in the time lags, though in two out of the five cases the theoretical curve also intersected the observed time-settlement curve. In the other three cases the "final" settlements agree rather well.

One can agree with the conclusion that the permeameter measures primarily the lateral permeability whereas the rate of consolidation in the (routine) laboratory test depends mostly on the vertical permeability. In three cases the author found a considerable discrepancy between permeabilities with ratios varying between 100 and 5000; in five cases between 5 and 40; and in twelve cases between 1 and 5. Nine measure-

ments belonging to the latter group were obtained in a rather uniform soft silty clay. The majority of the given ratios can be expected to occur in normally consolidated sediments. Ratios in the order of hundreds and thousands, however, cannot be explained by preferred orientation of soil particles resulting from normal consolidation in the vertical direction.

The use of the extremely high in situ values has resulted in a better agreement between predicted and observed rates of consolidation in all cases. The "final" settlement of the embankments proved to be in close agreement with the 100 percent consolidation compression, except in one case. This fact would seem to indicate that the a_v values obtained from the pressure-void ratio curves were appropriately chosen.

The fact remains, however, that the effect of the two-dimensional nature of the deformation and flow problem cannot be neglected in a prediction of long-term settlements. Although piezometers were placed at significant depths, there are no indications in the paper that the piezometric measurements were used to check the theoretical pore pressure vs time curves. Such comparisons would have served the purpose of evaluating the validity of the assumptions used in the prediction of the settlements.

SOIL BEARING TESTS USING A SPHERICAL PENETRATION DEVICE

Authors Butt, Demirel, and Handy investigated the use of a spherical shape loading surface in penetration techniques. It was found that reproducibility of test results with this device was far better than of results obtained with other penetration devices. Satisfactory agreement was also obtained between the spherical bearing value and the unconfined compressible strength in clay soils. The ultimate bearing capacity obtained from Terzaghi's equation for shallow footings turned out to be close to the sphere bearing value. The authors did not include cone penetrometer results in their comparative studies.

CONCLUSIONS

A summary of conclusions of the Symposium papers is not a simple task in view of the different objectives set by the authors. On this basis a distinction can be made between the studies of Hanna and Adams and of Soderman, Milligan, and Kim on the one hand, and those of Schmidt and Gould and of Weber on the other. Whereas the first two papers attempted to determine the properties of clay deposits through the immediate effects of the release and application of loads, the last two papers are concerned with long-term prediction of the time-settlement behavior of embankment loads. The third paper, by Bromwell and Lambe, dealt with the case of short-term effects due to excavation and water table lowering at the top level of a clay layer.

A point common to four out of five papers is the assumption of the one-dimensional nature of the problems. Considering the agreement found by Schmidt and Gould and Weber, the effect of two-dimensional deformation and flow on the vertical rate of consolidation would not have been a significant factor. In the work reported by Bromwell and Lambe the effect of the three-dimensional nature of the problem could have been stronger. In all cases, conclusions concerning the magnitude of these effects on the basis of agreements or differences between predicted and observed behavior would be premature because of the influence of other significant factors.

The lack of similarity between laboratory or in situ testing procedures and deformation processes in the field may well be one of the most important factors. It is well-known that small loading increments in consolidation tests on clays may yield compression indexes varying from one-tenth to one-twentieth of the value obtained by the standard increment procedures. In several instances the authors have not found an acceptable relationship between the elastic deformation properties of clays and the undrained strength of clays. In other instances no noticeable increase of the undrained strength was found in the field at the end of the primary consolidation period. These instances demonstrate a basic fallacy in the definition of strength and the methods used for the measurement of this quantity.

If effects of the multidimensional nature of problems are to be included in the prediction of the rate of consolidation we have to be aware of the small strain type solutions

presently available. Test results obtained from large incremental load programs are not applicable to this kind of solution.

It therefore seems that progress in the prediction of settlement behavior in the near future requires improvement of testing techniques, both in the laboratory and in situ, before more sophisticated techniques of computation are attempted.

Comparisons between observed and predicted behavior as achieved by the authors of the Symposium papers are badly needed to realize the progress made in these attempts.

A similar problem exists regarding the use of a deformation modulus for the computation of instantaneous deformations under no drainage conditions. If a modulus is required it should take the initial in situ stress conditions into account.

REFERENCE

1. Geuze, E. C. W. A., The Uniqueness of the Mohr-Coulomb Concept in Shear Failure. ASTM STP 361, 1963.

Price: $2.60

Available from

Highway Research Board
National Academy of Sciences
2101 Constitution Avenue
Washington, D.C. 20418